

Dissertation zur Erlangung des Doktorgrades
der Fakultät für Chemie und Pharmazie
der Ludwig-Maximilians-Universität München

**RNA transfer by Epstein-Barr virus triggers early events
that regulate cell fate and promote immune evasion**



von

Simon Jochum

aus Koblenz

2011

Erklärung

Diese Dissertation wurde im Sinne von § 13 Abs. 3 bzw. 4 der Promotionsordnung vom 29. Januar 1998 von

- von Herrn Prof. Dr. Wolfgang Hammerschmidt betreut und
- von Herrn Prof. Dr. Horst Domdey vor der Fakultät für Chemie und Pharmazie vertreten.

Ehrenwörtliche Versicherung

Die Dissertation wurde selbständig, ohne unerlaubte Hilfsmittel erarbeitet.

München, den 15. April 2011

Simon Jochum

Dissertation eingereicht am 15. April 2012.

1. Gutachter: Prof. Dr. Wolfgang Hammerschmidt

2. Gutachter: Prof. Dr. Horst Domdey

Mündliche Prüfung am 16. Dezember 2012.

Parts of this study are published in the following research articles:

1. Jochum S., Moosmann A., Lang S., Hammerschmidt W. and Zeidler R. (2012)
The EBV immune evasion proteins vIL-10 and BNLF2a protect newly infected B cells from immune recognition and elimination.
PLoS Pathogens 8: e1002704.
2. Jochum S., Ruiss R., Moosmann A., Hammerschmidt W. and Zeidler R. (2012)
RNAs in Epstein-Barr virions control early steps of infection.
Proceedings of the National Academy of Sciences 109: E1396-E1404.

TABLE OF CONTENTS

Table of Contents	4
List of Figures	8
Abstract	10
Zusammenfassung	11
Introduction	12
1. The immune system	12
1.1 Mediators of cellular and humoral immune response	13
1.2 CD8+ T cells recognize intracellular infection	14
1.3 MHC: determining histocompatibility	15
1.4 Natural killer cells control for irregular MHC I surface levels	15
1.5 Recognition through CD4+ T cells	16
1.6 Cytokine signaling	17
1.6.1 Interferons	17
1.6.2 IL-10	19
2. Epstein Barr virus	20
2.1 Infection and tropism	20
2.2 From infection to latency	21
2.3 Certain herpes viruses transfer RNA to their target cells	22
3. The immune evasion strategies of EBV	23
3.1 BNLF2a: a unique factor that interferes with MHC I-loading	23
3.2 BCRF1, the viral homologue of cellular IL-10	23
4. Immune responses to EBV: immune control and fatal failure	25
4.1 Containment of EBV infection in immunocompetent hosts	25
4.2 EBV causes proliferative disorders and cancer	25
5. Experimental strategies to unravel processes of EBV infection	26
5.1 EBV-specific T cell clones as experimental tool	26
5.2 Genetically modified recombinant EBVs and their potential to unravel viral strategies	27
6. Aim of this study	28
 Results I	 30
1. Generation of <i>BCRF1</i> - and <i>BNLF2a</i> -deficient EBV	30
1.1 Selection of appropriate knock-out strategies	30
1.2 Confirmation of genetic mutations and virus titrations	31
2. Phenotypes of <i>BCRF1</i> - and <i>BNLF2a</i> -mutant EBV	33
2.1 Expression analyses of BCRF1 and BNLF2a and their influence on TAP levels	33
2.2 MHC surface levels of cells infected with BCRF1- and BNLF2a-deficient virus mutants	34
2.3 EBV-specific CD8+ T cell clones recognize BNLF2a-deficient EBV-infected cells significantly better	36
2.4 BCRF1 affects the peripheral cytokine response	38
2.5 BCRF1 impairs NK cell-mediated killing of EBV infected cells	40
2.6 CD4+ T cells stimulate NK cell-mediated killing	41
3. Effects on long-term immune control	43

Results II	45
1. The origin of early transcripts in EBV-infected B cells	45
1.1 Several EBV transcripts are present in B cells immediately upon infection	45
2. EBV particles contain RNAs	47
2.1 Preparation and validation of RNA from viral particles	48
2.2 Assessment of different transcript categories in viral particles	50
2.3 Levels of selected transcripts differ between virus producers and viral particles ..	52
2.4 The RNA shuttle-protein EB2 of EBV is present in virions	54
3. Virion-transferred transcripts are translated in recipient cells	55
3.1 Virion-incorporated transcripts are translated immediately in infected cells	55
3.2 The translation of transferred RNAs leads to antigen presentation	57
4. Virion-transferred RNAs modulate the immune response	59
4.1 Packaged BNLF2a-RNA decreases the recognition of infected B cells by CD8+ T cells	59
4.2 Packaged EBERs induce Ifn- α production in infected cells	60
4.3 Virion-transferred microRNAs decrease MICB surface levels on infected B cells	62
4.4 Packaged RNAs enhance EBV's capacity to transform B cells	64
Discussion	66
1. EBV balances immune evasion to prevent counter-mechanisms	66
1.1 Unraveling viral immune evasin mechanisms by reverse genetics	66
1.2 BNLF2a – a dedicated antagonist of antigen presentation	67
1.2.1 The early phase of infection reveals phenotypes of early lytic genes	67
1.2.2 TAP-dependent antigen presentation represents a vulnerable bottleneck	68
1.2.3 Endogenous BNLF2a expression leaves MHC I levels unaffected	69
1.3 <i>BCRF1</i> / <i>vIL10</i> – a secreted immune evasin with differences to hIL-10	70
1.3.1 Endogenous <i>BCRF1</i> expression does not influence specific T cell recognition <i>in vitro</i>	70
1.3.2 <i>vIL-10</i> and Th1 cytokines	70
1.3.3 <i>vIL-10</i> impairs NK cells	71
1.3.4 <i>vIL-10</i> and hIL-10 – homologues with different posttranscriptional regulation	72
1.4 EBV copes with innate and adaptive immunity	74
1.5 Concluding remarks	75
2. Viron packaged RNAs trigger early events in EBV infection	76
2.1 Which events trigger the initial lytic phase of EBV?	76
2.2 Translation of transferred RNA proves the concept	77
2.3 Linking RNA transfer to function	78
2.3.1 Counteracting RNA induced immunogenicity	78
2.4 Effects of non-coding RNA	78
2.4.1 EBERs and their functions	79
2.4.2 MicroRNA regulated immune escape	79
2.5 RNA in particles: a coincidence or a selective mechanism?	80
2.6 RNA transfer increases the chances of virus establishment	82
2.7 Concluding remarks	82

Material & Methods	84
1. Material.....	84
1.1 General equipment	84
1.2 General consumables	85
1.3 Cell culture equipment	85
1.4 Cell culture consumables	86
1.5 Media and solutions for cell culture.....	86
1.6 Enzymes for molecular biology	87
1.7 Kits for molecular biology and biochemistry	87
1.8 Chemicals and reagents.....	88
1.9 Media, solutions and buffers.....	89
1.10 Antibodies	91
1.10.1 Antibodies for FACS stainings.....	91
1.10.2 Antibodies for immune biochemistry	91
1.11 Oligonucleotides.....	92
1.11.1 Primers for standard PCR:	92
1.11.2 Primers for maxiEBV cloning	92
1.11.3 Primers for quantitative PCR.....	93
1.11.4 Stem-loop primers and qPCR primers for microRNAs.....	93
1.12 Plasmids.....	94
1.13 maxiEBV BACs	94
1.14 Bacterial strains	95
1.15 Eukaryotic cell lines	95
1.16 EBV specific T cell clones	96
1.17 Primary cells.....	96
1.17.1 PBMCs.....	96
1.17.2 Adenoid tissue	96
1.18 Software.....	97
2. Methods	98
2.1 Molecular biology	98
2.1.1 Bacterial culture.....	98
2.1.2 Generation and transformation of chemically competent bacteria.....	98
2.1.3 Generation and electroporation of electro-competent bacteria.....	98
2.1.4 Engineering of recombinant EBV	99
2.1.5 Isolation of plasmid DNA from bacteria	101
2.1.6 Phenol-chloroform precipitation of DNA.....	101
2.1.7 Preparation of high quality maxiEBV BAC DNA	102
2.1.8 Measurement of DNA concentration.....	103
2.1.9 Enzymatic treatment of DNA and agarose gel electrophoresis.....	103
2.1.10 Southern blotting	104
2.1.11 RNA extraction.....	105
2.1.12 Reverse Transcription.....	105
2.1.13 quantitative PCR.....	106
2.1.14 Standard PCR	107
2.1.15 EBV genotyping PCR.....	108
2.2 Protein biochemistry	109
2.2.1 Cell lysis	109
2.2.2 Immunoprecipitation of BRLF1 protein from infected cells 2hpi.....	109
2.2.3 SDS polyacrylamide gel electrophoresis (SDS-PAGE)	109
2.2.4 Immunoblotting	110
2.2.5 Purification of His-tagged protein	110

2.2.6 ELISA.....	111
2.3 Cell culture.....	112
2.3.1 Culture of stable cell lines	112
2.3.2 Culture for EBV-specific CD8+ T cell clones	112
2.3.3 Freezing and thawing of eukaryotic cells.....	112
2.3.4 Transfection of 293 cells	113
2.3.5 Generation of virus producer cells.....	113
2.3.6 Induction of virus production in recombinant producer cell lines.....	114
2.3.7 Virus titration.....	114
2.3.8 Harvest of virus from spontaneously lytic B95.8 cells.....	116
2.3.9 Enrichment of virus particles by ultracentrifugation.....	116
2.3.10 Preparation of particles for RNA purification	116
2.3.11 Preparation of PBMCs from blood.....	118
2.3.12 Preparation of cells from human adenoids	118
2.3.13 FACS analysis of cells.....	118
2.3.14 Specific TCR staining by multimers	118
2.3.15 Cell sorting	119
2.3.16 Assessment of cell vitality by MTT	120
2.3.17 Cell counting.....	120
2.4 Functional assays with living cells.....	121
2.4.1 Infection of B cells	121
2.4.2 Inhibition of transcription and translation.	121
2.4.3 T cell recognition assays.....	121
2.4.4 Cytokine response of complete PBMCs to EBV infection.....	122
2.4.5 Killing assays with NK cells	122
2.4.6 Limiting dilutions and regression assays.....	123
Abbreviations.....	124
Literature	125
Danksagung.....	140
Curriculum Vitae	142
Publications and Presentations	143

LIST OF FIGURES

Figure	Title	Page
1.1	Activation and differentiation of lymphocytes in an immune response.	13
1.2	Infected cells present foreign antigen on MHC I and are eliminated by T cells.	14
1.3	Scheme of Th1 and Th2 cytokine function and interaction	18
1.4	vIL-10 and h-IL-10 show strong amino acid homology, but bind differently to the IL-10R1.	24
2.1	Insertional mutagenesis or single nucleotide exchange was the knock out strategy of choice, depending on the genomic situation.	30
2.2	Genotypes of EBV mutants were confirmed and virus supernatants were titrated for equal infection rates.	32
2.3	Following infection, BNLF2a and BCRF1 transcripts are present early and expression is maintained throughout infection.	33
2.4	MHC surface levels on B cells are not significantly altered upon infection with mutant EBV.	35
2.5	Lack of BNLF2a expression leads to earlier and stronger Ifn- γ signals of a T cell clone specific for EBV's BZLF1 protein.	37
2.6	BNLF2a reduces the presentation of TAP-dependent epitopes during the early phase of infection.	37
2.7	Δ BCRF1 infected cultures of PBMCs show elevated levels of cytokines that regulate inflammation.	39
2.8	BCRF1 affects NK cell mediated lysis of infected B cells and CD4 ⁺ T cell help.	41
2.9	NK mediated killing is partly rescued, CD4 effects are fully reverted by exogenous administration of IL-10.	42
2.10	Regression assays follow a Gaussian distribution <i>and</i> Limiting dilution of the viruses showed comparable transformation rates.	43
2.11	<i>In vitro</i> , only double deficiency of <i>BNLF2a</i> and <i>BCRF1</i> leads to improved long-term immune control.	44
3.1	EBV transcripts are detectable in B cells as early as two hours post infection.	46
3.2	Several transcripts are immediately detectable and remain stable in the first hours of infection.	47
3.3	Viral transcripts are located inside EBV particles.	49

Figure	Title	Page
3.4	B95.8 particles and TR ⁻ particles contain viral RNAs.	51
3.5	Viral particles and producer cells differ in their transcript levels.	53
3.6	EB2 protein is packaged into virions.	54
3.7	Particle transcripts are translated in newly infected cells.	56
3.8	CD8 T cell clones specific for lytic EBV epitopes recognize TR ⁻ VLP infected B cells.	58
3.9	The transfer of BNLF2a transcripts impairs immune recognition of infected cells immediately after infection.	59
3.10	The virus particle-mediated transfer of EBERs induces Ifn- α synthesis in infected B cells.	61
3.11	Within the first days of infection, TR ⁻ VLP pseudo-infection results in comparable MICB surface levels as on wildtype infected-B cells, indicating functional microRNA transduction.	63
3.12	Co-infection of primary B cells with EBV and TR ⁻ VLP enhances the transformation potential of B95.8 virus stocks.	65
4.1	Transcriptional and post-transcriptional regulation of hIL-10 and BCRF1.	73
4.2	Scheme of BNLF2a and BCRF1 mediated immune evasion.	75
4.3	Immediate effects of transferred RNA provide a supportive environment for EBV establishment.	83
5.1	Quantitative assessment of microRNAs.	106
5.2	Band patterns of the EBV genotyping PCR.	108
5.3	Workflow of the procedure to generate of recombinant EBV.	115
5.4	Workflow of virion-enrichment and preparation of packaged RNA.	117
5.5	FACS based Multiplex-ELISA	122

ABSTRACT

More than 90% of the worldwide population is infected with Epstein Barr virus (EBV). In general, the infection remains asymptomatic and the virus persists for life in latently infected B cells. During this state, viral activity is reduced to the maintenance of the viral genome such that EBV-infected cells are not efficiently recognized by the immune system. However, the first days of primary infection are characterized by a period of lytic gene expression that contributes to successful virus establishment (Kalla et al., 2010). The abundant expression of “foreign” protein renders the infected cell prone to immune recognition and requires viral counter-measures to evade immune responses.

The first part of this work focuses on the importance of two immune evasins of EBV during this early phase of infection: *BCRF1* and *BNLF2a*, encoding the viral homologue of the anti-inflammatory cytokine IL-10 and a unique inhibitor of epitope loading on MHC I molecules, respectively. To study their impact on immune responses to freshly infected B cells, I generated recombinant EBV mutants, which are deficient in expressing either *BCRF1* or *BNLF2a* or both. I observed significant immunological consequences during the first days of infection, but, unexpectedly, the MHC I surface pattern of infected B cells was not affected. Deficiency in *BNLF2a* expression in infected cells resulted in a drastically increased response of EBV-specific CD8⁺ T cells. *BCRF1* did not participate in this effect, but instead severely impaired the cytokine response to viral infection and protected infected cells from elimination by NK/NKT cells. Thus, both immune evasins have important functions during the early phase of infection and are instrumental for the establishment of latency. Their balanced activity illustrates the perfect adaptation of the virus to the host’s immune system.

The second part of this work builds upon my initial observation that viral transcripts are present in the infected cell almost instantly following virus entry. I found that EBV particles represent the source of these transcripts as I identified them to contain viral RNA which is transferred to and expressed in the infected cell. I could further demonstrate that these packaged transcripts exert important biological functions in the infected cells by triggering the initial viral transcription program or acting as immune modulators. In sum, delivered RNAs apparently create a supportive environment that promotes virus establishment in infected B cells. Thus, despite EBV’s classification as a DNA virus, also packaged RNAs are apparently essential for its infectious nature.

ZUSAMMENFASSUNG

Mehr als 90% der weltweiten Bevölkerung sind mit Epstein Barr Virus (EBV) infiziert. In B Zellen etabliert das Virus eine latente Infektion, die normalerweise asymptomatisch verläuft und lebenslang bestehen bleibt. In Latenz liegt nur sehr begrenzte Virusaktivität vor, die das Immunsystem nicht erkennt und infizierte Zellen somit nicht eliminiert. In den ersten Tagen nach der Infektion von B Zellen kommt es jedoch zur Expression einer Vielzahl lytischer Gene, die wichtig für die erfolgreiche Virusetablierung ist (Kalla et al., 2010). Dies geht einher mit einer starken Last an Virusprotein in der Zelle, welche das Risiko einer Immunreaktion deutlich erhöht. In dieser Phase sind virale Gegenmaßnahmen zur Immunerkennung von besonderer Bedeutung.

Im ersten Teil dieser Arbeit habe ich den Einfluss und das Zusammenspiel zweier viraler Faktoren auf die frühe Immunantwort untersucht: (i) *BCRF1*, ein EBV-Homolog des anti-inflammatorischen humanen IL-10, und (ii) *BNLF2a*, ein EBV-spezifischer Inhibitor der Antigenpräsentation auf MHC I. Um ihre physiologische Bedeutung zu erfassen, habe ich EBVs hergestellt, die entweder defizient für *BCRF1* oder *BNLF2a* oder beide Gene sind. Die Infektion mit diesen Viren verursachte eine stark veränderte frühe Immunantwort: *BNLF2a*-Defizienz resultierte in einer bedeutend stärkeren Aktivierung von EBV-spezifischen CD8+ T Zellen, während *BCRF1* die Zytokin-Antwort im Rahmen einer Infektion zugunsten des Virus deregulierte. Darüber hinaus zeigte sich, dass *BCRF1* infizierte Zellen vor der Eliminierung durch NK/NKT Zellen schützt. Somit konnte ich für beide Faktoren wichtige Funktionen bei der Umgehung der frühen Immunantwort nachweisen, einem essentiellen Schritt bei der Etablierung einer latenten Infektion.

Der zweite Teil meiner Arbeit basierte auf der initialen Beobachtung, dass EBV-Transkripte bereits unmittelbar nach Infektion in den Zielzellen präsent sind. Meine Experimente zeigen, dass EBV Partikel selbst diese RNA enthalten und bei einer Infektion in die Zelle transferieren. Diese Transkripte haben eine wichtige Funktionen im Rahmen der Infektion. Sie kodieren zum einen für Initiatoren des frühen lytischen Transkriptionsprogramms, zum anderen dämpfen sie das Ausmaß einer antiviralen Immunantwort des Wirtes. Der Transfer von RNA generiert offenbar zelluläre Bedingungen, die sich positiv auf den Infektionserfolg des Virus auswirken. Somit konnte ich dem klassischen DNA-Virus EBV erstmalig auch Eigenschaften eines RNA-Virus nachweisen.

INTRODUCTION

1. The immune system

Defense against pathogens is essential for the survival of an organism. Even the most basic forms of life exhibit protection mechanisms like restriction of foreign genome sequences or phagocytic activity. With the onset of evolution, organisms became more complex and developed a dedicated compartment of many different but interacting cell types, called the immune system (IS). It can be divided into two subsets: the innate IS and the adaptive IS. The innate IS comprises granulocytes, macrophages, dendritic cells, mast cells and natural killer cells as effectors whose basic progenitors can already be found in invertebrates. These cells carry germline-encoded receptors to target rather invariant pathogen-associated molecular patterns (PAMPs), like bacterial lipopolysaccharides (LPS). The ability to react immediately on the invasion of pathogens is the major advantage of this arm of the IS. Therefore, most of these effectors are located in classical entry tissues, such as submucosa, however are also present in lymph and blood flow.

The innate IS limits pathogen spread but is rarely able to eliminate the invaders on its own. Instead, elimination of pathogens is usually achieved by engagement of the second arm of the IS, called the adaptive IS. It evolved in higher life-forms starting from jawed vertebrates and consists of two major types of effector cells: T lymphocytes that can be further subdivided into CD4⁺ T cells (T helper cells) and CD8⁺ T cells (T killer cells), as well as B lymphocytes. The characteristic feature of lymphocytes is their antigen receptor, whose specificity is not germline-encoded but generated by somatic recombination of gene segments and is therefore unique to each cell. Expression of these random products leads to the development of cells that recognize epitopes of either 'foreign' or 'self' origin. Self-reactive cells would result in threatening autoimmunity. Therefore, highly effective processes of selection during development of lymphocytes ensure that only cells with non-self specificity are engaged in maturation.

Mature naïve lymphocytes then bear individual non-self reactive antigen receptors, but still require the arming of effector functions. This occurs in lymphoid tissue upon primary encounter of matching antigen in combination with secondary signals from professional antigen presenting cells (APC), or T helper cells. Subsequently, armed cells undergo clonal expansion, leave the lymph node and deploy immediate effector function when their antigen receptor is triggered (independently of secondary signals). Within five to seven days, this

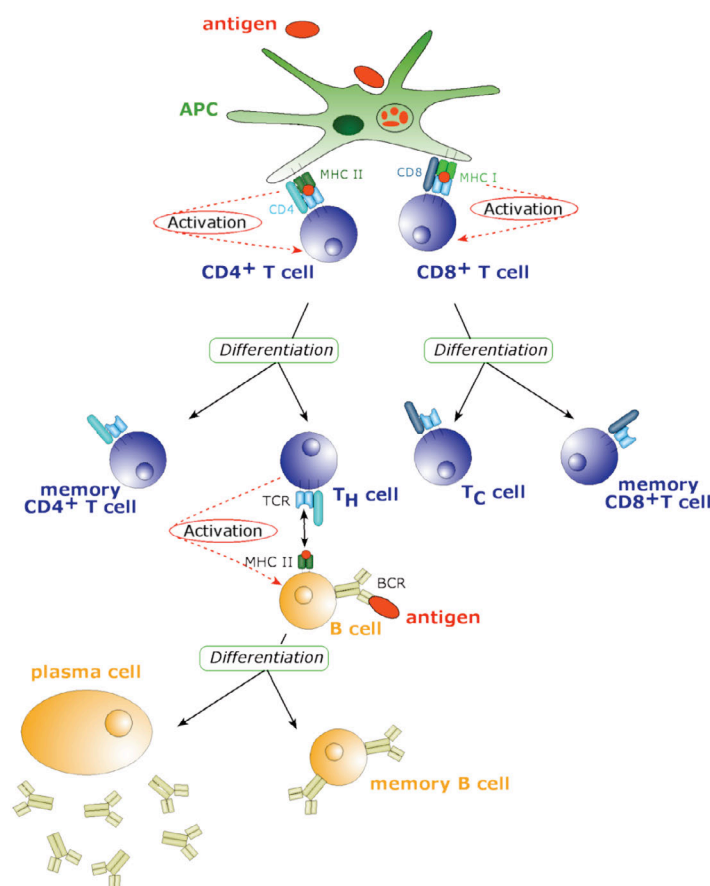


Figure 1.1: Activation and differentiation of lymphocytes in an immune response. The phagocytic uptake of antigen results in presentation on MHC I and MHC II on APCs and triggers T cell activation. B cells also present antigen on MHC II, which is recognized by CD4 T cells that in turn activate the presenting B cell. APC, antigen presenting cell; TCR, T cell receptor; BCR, B cell receptor; T_H cell, T helper cell; T_C cell, cytotoxic T cell.

process generates a large amount of potent effectors with specificity against the invading pathogen, which is generally sufficient to eliminate the infection.

A further hallmark of the adaptive immune response is the generation of an immunologic memory: A minor subpopulation of effector cells acquires a memory phenotype during clonal expansion. These cells are of extreme longevity and reside in the body for many years. In contrast to naïve lymphocytes, they reactivate and undergo clonal expansion immediately upon encounter of antigen, as they do not need to be armed. Hence, re-infection with the same pathogen is eradicated in a faster and more efficient way, frequently without manifestation of any symptoms. This principle is

exploited by vaccination: The IS is triggered to mount immunity to an attenuated or inactivated pathogen generating memory cells that provide long-term protection against the naturally occurring, infectious pathogen (Janeway, 2005).

1.1 Mediators of cellular and humoral immune response

The adaptive immune system can evoke cellular and humoral responses. Cellular immune responses are mediated by T cells and to some extent also by natural killer (NK) cells, with the latter belonging to the innate IS. They confer cytotoxic effector functions through direct cellular contact and thereby eliminate infected cells. $CD4^+$ T cells also belong to the cellular response, but contribute secondary activating signals by direct cell contact and cytokine secretion.

Humoral immune responses are defined by shedding of pathogen-specific antibodies to the ‘humours’, *i.e.* any kind of body fluid. This function is accomplished by plasma B cells that secrete soluble forms of their respective B cell receptors. As described above, initial encounters of matching antigen and costimulatory signals from CD4⁺ T cells are mandatory to trigger this feature. Antibodies deploy neutralizing functions by covering adhesion molecules of the pathogen and tagging them for one of two processes: either phagocytosis by macrophages, or antibody dependent cellular cytotoxicity (ADCC), carried out by NK cells and eosinophils (Metzger, 1990).

For reasons of clarity, cells of the IS are assigned to functional categories. An efficient immune response, however, comprises effectors from all arms of the IS, which operate as highly synchronized network of defense.

1.2 CD8⁺ T cells recognize intracellular infection

In many instances, pathogens are neither sufficiently intercepted nor recognized before they enter a cell, which is usually the case with virus infections. Still, the IS can recognize intracellular infections by means of pathogen-derived antigens, which are presented on the surface of infected cells in the context of class I major histocompatibility complexes (MHC I). Therefore, peptides that are generated by protein degradation in the proteasome are actively translocated to the endoplasmic reticulum (ER) by the transporter associated with antigen- presentation (TAP). Once in the ER, the correct loading of peptides to MHC I is mediated by tapasin and the chaperones calreticulin and Erp57. Loaded MHC I molecules then migrate via the Golgi network to the cell surface to present the peptides. Circulating CD8⁺ T cells scan these molecules for a putative match with their respective T cell receptor (TCR). As mentioned above, immune effectors are selected for their specificity to recognize non-self

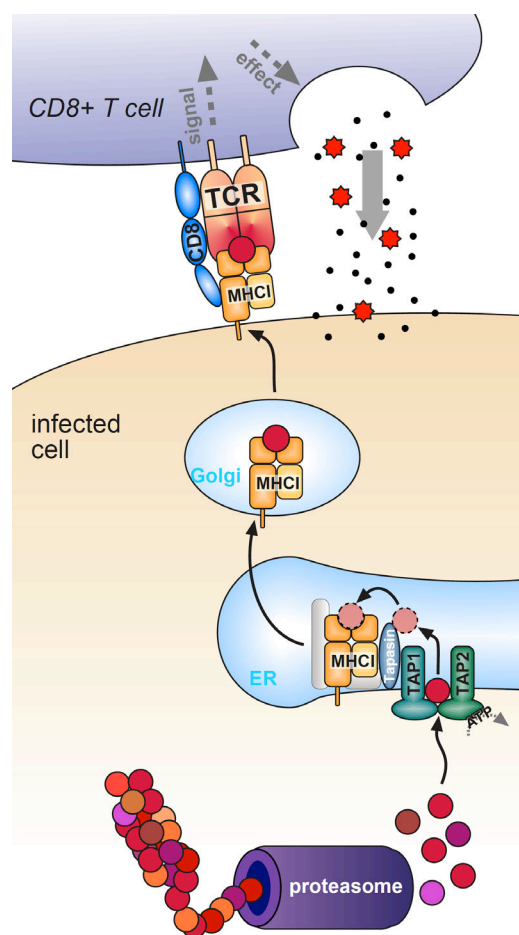


Figure 1.2: Infected cells present foreign antigen on MHC I and are eliminated by T cells. See text for details. ER, endoplasmic reticulum; MHC major histocompatibility complex; TCR, T cell receptor.

structures. Hence, if a TCR matches a presented peptide, it is in general of foreign origin and indicates the infection of the cell. The TCR match activates effector mechanisms, which in case of cytotoxic CD8⁺ T cells lead to elimination of the infected cell via cytolytic effector functions (Germain, 1994).

1.3 MHC: determining histocompatibility

T cell recognition of infected cells is not only dependent on the presented peptide but also on the presenting MHC molecule. A T cell's co-receptor assist in antigen recognition: CD8 binds to MHC I, which can be found on nearly every nucleated cell. CD4 binds to MHC II, which is present on APCs only. But the TCR itself also has to match the MHC molecule and is positively selected for this property during thymic maturation.

In humans, the MHC is also termed human leukocyte antigen (HLA). Whereas MHC I heavy chains are encoded by the HLA-A, B and C genes, MHC II chains are encoded by HLA- DP, DQ and DR, all of them located on chromosome 6. Most of these genes have more than ten alleles, some of them have even more than 100. Thus, the HLA genes show a high degree of variation between individuals, far more than other human genes. Each individual inherits a paternal and a maternal allele of each locus. Both alleles of all HLA genes are co-dominantly expressed on the same cell and form the repertoires of MHC I (max. 6 different molecules) and MHC II (max. 12 different molecules). The individual entity of MHC molecules defines the tissue as 'self' and T cells of this individual will only tolerate self-MHC. Correct recognition of infected cells is hence based on self-MHC loaded with foreign peptide, whereas foreign MHC will lead to immunologic rejection by T cells recognizing 'non-self' structures. MHC incompatibility is a major obstacle in transplantation. Thus, there is a requirement for at least partly matching HLA in donor and recipient (Murphy, 1999).

1.4 Natural killer cells control for irregular MHC I surface levels

Natural killer (NK) cells represent another type of potent cellular effectors of the immune system. They are characterized by the expression of the cell adhesion molecule CD56 and the Fc- γ receptor III (CD16) and account for 5-25% in PBMCs. NK cells belong to the arm of innate immunity, as they rely on conserved, invariant receptors. Regarding their evolution, NK cells are considered as the link between innate and adaptive immunity, as the relation to cytotoxic T cells is obvious and even a subset of NK cells with an invariant TCR has been

described (termed NKT cells) (Fowlkes et al., 1987; Godfrey et al., 2004).

Most importantly, NK cells recognize pathogen induced MHC I downregulation on infected cells and eliminate them by deploying cytolytic function. To decide on activity, NK cells integrate activating and inhibitory signals, which they perceive by a variety of receptors scanning the surface of other cells. Dominant signals are usually derived from killing inhibitory receptors (KIRs) or CD94:NKG2 receptor dimers, which bind to MHC I molecules and minor-histocompatibility complexes, respectively. These signals dominate any potentially activating signals from cell contact sensing receptors. In case NK cells scan cell surfaces with low or absent MHC I molecules and simultaneously receive signals from activating receptors, the signal balance is shifted towards activation and causes the directed release of cytotoxic components like perforin and granzyme. Through their immediate presence and their unique potential to sense downregulated antigen presentation, NK cells are highly important for the restriction of viral infections (Vivier et al., 2011).

1.5 Recognition through CD4+ T cells

CD4+ cells recognize their targets similarly to CD8+ T cells, the difference being that their TCR in combination with the co-stimulatory CD4 molecule specifically binds to MHC II. MHC II is found exclusively on professional antigen presenting cells (APC) comprising dendritic cells, activated B cells and macrophages. These cells are able to engulf recognized pathogens or apoptotic cells for endocytosis. The load is processed by acidification and protease activation in endosomes, leading to the generation of peptides. Other vesicles with ready-to-load MHC II molecules fuse, however these MHC II still carry a placeholder (CLIP) in the peptide-binding groove. HLA-DM molecules mediate the replacement of CLIP with processed peptides and the then loaded MHC II molecules finally migrate to the cell surface (Pieters, 2000). In analogy to CD8+ recognition, scanning T cells are activated when their TCR matches the epitope and CD4 binds to MHC II. CD4+ T cells exhibit a so-called helper function by releasing cytokines that modulate the presenting cell's properties, thereby initiating the differentiation of B cells into antibody secreting plasma cells and memory cells, for instance (London et al., 2000).

1.6 Cytokine signaling

The fate and behavior of cells of the immune system depend on signals derived not only from direct contact with other cells, but also on the presence of soluble signaling molecules, called cytokines. These include chemokines, which are important in chemoattraction of immune cells to a focus of inflammation, for example, and interleukins (ILs), initially named for their function of mediating communication between leukocytes. The major source of cytokines are CD4⁺ T cells, also termed T helper (Th) cells. Depending on their differentiation, they promote either cellular immune responses (Th1) or humoral immune responses (Th2) (Romagnani, 1999; O'Garra and Arai, 2000). These distinct functions are associated with the secretion of characteristic cytokines: Th1 cytokines like IL-2, Ifn- γ , IL-12 and TNF- β boost T and NK cell responses, while Th2 cytokines like IL-4, IL-5, IL-6, IL-10 and IL-13 induce B cell differentiation and proliferation. However, these cytokines are also produced by other cell types, among them CD8⁺ T cells, monocytes, NK cells, B cells and mast cells.

Cytokines form a complex network of communication that orchestrates the different IS compartments to respond in an appropriate manner. As such, certain cytokines act mutually antagonistic and the kind of immune response within a certain phase of an infection is determined by the predominant subset of cytokines: Ifn- γ , for example, hampers cytokine secretion of Th2 cells, whereas Th2 cytokines, such as IL-10 can suppress Th1 production and function (Fiorentino et al., 1989; Modlin and Nutman, 1993; Spellberg and Edwards, 2001).

Table 1.1 represents the most important sources and functions of the cytokines analyzed in this study.

1.6.1 Interferons

Interferons (Ifn) represent the subgroup of cytokines which is predominantly associated with antiviral defense (Biron, 1994) and hence is of special interest in this work. So far, three different types of interferon have been defined depending upon their receptor affinity: type I consisting of the subgroups Ifn- α and β , type II represented by Ifn- γ and type III represented by Ifn- λ . Although type III Ifn form an individual subfamily due to structural and genetic characteristics, their way of induction and function highly resemble those of type I Ifn (Kotenko et al., 2003; Sheppard et al., 2003).

Table 1.1: Th1 and Th2 cytokine sources and functions. The most important source cells and functions are listed (Thomson and Lotze, 2003).

	Cytokine	Sources	Major effects
Th1 cytokines	Ifn- γ	Activated NK and T cells (major source: Th1 cells), enforced secretion by IL-2 signaling	Inhibits the proliferation of infected cells and induces an “antiviral“ state, promotes cellular immune response and proliferation of NK and T cells
	TNF- α/β	Activated T cells and other leukocytes, induced by Ifn and IL-2 signaling	Induction of apoptosis or cytostasis in none-immune cells, induces chemoattractants, enhances proliferation of T cells, the spectrum of TNF- α and - β is similar, but TNF- α is more potent
	IL-1	Maturing monocytes, neutrophils, fibroblasts, lymphocytes (low level)	Stimulation of IL-2 secretion in T helper cells, activation of T, NK and also B cells
	IL-2	Activated Th1 cells but also other T cells	Induction of Ifn- γ , drives T cells into cell cycle and promotes clonal expansion, induces the secretion of IL-1 and TNF- α/β
	IL-12	Induced peripheral lymphocytes, mainly T cells	Contributes to the proliferation of lymphoblasts during clonal expansion, activates NK cells in combination with TNF- α , induces IL-2, Ifn- γ and TNF- α in Th1 cells
Th2 cytokines	IL-4	Activated Th2 cells	Proliferation and differentiation of activated B cells, increases antigen presentation on MHC II, inhibits IL-6 synthesis
	IL-5	Activated Th2 T cells	Stimulation of B cell growth and immunoglobulin secretion
	IL-6	All stimulated leukocytes	Pleiotropic promotion of inflammatory responses, inhibits TNF- α/β production
	IL-10	Regulatory T cells and activated B cells, also monocytes	Pleiotropic anti-inflammatory cytokine, strong inhibitor of Th1 cytokine production and also of IL-6 synthesis, limits immune responses, promotes B cell growth

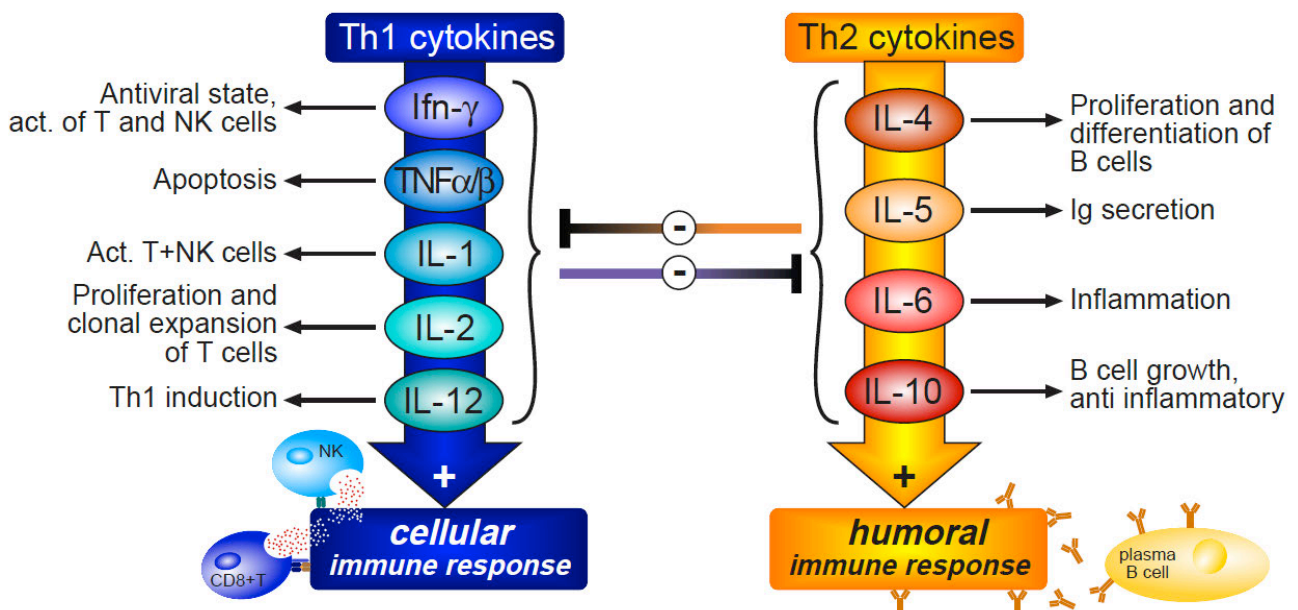


Figure 1.3: Scheme of Th1 and Th2 cytokine function and interaction.

Interferon alpha and beta

In humans, Ifn- α comprises 14 different subtypes, which are mainly secreted by leukocytes (Hardy et al., 2004). Ongoing research is trying to elucidate the biological characteristics of the various family members and their respective sources. Ifn- α secretion is induced by downstream signaling of TLR-3 and RIG-I that both recognize the PAMP of double-stranded RNA (Meylan and Tschopp, 2006). Ifn- α exhibits antiviral effects that manifest in inhibition of proliferation and the expression of interferon-stimulated response factors. As a consequence, activated immune effectors are recruited and triggered to eliminate infected cells. Ifn- β is similar to Ifn- α with regards to structure and function but is predominantly produced by fibroblasts and epithelial cells (Theofilopoulos et al., 2005).

Interferon gamma

The major sources of Ifn- γ are activated Th1 cells, cytotoxic T cells and NK cells that encounter infections. Ifn- γ inhibits the growth of surrounding cells and increases antigen presentation. Therein, it shows the most pronounced effect of all known interferons. Ifn- γ represents the prototypic Th1 cytokine and its immune modulating properties promote a cellular immune response (Schroder et al., 2004; Schoenborn and Wilson, 2007). *In vitro*, secreted IFN- γ is often used as an indicator for T cell activity (Sitkovsky, 1988).

1.6.2 IL-10

IL-10 is a very remarkable member of the interleukin family. It was first discovered as cytokine synthesis inhibitory factor (CSIF) produced by Th2 cells (Fiorentino et al., 1989). Later, it was shown that regulatory T cells, B cells and NK cells are also significant sources for IL-10 (Groux et al., 1997; Bouaziz et al., 2008; Vivier and Ugolini, 2009). Whereas most cytokines display growth-promoting or response-boosting activities, IL-10 in contrast has turned out to be a key player in inhibiting inflammation and terminating an immune response (Moore et al., 2001). Many studies revealed inhibitory functions of IL-10, including the decrease of cytotoxic effector molecules and reduced antigen presentation through decreased MHC I and MHC II surface levels (de Waal Malefyt et al., 1991a; Gazzinelli et al., 1992; Ralph et al., 1992). However, stimulatory effects on the proliferation and humoral activity of B cells have also been described (Go et al., 1990; Rousset et al., 1992a). They are in line with IL-10 as the canonical Th2 cytokine and its strong potential to attenuate cell-mediated immune reactions in favor of a humoral response

(Fiorentino et al., 1991). IL-10 deficient mice suffer from chronic inflammatory Bowel disease and exaggerated inflammatory responses in general (Kuhn et al., 1993; Berg et al., 1995). Thus, the major function of IL-10 is obviously the containment and eventual termination of immune responses to prevent immunopathology. Therapeutic applications of IL-10 in humans suffering from autoimmune or inflammatory conditions were analyzed in several clinical studies, but always faced the risk of opportunistic infections due to the systemic immune suppressive effects of IL-10 (Opal et al., 1998).

Taken together, IL-10 is a highly pleiotropic cytokine. The functional outcome of IL-10 signaling appears to be highly dependent on its own concentration and that of concomitantly present cytokines as well as on the type and state of the target cell.

2. Epstein Barr virus

Epstein Barr virus (EBV) is an enveloped virus with a large double-stranded DNA genome (172kb) and an approximate particle size of 200nm. It belongs to the family of herpes viruses and the official nomenclature terms it human herpes virus 4 (HHV-4). EBV is one of the most widespread human pathogens and more than 90% of the worldwide population is infected (Epstein and Achong, 1979). EBV establishes a latent infection in B cells and only a minute number of viral proteins are expressed, thus preventing recognition by the IS. Sporadic reactivation from this reservoir is sufficient for eventual spread to other hosts and to enable life-long persistence of EBV in an infected individual. This strategy and tropism qualifies EBV as a classical lymphocryptovirus or γ 1-herpes virus (Rickinson and Kieff, 2007).

2.1 Infection and tropism

EBV enters its host via the epithelial cells of the oral mucosa from where it spreads to the B-cell compartment. Infection of B cells occurs through binding of the viral envelope glycoprotein 350 (gp350) to the cellular complement receptor 2 (CR2, *i.e.* CD21) and additional interaction of viral gp42 with cellular MHC II (Nemerow et al., 1987; Wang and Hutt-Fletcher, 1998). This interaction leads to the endocytosis of the particle, which in turn triggers the viral mechanism for membrane fusion, mediated by viral gHgL and viral gB, and finally releases the particle content including the viral capsid into the cytoplasm. The capsid is then transported to the nucleus where it discharges the linear viral genome, which forms a circle, replicates to several copies and is finally tethered to peri-chromatic regions of the

cellular genome (Kanda et al., 2001; Deutsch et al., 2010). Once established, the viral DNA replicates in synchrony with the cellular genome and is maintained as extrachromosomal viral plasmid, termed episome. *In vitro*, infection of B cells generates continuously proliferating lymphoblastoid cell lines (LCLs), which provide a reliable surrogate system to study many aspects of the interaction between the virus and its target cells.

EBV is also able to infect epithelial cells. Their infection occurs by the same gp350/CD21 interaction, however fusion is rather inefficient *in vitro* – presumably due to the lack of MHC II molecules and thus the lack of a gp42 interaction partner (Wang et al., 1998; Shannon-Lowe et al., 2009).

2.2 From infection to latency

In vivo, EBV preferentially infects naïve and memory B cells, both showing a resting phenotype (Joseph et al., 2000). The initial, virally triggered signaling events reactivate the cells. Upon infection, an immediate lytic phase is initiated that intriguingly does not give rise to progeny virus. This early lytic phase is presumably induced by the spontaneous expression of the two viral transcription factors Zta and Rta, encoded by the immediate-early genes *BZLF1* and *BRLF1*, respectively. Together they drive infected cells from G0/G1 to S phase (Guo et al., 2010; Kalla et al., 2010). These viral transactivators also induce numerous early lytic transcripts that contribute to the transient activation of the target cell. The early lytic phase eventually subsides and infected cells enter latency. Based on this strategy, the virus persists in its host with rare episodes of reactivation to spread to other cells and to ensure an infection of the host organism for life. *In vivo*, an efficient immune control counteracts the growth transforming potential of EBV. EBV associated diseases are usually linked to immune deficiency or secondary infections that trigger lymphomagenesis (see also chapter 4.2). *In vitro*, growth-limiting effectors are absent and infection of B cells with EBV leads to growth transformation and continuously proliferating lymphoblastoid cell lines.

Latently infected cells differ with respect to the number of expressed viral genes, which led to their classification in four different subtypes (see table 1.2).

Latency	expressed EBV genes					associated cells / malignancy
	<i>EBERs</i>	<i>EBNA-1</i>	<i>LMP1</i>	<i>LMP2A</i>	<i>EBNA-2,-3,-LP</i>	
0	+	n.d.	-	-	-	peripheral B cells*
I	+	+	-	-	-	BL, PEL
II	+	+	+	+	-	HL, NPC
III	+	+	+	+	+	IM, PTLD, LCL

Table 1.2: Latency programs are defined by the gene expression pattern and associated with distinct cellular phenotypes and malignancies. BL, Burkitt lymphoma; PEL, primary effusion lymphoma; HL, Hodgkin lymphoma; NPC, nasopharyngeal carcinoma; IM, infectious mononucleosis; PTLD, post-transplant lymphoproliferative disorder; n.d., not determined; *: resting phenotype; (see also Kuppers, 2003)

2.3 Certain herpes viruses transfer RNA to their target cells.

The discovery of packaged transcripts in virions of human cytomegalovirus (hCMV) added a new aspect to the field of herpes virus biology (Bresnahan and Shenk, 2000). Concomitant to the fusion of virus particles with the target cell, the RNA molecules are transferred and translated immediately. Initial synthesis of viral protein is hence independent of *de novo* transcription from the viral DNA genome and presumably contributes to the success of hCMV infection.

Similar reports exist for Herpes simplex virus I (HSV1). Here, a tegument protein binds viral transcripts and thus mediates the incorporation of RNA into HSV1 virions and their transfer to recipient cells (Sciortino et al., 2001; Sciortino et al., 2002). This finding suggests an intentional mechanism for directed RNA transfer by HSV1 virions to fulfill a role in the immediate-early steps of viral infection.

Virions of Kaposi sarcoma herpes virus (KSHV) have also been identified to contain RNA (Bechtel et al., 2005). This finding is of special interest as KSHV and EBV are highly related in terms of genomic structure and viral mechanisms. The establishment of a KSHV infection is also characterized by an initial lytic phase, for instance. Intriguingly, all of the transcripts that are contained in KSHV virions are also found during the initial lytic phase. Their transfer might thus represent the necessary trigger to engage the lytic phase, however functional correlations are still missing. With the given homology to KSHV and the similar transcriptional program during the first few days after infection, EBV might follow a similar strategy.

The findings described above have reshaped the dogma of the strict dependency on DNA genomes in herpes virus biology (Roizman, 2000). RNAs could give the virus a head start by counteracting cellular defense mechanisms and shaping a supportive intracellular environment for a successful infection. Thus, packaged EBV RNAs might event promote the establishment of latency.

3. The immune evasion strategies of EBV

The epidemiological success of EBV is owed in large extent to its potential to escape from immune responses of the host. In addition to the strategy of hiding in latency, EBV has acquired sophisticated active immune evasion strategies that are of major importance during the lytic phase. These strategies range from global reduction of transcription by a host shutoff factor to specific interference with antigen presentation (Rowe et al., 2007; Rensing et al., 2008; Long et al., 2011). Interference with the inflammatory response of immune cells and the decrease of antigen presentation provide the virus with additional potent features to ascertain its persistence within the host. In this context, two immune evasins of EBV are of special interest: *BNLF2a*, encoding a unique inhibitor of epitope loading on MHC I molecules and *BCRF1*, encoding the viral homologue of human IL-10.

3.1 BNLF2a: a unique factor that interferes with MHC I-loading

Pudney and colleagues reported a steady decrease of antigen-presentation in EBV-infected cells with the onset of the lytic cycle that is not observed in other herpes viruses to this extent (Pudney et al., 2005). This observation drove the idea to screen for unique immune evasins of EBV that led to the identification of BNLF2a to act in an immune evasive manner (Hislop et al., 2007). Functional analyses revealed that BNLF2a blocks the binding of both ATP and peptides to TAP1. This impairs the function of TAP to translocate peptides to the ER and thereby diminishes the load of antigen to MHC class I molecules (Horst et al., 2009). Ectopic expression of high levels of BNLF2a even leads to decreased MHC I surface levels. In the context of EBV infection, BNLF2a supports the immune escape of established LCLs that undergo the lytic phase (Croft et al., 2009).

No information about the impact of BNLF2a on the success of the initial infection is available. During these early days of virus infection, cells support the expression of lytic genes (Kalla et al., 2010), which leads to high antigen loads. This requires an efficient strategy to counteract the risk of recognition in an immune host, with the presumably important participation of BNLF2a.

3.2 BCRF1, the viral homologue of cellular IL-10

Considering the functions ascribed to IL-10, it can be rated as immune dampening, but also as a pro-viral factor. Indeed, several viruses have included a variant of the IL-10 gene in their genomes. So far, orthologues have been found in Epstein Barr virus (EBV), equine herpes virus type 2 (EHV2), poxvirus Orf, and human cytomegalovirus (hCMV) (Hsu et al.,

1990; Moore et al., 1990; Vieira et al., 1991; Rode et al., 1993; Fleming et al., 1997; Kotenko et al., 2000). The EBV variant of IL-10 is encoded in the BCRF1 open reading frame and shows 84% homology to human IL-10 on the protein level, with most of the differences located in the N-terminal 20 amino acids. Additionally, a single amino acid exchange at position 87 was identified and crystal structures revealed this amino acid to be decisive for folding and dimerization, which is essential for receptor binding. Compared to human IL-10, this modification results in a drastically reduced affinity of viral IL-10 (vIL-10) to the IL-10 receptor (Liu et al., 1997; Ding et al., 2000; Yoon et al., 2005).

Assumingly, the viral IL-10 derivative still supports proliferation of B cells and decreases antigen presentation, but does not activate T cells (MacNeil et al., 1990; de Waal Malefyt et al., 1991b; Rousset et al., 1992b; Suzuki et al., 1995). This evolutionary adaption renders vIL-10 even more favorable for the virus' purposes and its value is reflected in its high conservation (Kanai et al., 2007). Moreover, previous work points to a specific contribution of vIL-10 to EBV's immune evasion strategy (Zeidler et al., 1997).

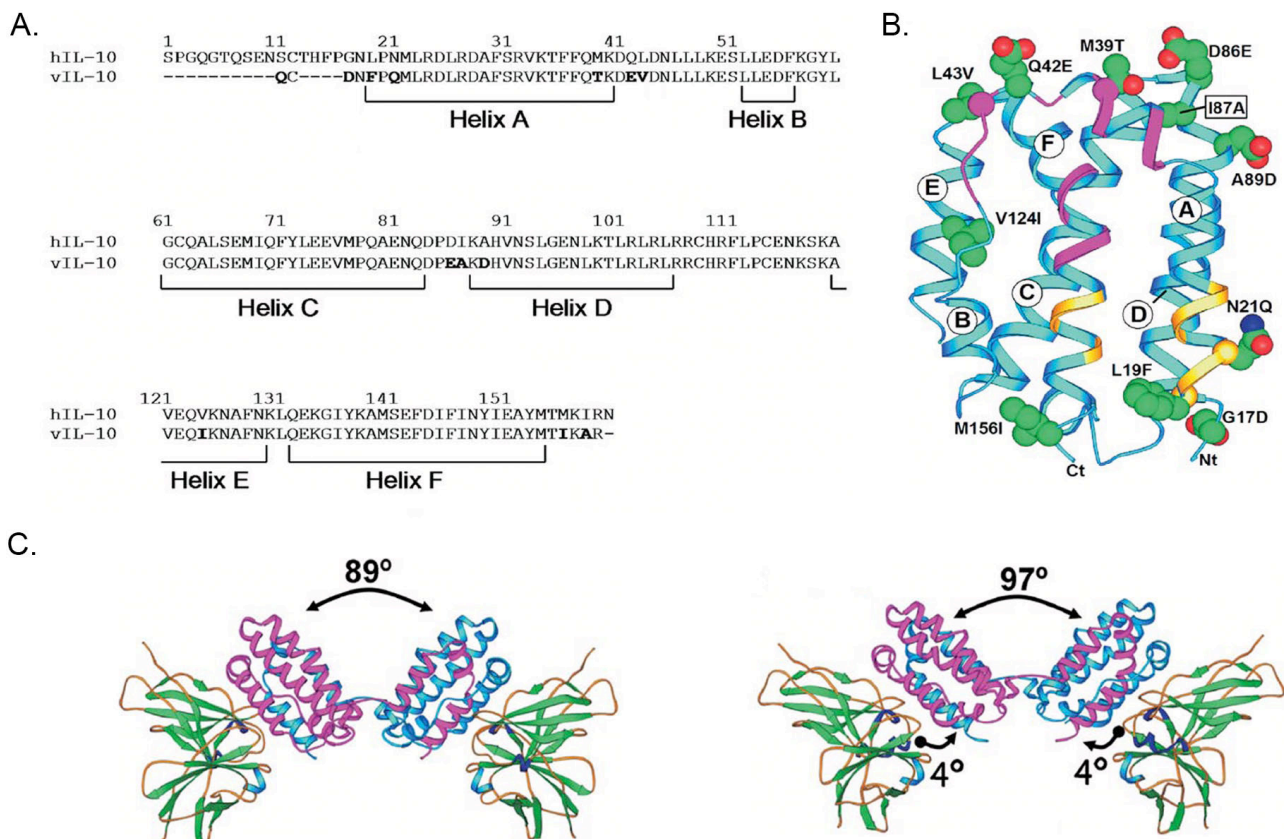


Figure 1.4: vIL-10 and h-IL-10 show strong amino acid homology, but bind differently to the IL-10R1. A. Amino acid sequence alignment, differences are shown in bold letters, helix forming stretches are indicated. B. Ribbon diagram of a vIL-10 monomer, helices and changed amino acids are indicated (compare to A), box: the change of isoleucine 87 to alanine is responsible for different angles in C. C. Interdomain angles in vIL-10 (left) and hIL-10 (right) dimers and their orientation upon binding to the soluble IL-10 receptor 1 chain. Adapted from Yoon et al., 2005.

4. Immune responses to EBV: immune control and fatal failure

4.1 Containment of EBV infection in immunocompetent hosts

Virus-infected cells are usually recognized and eliminated by CD8⁺ T cells and NK cells that represent the effectors of the anti-viral compartment of the immune system. CD4⁺ T cells contribute to the elimination by provision of secondary signals that are essential for CD8⁺ cytotoxicity. EBV infection is usually asymptomatic during early childhood, but primary infection in adolescents or adults often manifests as infectious mononucleosis (IM) caused by antiviral immune responses. During acute IM, high numbers of T and NK cells as well as infected proliferating B cells are present (Young and Rickinson, 2004). It is their dramatic increase in number that causes the characteristic strong swelling of oropharyngeal lymph nodes. Analyses of the TCR repertoire revealed an oligoclonal character of the T cell population due to the expansion of EBV-specific T cells upon encounter of virus-infected cells (Callan et al., 1996).

The exact contribution of NK cells to EBV control is largely unknown. Tonsillar NK cells can be primed by co-resident dendritic cells *in vitro* to produce Ifn- γ in amounts sufficient to inhibit B cell proliferation (Strowig et al., 2008) and kill EBV infected B cells *in vitro* (Wilson and Morgan, 2002). Moreover, EBV-encoded microRNA miR-BART2-5' has been shown to reduce the expression of MICB, an NK-activating ligand (Nachmani et al., 2009). Of note, T and NK cell-mediated immunity efficiently limits virus spread, mainly by eradication of infected cells that show a transformed phenotype (latency III) or are in the lytic phase. Cells in latency 0 are spared in this process and represent the virus reservoir and their eventual reactivation ensures the life-long persistence of the infection in the host.

4.2 EBV causes proliferative disorders and cancer

EBV has also been aetiologically linked to several malignant diseases, including Burkitt lymphoma (BL), Hodgkin Lymphoma (HL) and post-transplant lymphoproliferative disorder (PTLD). Whereas BL and HL are associated with EBV infection but arise due to secondary events (such as *c-MYC* translocation in BL), PTLD exclusively occurs in immunocompromised individuals (Gottschalk et al., 2005b). More than 90% of all PTLDs occur due to missing immune surveillance of EBV infected B cells (Snow and Martinez, 2007). In contrast to the prevalent state of latency 0 in B cells of healthy individuals, the immunological imbalance in PTLD permits for the continuous growth of B cells with a latency III expression pattern, which expand in these individuals and thus display a similar phenotype as LCLs *in vitro*. Three different conditions predominantly foster the development

of PTLDs: (i) EBV-positive solid organ recipients when their own EBV infected B cells reactivate after transplantation, (ii) EBV-negative recipients are transplanted with an organ from an EBV-positive donor containing EBV-infected B cells, and (iii) bone marrow transplants from EBV-positive donors with a high percentage of EBV infected B cells that cannot be controlled under immunosuppression. Standard treatment of acute PTLD includes the reduction of immunosuppression and the use of anti-CD20 antibodies that target B cells (Meijer and Cornelissen, 2008). Clinical trials with the adoptive transfer of autologous or HLA-matched EBV-specific T cell clones show a certain success of treatment in patients, but problems with preparation of cells in sufficient amounts in the given time are difficult to overcome (Papadopoulos et al., 1994; Rooney et al., 1998; Gottschalk et al., 2005a; Moosmann et al., 2010). Vaccination would provide the most adequate solution to reduce the risk of EBV-associated diseases, as immune hosts would eliminate infected cells before the virus could establish a latent infection. Promising results were obtained in our group with an attenuated vaccine of replication-incompetent EBV-like particles that induced immunity in humanized mice (Ruiss et al., 2011).

5. Experimental strategies to unravel processes of EBV infection

5.1 EBV-specific T cell clones as experimental tool

EBV-specific T cell clones can be raised from PBMCs of EBV-positive donors by specific stimulation over several weeks (Bollard et al., 2008; Moosmann et al., 2010). Besides their intended use in therapy, they are also of great use in basic EBV research. T cells are highly sensitive tools to detect EBV infection of B cells and allow for the characterization of epitope presentation patterns during the different phases of infection. To this end, infected B cells of matching HLA are incubated with clonal CD8⁺ T cells of known epitope specificity for several hours. Shedding of Ifn- γ correlates with CD8⁺ T cell activation and indicates antigen recognition. Ifn- γ levels in the supernatant can be assessed by ELISA and allow to deduce whether B cells presented the cognate T cell epitope and thus expressed the viral protein. This approach requires only a few cells and is far more sensitive than protein detection by Western immunoblotting, for instance. The combination of this immunological assay with genetically modified recombinant EBV can furthermore provide information on the physiological impact of defined viral factors with regards to viral immune escape abilities, for example (see next chapter).

5.2 Genetically modified recombinant EBVs and their potential to unravel viral strategies

The functions of BNLF2a and vIL-10 were identified in studies that expressed the proteins ectopically or in assays that used high doses of exogenous vIL-10 (Zeidler et al., 1997; Hislop et al., 2007). These results were sufficient to support the conclusions but did not measure the precise contribution of either BNLF2a or vIL-10 in the context of a virally infected cell.

Loss-of-function situations are usually more specific and thus appropriate to unravel the physiological impact of proteins. This strategy has become available for EBV since Hammerschmidt and colleagues generated a recombinant EBV genome and established an inducible virus producer cell line (Delecluse et al., 1998). In brief, the complete EBV genome of the laboratory strain B95.8 was engineered onto an F-factor plasmid to yield a so-called bacterial artificial chromosome (BAC). A hygromycin resistance gene and an eGFP expression cassette were included, both constitutively expressed from heterologous promoters. The successful transduction of the BAC could thus be visualized by GFP fluorescence and stable clones could be selected. Out of several cell lines tested, HEK293 cells were found to be permissive for virus production when transfected with an expression plasmid encoding the viral transcription factor BZLF1, both sufficient and essential for the induction of EBV's lytic cycle. This seminal work enabled detailed studies on distinct features of single genes of EBV. The technology also allowed for the generation of the first EBV packaging cell line. The deletion of the terminal repeats (TR) that serve as genome-packaging signals during virus egress provided a helper genome that cannot be encapsidated. Producer cells carrying these genomes exclusively give rise to genome-free virus like particles (TR⁻ VLP) upon induction of the viral lytic phase (Delecluse et al., 1999). These particles served as vehicles for EBV-based gene vectors (Hettich et al., 2006), and have demonstrated their potential as vaccine candidates recently (Ruiss et al., 2011).

A new strategy for BAC modifications through induced recombination sustainably facilitated the generation of new EBV variants (Warming et al., 2005). The approach enables straightforward gene replacement as well as traceless mutagenesis of single nucleotides in the context of the BAC of 180kb in size. I made use of this strategy, which is described in detail in the 'Material and Methods' section.

The option to apply reverse genetics to this recombinant EBV genome has already contributed many details to the understanding of very different viral mechanisms. The facilitated and efficient method of BAC engineering will give rise to many other studies in the near future.

6. Aim of this study

Given an infection rate of more than 90% of the worldwide population, Epstein Barr virus can be considered an extremely successful virus. This success is largely owed to EBV's ability to persist in latently infected cells that are not recognized by the host's immune system. Primary infection, however, is characterized by an initial lytic phase that promotes the successful infection of quiescent B cells and the establishment of latency (Kalla et al., 2010). This phase is characterized by the transcription of many different viral genes and concomitant antigen presentation, resulting in an increased probability for infected cells to be eliminated by immune effectors. Several sophisticated strategies to evade the immune response of the host have been associated with distinct gene functions of EBV (Ressing et al., 2008), but knowledge on their impact during the early lytic phase is still missing.

In the early lytic phase of EBV infection the viral transactivators BZLF1 and BRLF1 are expressed which presumably induce the subsequent expression of additional viral genes. The initial trigger for the expression of both BZLF1 and BRLF1 is enigmatic and needs to be determined.

This study intends to expand the understanding of events during the first few days of infection and their contribution to the successful establishment of the virus in infected B cells. To this end, this work is divided into two parts:

1. Analysis of active immune evasion by EBV during the first days of infection with focus on BCRF1 and BNLF2a

Previous work done by our group and others indicated that *BCRF1*, encoding the viral IL-10 homologue (vIL-10), and *BNLF2a*, an immune evasin unique to EBV, account for a reduced antigen presentation by interference with MHC I loading (Zeidler et al., 1997; Hislop et al., 2007). A general decrease of MHC I surface levels on EBV infected cells has been described and overexpression experiments have suggested that both factors contribute to this effect. In this work, I addressed the physiological roles of *BCRF1* and *BNLF2a* expression by generating recombinant EBV deletion mutants. I assessed the responses of EBV-specific CD8⁺ T cell clones and NK/NKT cells to B cells infected with these mutants to investigate the impact of vIL-10 and BNLF2a on specific cellular immunity. It is not exactly known to which extent vIL-10 reflects the capacities of cellular IL-10 to modulate the expression of other cytokines. I investigated the influence of *BCRF1*/vIL-10 deficiency on cytokine responses of PBMCs to infected B cells and

also analyzed BNLF2a effects in this regard. Finally, the importance of *BCRF1* and *BNLF2a* expression for the success of virus infection in presence of immune effectors was evaluated in regression assays.

2. Investigation on RNA transfer by EBV virions and their role as a trigger of initial events in EBV infection

In the last few years, it became evident that several members of the Herpes virus family incorporate RNA into their virions in addition to their DNA genomes (Bresnahan and Shenk, 2000; Sciortino et al., 2001; Bechtel et al., 2005). During infection, RNAs are transferred to target cells and immediately translated. The contribution of these RNAs for the success of infection is still unclear. So far, RNA transfer has not been reported for EBV but could present a plausible explanation for the lytic program following infection. I intended to assess the presence of RNA in EBV particles and their putative transfer during infection. I evaluated the function of selected transcripts during early infection with the help of recombinant EBV mutants. The importance of immediate transcript presence with regards to the success of an infection was analyzed by the impact of virion RNA on viral transformation rates.

RESULTS I

- The contribution of BCRF1 and BNLF2a to the immune evasion of EBV -

1. Generation of *BCRF1*- and *BNLF2a*-deficient EBV

The contribution of BCRF1 and BNLF2a to the immune evasion of EBV was analyzed in a straightforward approach by generating viruses that are deficient for one or both of these two genes. The seminal work of Hammerschmidt and colleagues made reverse genetics available for EBV. They succeeded in cloning a recombinant EBV genome (p2089) in *E.coli* as a bacterial artificial chromosome (BAC), termed ‘maxi EBV’, and established the means to reconstitute infectious virus in HEK293 producer cells (Delecluse et al., 1998). Viruses based on the cloned EBV genome p2089 carry the genome of the B95.8 EBV strain together with the phenotypic markers of hygromycin resistance and GFP fluorescence. The availability of the viral genome as a BAC enables modifications by standard molecular cloning procedures.

1.1 Selection of appropriate knock-out strategies

To generate *BCRF1*-deficient EBV, I replaced the *BCRF1* open reading frame (ORF) in the recombinant wildtype EBV genome (p2089) with a prokaryotic kanamycin resistance expression cassette. This strategy seemed appropriate, because *BCRF1* does not overlap with other genes or cis-acting elements, which renders off-target effects unlikely (figure 2.1).

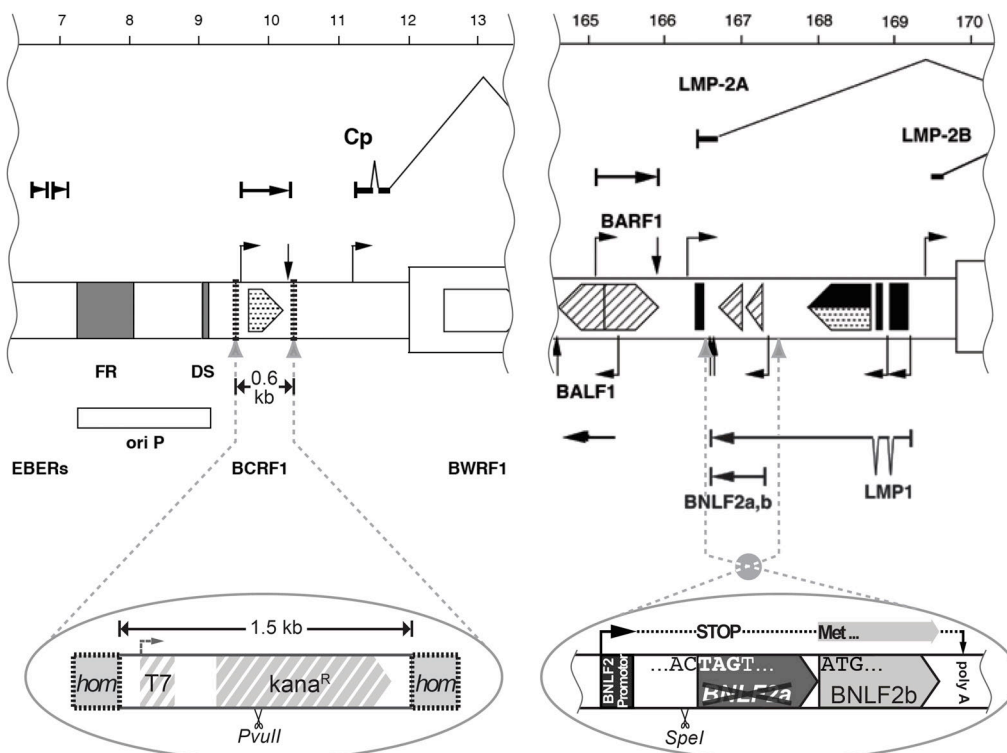


Figure 2.1: Insertional mutagenesis or single nucleotide exchange was the knock out strategy of choice, depending on the genomic situation. The *BCRF1* gene in the recombinant wildtype EBV-BAC (p2089) was replaced by a prokaryotic expression cassette for kanamycin resistance by homologous recombination. By traceless mutagenesis of 5 nucleotides, the Methionine1-codon of *BNLF2a* was replaced by a STOP-Codon and an additional *SpeI* site was introduced (see Materials and Methods for details). Numbers indicate the genetic position in kbp in the recombinant EBV genome (p2089).

The more complex genomic situation of *BNLF2a* necessitated a different cloning strategy, as the gene shares the transcript with *BNLF2b* and is situated in the first intron of *LMP2A*. Moreover, the area contains the 3' untranslated region of *BNLF1* encoding the latent membrane protein 1 (LMP1). Hence, the first codon of *BNLF2a* was mutated to a STOP-codon in combination with the insertion of an additional SpeI site for diagnostic purposes. This minimal invasive exchange of four nucleotides only reduced the risk of unintended and adverse interference with expression or regulation of neighboring genes (Figure 1B).

Three EBV mutants were constructed. Two single mutants were null for *BCRF1* and *BNLF2a* and one double mutant combined both disabled alleles. Table 2.1 lists the used maxi EBVs and their genotypes.

Table 2.1: Genotypes of used recombinant EBVs.

Explicit name in this study	Genotype	clone # (AGV database)
recombinant wildtype (rec.wt.)	B95.8 genome (Baer et al., 1984) on an F-factor BAC, contains CMV promoter-driven expression cassettes for hygromycin resistance and GFP (Delecluse et al., 1998)	p2089
$\Delta BCRF1$	derived from p2089, a prokaryotic kanamycin resistance expression cassette (1.5kb) replaces the <i>BCRF1</i> ORF (nt 9670-10200 in p2089)	p3912
$\Delta BNLF2a$	derived from p2089, mutation of 5'-AGATGG-3' to 5'-ACTAGT-3' (negative strand, nt 177322-177317 in p2089) results in a functional <i>BNLF2a</i> knock-out	p4030
double knock-out (double k.o.)	derived from p4030, combines both $\Delta BCRF1$ and $\Delta BNLF2a$	p4031

1.2 Confirmation of genetic mutations and virus titrations

I established virus producers from stably transfected HEK293 cells by selecting for hygromycin resistant single cell clones and testing for virus production-permissive cells. The genotypes were confirmed by Southern blot hybridization (figure 2.2A) and the titers of infectious virus in the supernatants were calculated from the percentage of GFP-positive Raji cells after infection, denoted as “green Raji units” (GRU). In subsequent steps of “back-titrations”, I repeatedly performed these infection experiments to precisely adjust the calculated titers of the different recombinant viruses (figure 2.2B, see also Material and Methods). Infected B cells were routinely genotyped by PCR to confirm infection with the correct virus mutant (figure 2C), including a virus strain-specific multiplex PCR to exclude contamination with the B95.8 laboratory strain or EBV field strain-infected B cells from EBV-positive blood donors.

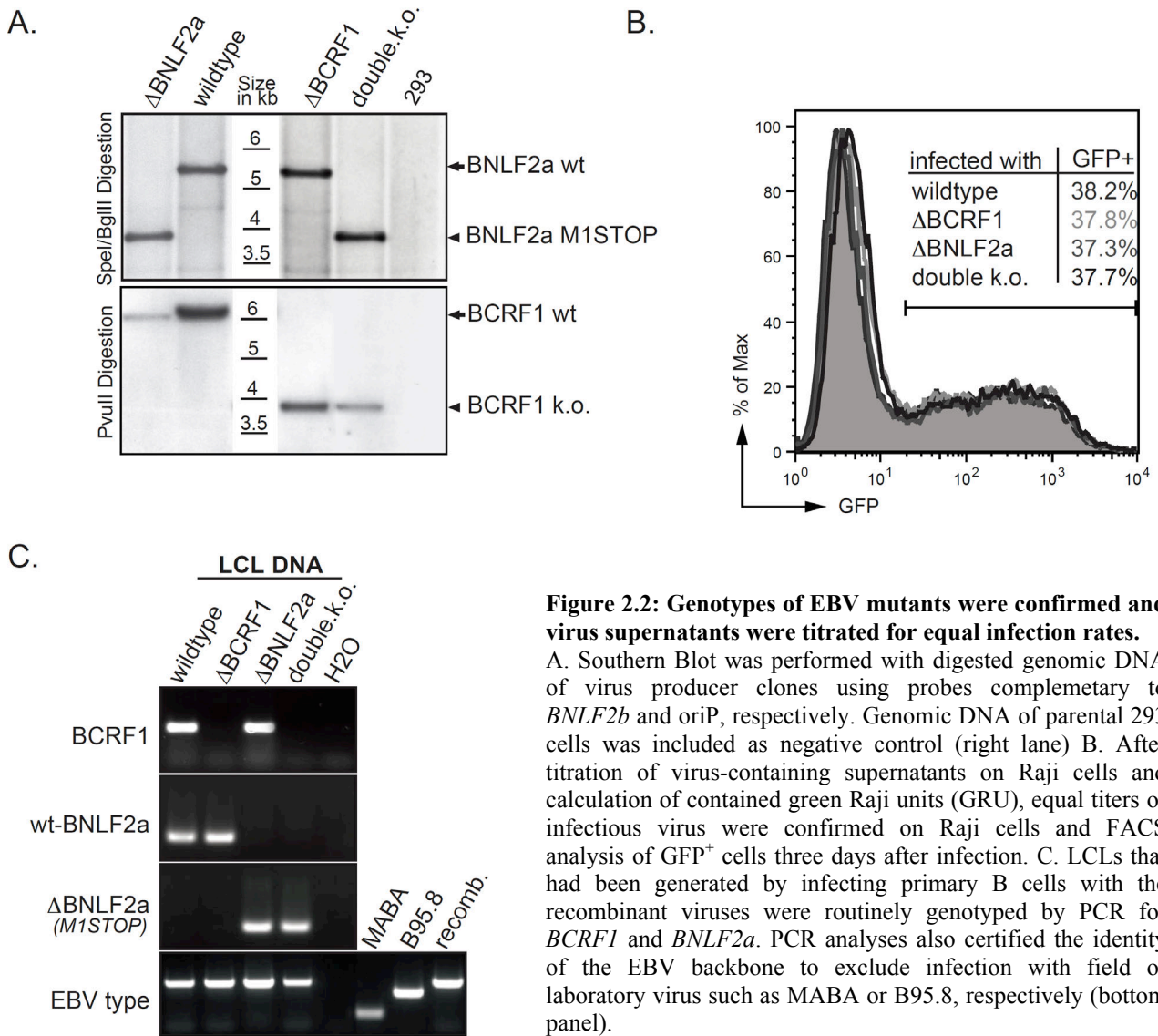


Figure 2.2: Genotypes of EBV mutants were confirmed and virus supernatants were titrated for equal infection rates.

A. Southern Blot was performed with digested genomic DNA of virus producer clones using probes complementary to *BNLF2b* and oriP, respectively. Genomic DNA of parental 293 cells was included as negative control (right lane) B. After titration of virus-containing supernatants on Raji cells and calculation of contained green Raji units (GRU), equal titers of infectious virus were confirmed on Raji cells and FACS analysis of GFP⁺ cells three days after infection. C. LCLs that had been generated by infecting primary B cells with the recombinant viruses were routinely genotyped by PCR for *BCRF1* and *BNLF2a*. PCR analyses also certified the identity of the EBV backbone to exclude infection with field or laboratory virus such as MABA or B95.8, respectively (bottom panel).

2. Phenotypes of *BCRF1*- and *BNLF2a*-mutant EBV

2.1 Expression analyses of BCRF1 and BNLF2a and their influence on TAP levels

BCRF1 expression becomes detectable as early as a few hours after infection of B cells (Miyazaki et al., 1993). This finding has been interpreted in a way that BCRF1 acts prior to the cellular expression of human IL-10, which is induced later on in EBV infected B cells. Strong expression of BNLF2a was observed in lytic cells and was described to be directly driven by BZLF1 (Yuan et al., 2006; Bergbauer et al., 2010). An initial lytic phase was observed during the first few days after infection (Kalla et al., 2010), which might also include expression of BNLF2a to prevent the early recognition of virus infected cells.

It was of principal interest to evaluate the kinetics of BCRF1 and BNLF2a expression, specifically with regards to the timing of immunological assays. Additionally, I intended to verify the antagonistic effect of vIL-10 (encoded by *BCRF1*) on TAP2 transcript levels that had been causally linked to decreased MHC-I levels (Zeidler et al., 1997).

To this end, I analyzed the transcript levels of BNLF2a, BCRF1, hIL-10, TAP1 and TAP2 in primary B cells at different time points post infection. Primary B cells were infected with a multiplicity of infection (MoI) of 0.1 GRU per B cell, uninfected cells were included as controls. I observed BNLF2a expression already two hours post infection (hpi). The transcript

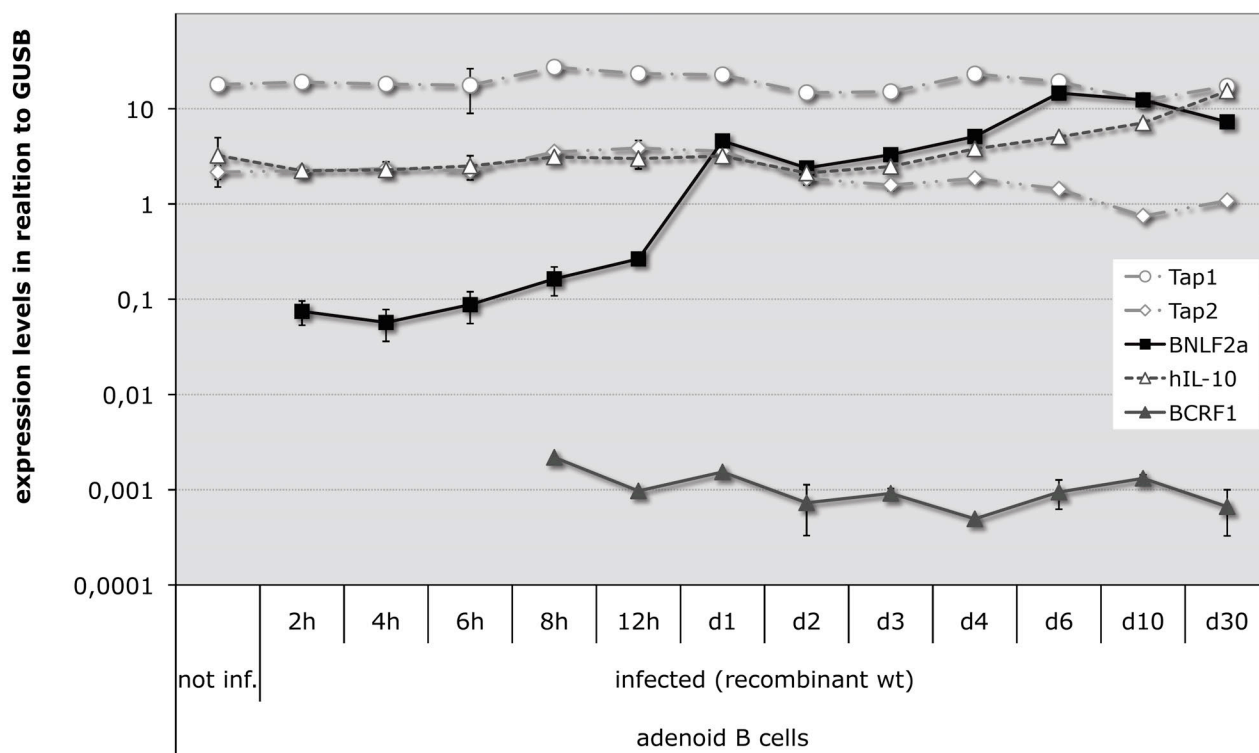


Figure 2.3: Following infection, BNLF2a and BCRF1 transcripts are present early and expression is maintained throughout infection. Quantitative PCR (qPCR) analyses were performed on cDNA from adenoid B cells that had been infected with recombinant wildtype EBV (2089) at an MoI of 0.1 GRU/cell. Uninfected adenoid B cells were included as negative control. Transcript levels were related to expression levels of glucuronidase beta (GUSB) that served as housekeeping gene.

level stayed stable until an induction of expression occurred at 8 hpi and reached a level that was approximately maintained during the period of analysis (30 days) (figure 2.3, squares). The two-tiered characteristics in combination with the immediate presence of stable levels as early as 2 hpi came as a surprise, and are the topic of investigation in the section “Results II”.

BCRF1 expression was not detectable until around 6hpi (figure 2.3, filled triangles), confirming the semi-quantitative data on BCRF1 expression (Miyazaki et al., 1993). However contrasting that publication, the present analysis also shows constantly high levels of cellular IL-10 expression in uninfected B cells prepared from adenoids (Figure 2.3, empty triangles). This observation was confirmed with EBV-infected peripheral B cells (not shown).

BCRF1 expression did not affect TAP2 transcript levels and thus did not contribute to a detectable extent to the postulated antagonistic effects of IL-10 on TAP2 transcripts (Zeidler et al., 1997). But my analysis could confirm the general inverse correlation of TAP2 and IL-10 transcript levels, as raising hIL-10 expression starting 3 days post infection (dpi) was accompanied by a decrease of TAP2 expression (figure 2.3, triangles and rhombuses), but TAP1 expression remained unaffected (circles). In general, the observed physiological impact of both forms of IL-10 did not reflect observations from a study with exogenously administered IL-10 (Zeidler et al., 1997).

2.2 MHC surface levels of cells infected with BCRF1- and BNLF2a-deficient virus mutants

Both vIL-10 and BNLF2a reduce MHC I surface levels (Zeidler et al., 1997; Hislop et al., 2007). B cells show high surface levels of MHC I and, due to their function as professional antigen presenting cells (APC), also carry MHC II on their surface.

I analyzed B cells that had been infected with recombinant wildtype, $\Delta BCRF1$, $\Delta BNLF2a$, or double k.o. EBV for MHC surface levels by FACS analysis one, three, six and nine dpi. Primary B cells showed a dramatic increase of MHC I levels at day 3 post infection. Data in figure 2.4A indicate that MHC I surface levels are not affected by physiological expression of BCRF1 and BNLF2a or that differences are too weak to be resolved by FACS analysis.

The analysis of MHC II levels revealed slightly increased surface levels in cells infected with *BCRF1*-deficient EBVs (figure 2.4B). Despite the general low BCRF1 transcript abundance (figure 2.3), expression was obviously sufficient to influence MHC II levels.

IL-10 has already been described to decrease MHC-II levels on macrophages and dendritic cells (de Waal Malefyt et al., 1991b; Steinbrink et al., 1997). Whether the detected minute differences are sufficient to alter CD4+ T cell activation remains to be clarified.

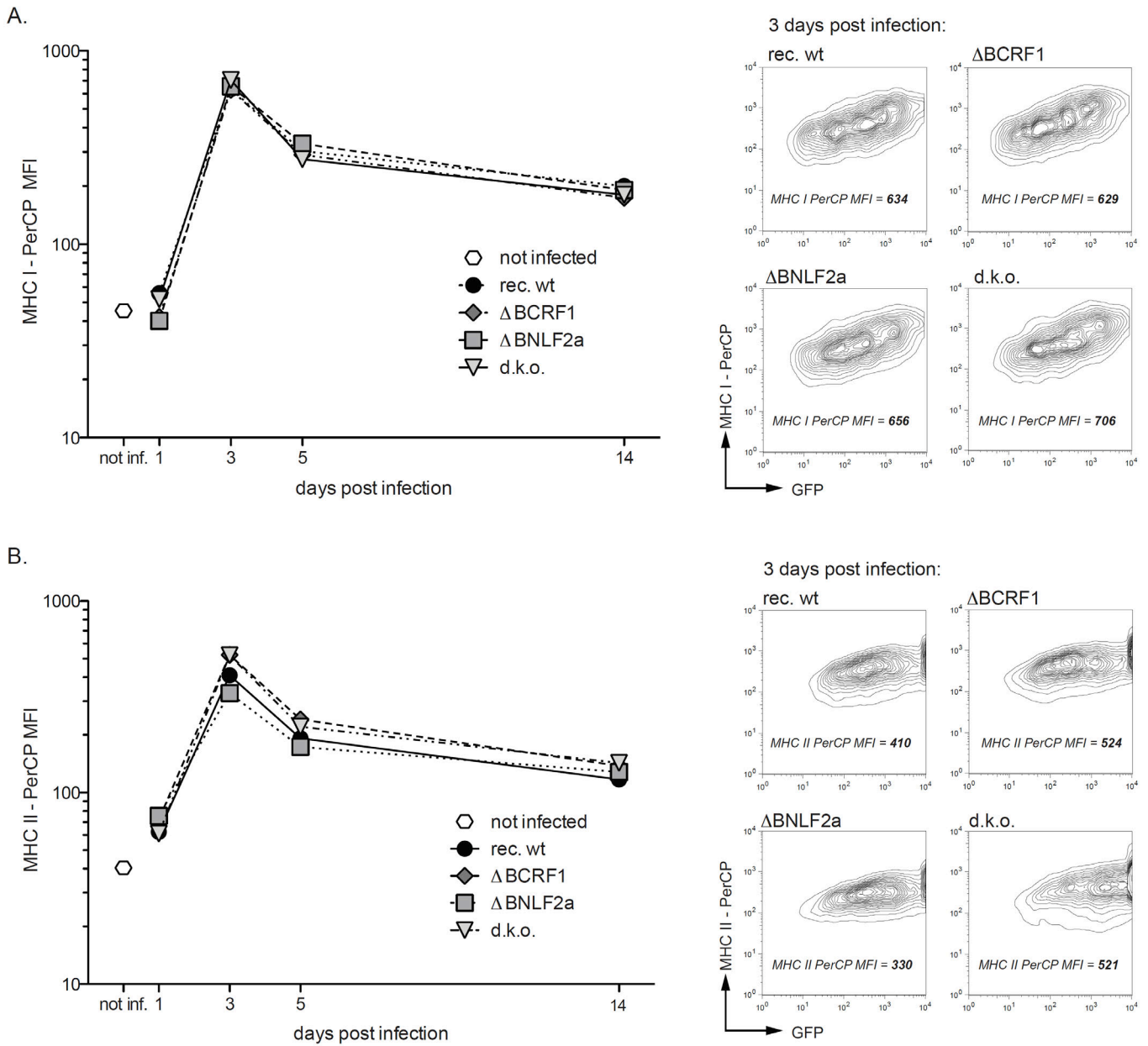


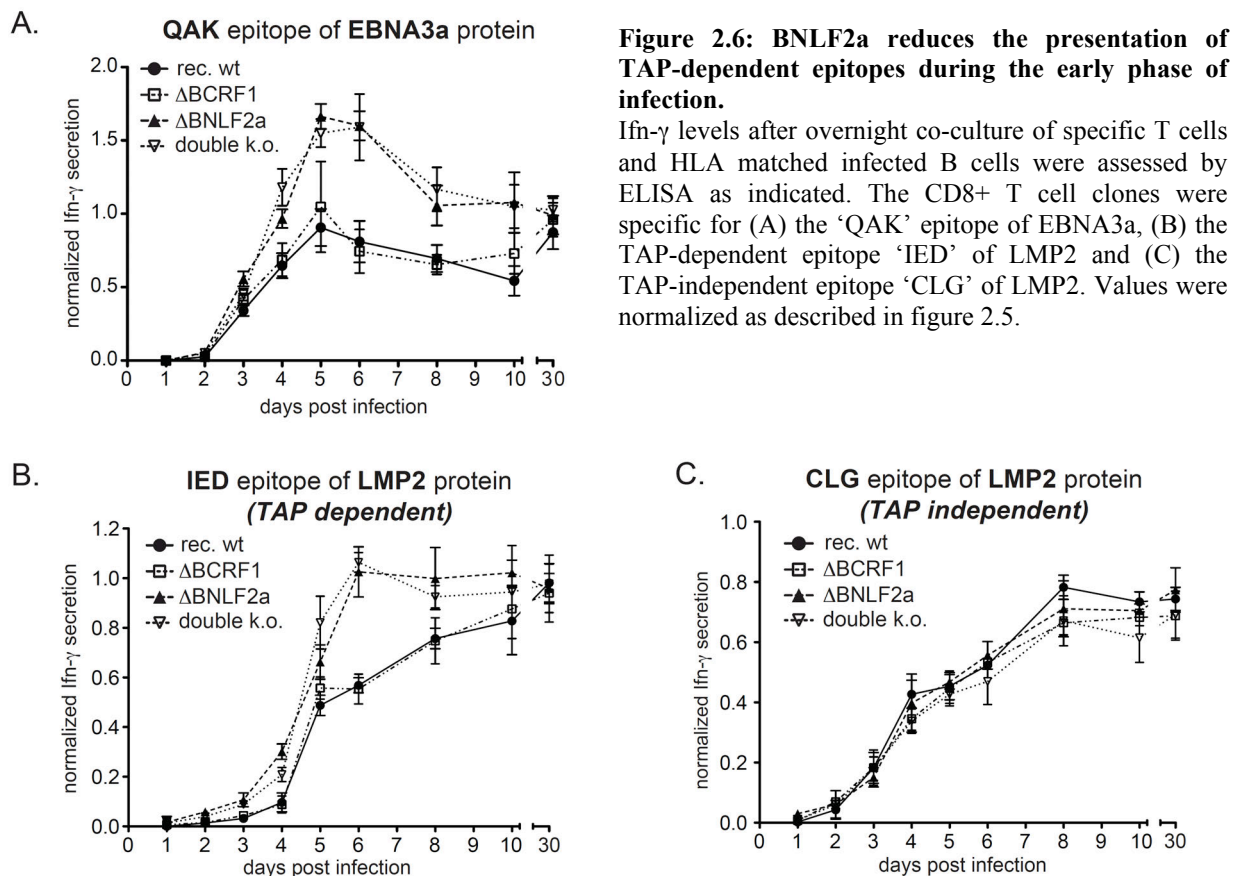
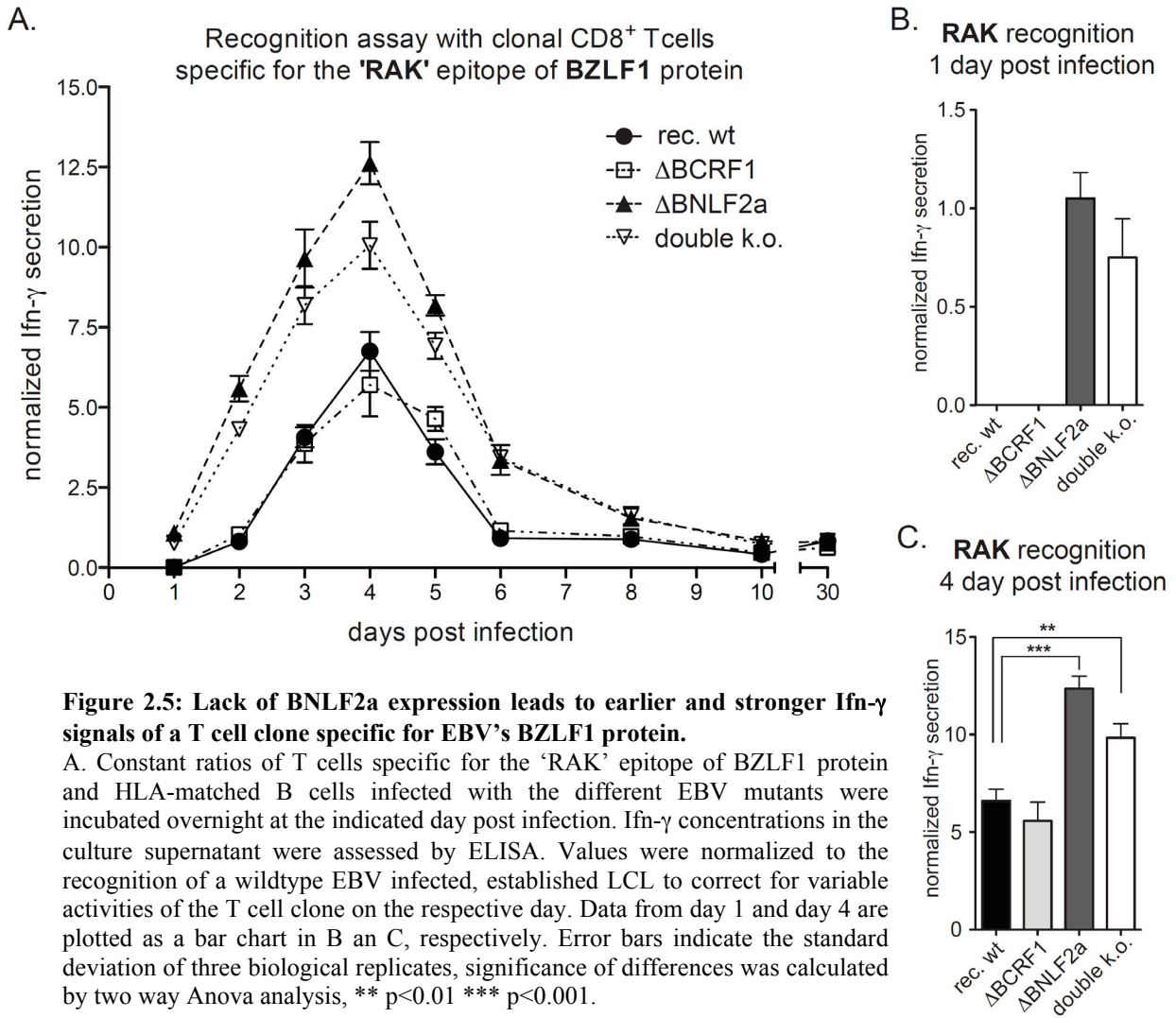
Figure 2.4: MHC surface levels on B cells are not significantly altered upon infection with mutant EBV. Adenoid B cells were infected with different virus constructs and surface levels of MHC I (A) and MHC II (B) were assessed by FACS (independent experiments). Diagrams show mean fluorescence intensities (MFI) of MHC signals at the indicated day after infection. Examples of FACS data at 3dpi are shown on the right.

2.3 EBV-specific CD8⁺ T cell clones recognize BNLF2a-deficient EBV-infected cells significantly better

EBV specific CD8⁺ T cell clones constitute a valuable tool to assess immune evasive capacities of EBV in infected cells. T cell clones are generated by selective enrichment of EBV-specific T cells from PBMCs of EBV-positive donors followed by the subcloning of single T cells. Clonal cells share the same TCR and thus are specific for a single EBV epitope and the associated MHC I allele. Clonality is confirmed in FACS analyses by the use of fluorescent tags that mimic a specific EBV epitope/MHC complex (tetra- and pentameres) that bind to the matching TCR. A homogeneously positive staining indicates unique TCR specificity as hallmark of a clonal T cell population. Upon recognition of a matching epitope, T cells are activated and secrete Ifn- γ , which is quantified in ELISA assays and serves as a measure for T cell activity.

I intended to gain insight into the kinetics of epitope presentation as well as differences between cells infected with recombinant wildtype and mutant EBVs. Therefore, I performed time course experiments on T cell recognition of B cells that had been infected with recombinant wildtype, $\Delta BCRF1$, $\Delta BNLF2a$ or double k.o. viruses. Starting on day one after infection, T cells of defined specificity were co-incubated overnight with HLA-matched, infected B cells in a constant effector/target ratio of 1:2. The supernatants were subsequently assessed for Ifn- γ levels.

A first analysis was performed with T cells specific for the “RAK” epitope of BZLF1 (Bogedain et al., 1995). HLA-matched B cells that were infected with the *BNLF2a*-deficient EBV variants led to a significantly stronger Ifn- γ secretion of the RAK-specific CD8⁺ T cell clone (figure 2.5A). Furthermore, these T cells recognized $\Delta BNLF2a$ -infected B cells already 1dpi, which was not the case with infected cells that could express BNLF2a (figure 2.5B). The difference in RAK recognition peaked at day 4 (figure 2.5C), was detectable during the first ten days of infection, but finally disappeared 30dpi with the establishment of latency.



I obtained comparable results with T cell clones that recognized the epitopes “QAK” (Burrows et al., 1994) and “IED” (Burrows et al., 1994; Lee et al., 1996) native to the EBV-proteins EBNA3a and LMP2, respectively (figure 2.6A and B). These epitopes were recognized later than the “RAK” epitope, indicating different epitope-specific presentation kinetics in this early phase of infection that were also observed in another study (Iskra et al., in preparation). In contrast to all other epitopes tested, the T cell response to the CLG epitope of LMP2 protein (Lee et al., 1993) proved to be independent of BNLF2a effects (figure 2.6C). This epitope is known to be loaded TAP-independently onto MHC I molecules, because its high hydrophobicity enables passive diffusion through the ER membrane (Lautscham et al., 2001). As BNLF2a was found to reduce antigen presentation through impairment of TAP function (Hislop et al., 2007; Horst et al., 2009), the postulated mechanism was confirmed by these results.

I could find that physiologic expression of BNLF2a was sufficient to inhibit epitope loading on MHC I although MHC I surface levels on infected B cells were not altered (figure 2.4A). Cells that were infected with *BNLF2a*-negative virus experienced a stronger and earlier recognition through specific CD8⁺ T cells. These findings were in line with previous reports that described strong inhibitory effects of BNLF2a on TAP-dependent epitope loading to MHC class I (Hislop et al., 2007; Croft et al., 2009; Horst et al., 2009). My results extend the importance of BNLF2a to the early lytic phase of EBV, as effects were observed already during the early days of infection.

Viral IL-10 did not influence the outcome of these targeted T cell recognition experiments: Δ *BCRF1* virus-infected cells were identical to recombinant wildtype virus whereas the double k.o. virus simply reflected the phenotype of Δ *BNLF2a* virus (figures 2.5 and 2.6).

2.4 BCRF1 affects the peripheral cytokine response

The T cell assays described above did not reveal an immunological phenotype of vIL-10. Nevertheless, its conservation during evolution (Kanai et al., 2007) and the strong immune modulatory capacity of its cellular homologue both suggest a beneficial role of vIL-10 in EBV infection.

Human IL-10 plays an important role in the orchestration of cytokine secretion and affects a broad range of immune effector cells (Moore et al., 2001). Because Th1/Th2 cytokines are to some extent indicative for the systemic immune response, I compared their levels in the supernatant of PBMC cultures infected with the different virus mutants. I prepared PBMCs of

an EBV positive donor and infected them at a MoI of 0.1 GRU/B cell. Cells were kept in dense cultures (5×10^6 cells/ml) and aliquots of the supernatants were sampled every three days for multiplex ELISA analysis.

Elevated levels of the Th1 cytokines Ifn- γ , IL-2 and TNF- β were observed in both Δ BCRF1 and double k.o. infected cultures and levels of the Th2 cytokine IL-10 were also found to be increased in these samples. These differences were detectable starting from day 3 after infection and peaked at day 9 (figure 2.7). Similar results were obtained with different donors in independent experiments. My findings indicate that BCRF1 expression early after infection influences the peripheral cytokine release. CD4⁺ T cells usually constitute more than 50% to PBMCs and are the major source of Th1 and Th2 cytokines. Hence, a direct effect of BCRF1 expression and vIL-10 secretion on the cytokine response of CD4⁺ cells seemed likely.

		Ifn-γ	IL-2	IL-6	IL-10	TNF β
not infected	pg/ml	90	33	16	0	11
	rel. to wt (%)	6	67	2	0	33
rec. wt.	pg/ml	1592	49	922	1024	35
	rel. to wt (%)	100	100	100	100	100
delta BCRF1	pg/ml	2071	67	772	1725	69
	rel. to wt (%)	130	136	84	168	197
delta BNL2a	pg/ml	1497	42	1179	1116	26
	rel. to wt (%)	94	86	128	109	75
double k.o.	pg/ml	3191	102	917	1626	111
	rel. to wt (%)	200	208	99	159	315

not altered: IL-1, IL-5, IL-8, TNF α

not detected: IL-4, IL-12

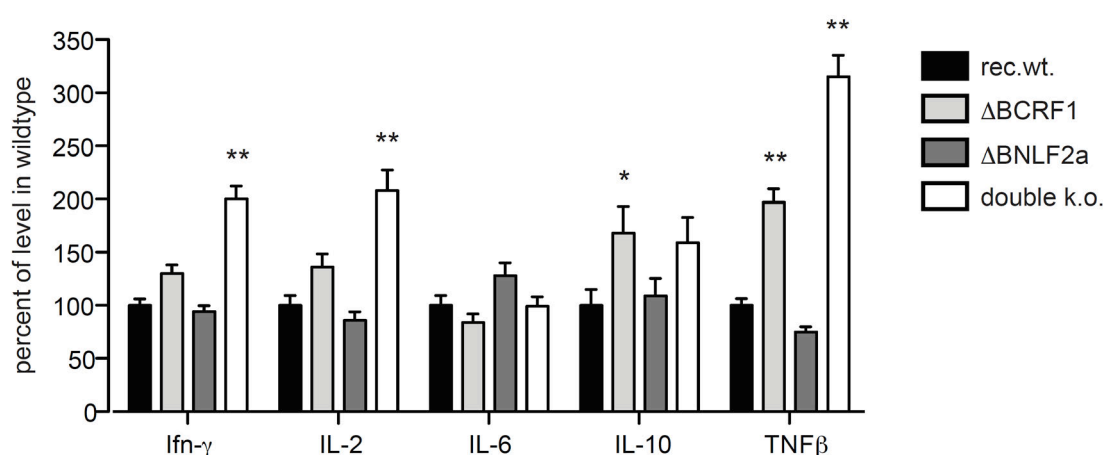


Figure 2.7: Δ BCRF1 infected cultures of PBMCs show elevated levels of cytokines that regulate inflammation.

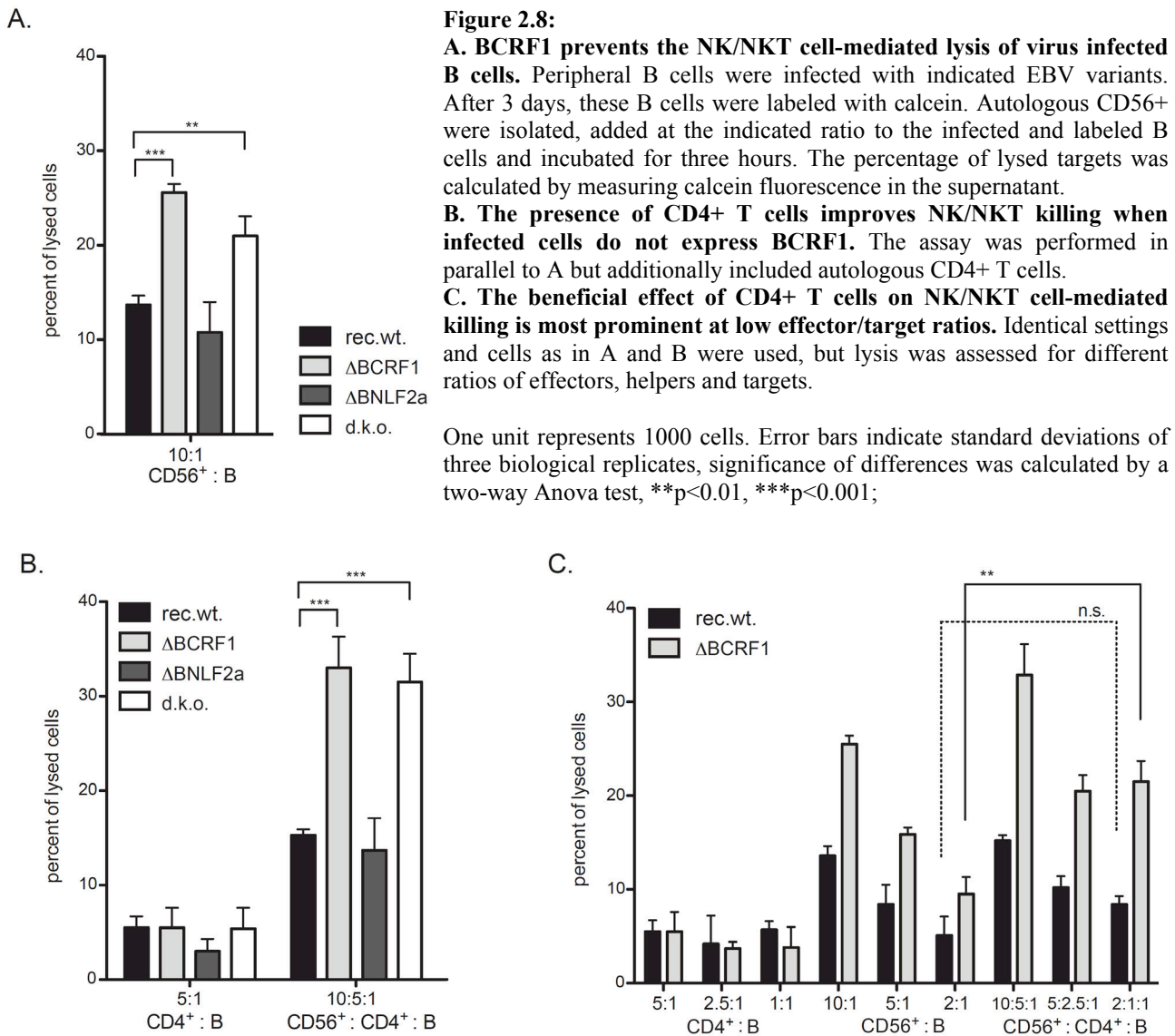
PBMCs were infected with different viruses (MoI = 0.1 GRU/ B cell) and kept in dense culture (5×10^6 cells/ml). On day 9 post infection, supernatants were analyzed by multiplex-ELISA for Th1/Th2 cytokines. Error bars indicate the coefficient of variance of the analyte. Statistical significance of difference to cytokine level in recombinant wildtype samples was calculated by a two-way Anova using the Bonferroni-Post-Test, * $p < 0.05$, ** $p < 0.01$. Percentage of cytokine levels in relation to those in wildtype infected PBMCs are plotted in the bar chart. Results represent one out of five independent experiments (5 different donors) with comparable results.

The loads of the cytokines $\text{Ifn-}\gamma$, IL-2 and TNF- β in double k.o.-infected PBMCs were consistently higher than in cultures infected with ΔBCRF1 EBV. Presumably, the stronger activation of EBV specific CD8⁺ T cells in absence of BNLF2a accounted for this synergistic effect. High hIL-10 concentrations in those cultures that had been infected with ΔBCRF1 EBV suggested a secondary induction of hIL-10 expression as a dampening response to the elevated immune stimulatory signals ($\text{Ifn-}\gamma$, IL-2, TNF β). As IL-10 antagonizes IL-6 expression, the slightly lower levels of IL-6 might have resulted from high hIL-10 concentrations.

2.5 BCRF1 impairs NK cell-mediated killing of EBV infected cells

In vivo, the frequency of EBV-specific CD8⁺ T cells is usually low and reactivation and clonal expansion takes several days. This delay of the adaptive response to viral infections causes a gap in defense, which has to be contained by so-called “first line effectors” of the innate IS (Janeway, 2005). With regards to viral infections, NK and NKT cells represent the most important innate effectors and were shown to be efficient in the killing of EBV-infected cells (Blazar et al., 1980; Pappworth et al., 2007). The early expression of BCRF1 and BNLF2a (figure 2.3) suggested that their gene products influence first line effectors as well. Therefore, I decided to investigate the impact of BNLF2a and BCRF1 expression on NK cell-mediated killing of B cells infected with the different EBV mutants.

For this purpose, B cells were isolated from peripheral blood and infected with the four different viruses. After three days, autologous CD56⁺ cells (*i.e.* NK and NKT cells, about 10-20% of PBMCs) were added and specific lysis of B cells was assessed after 3 hours of co-incubation (for details see “killing assay”, chapter 2.4.5 in section “Materials and Methods”). B cells infected with ΔBCRF1 virus were lysed preferentially. In contrast, only a faint reduction of lysis was observed for B cells infected with the ΔBNLF2a virus. B cells infected with the double-k.o. virus were lysed to an intermediate level which could be interpreted as the net sum of both effects (figure 2.8, mid panel).



2.6 CD4⁺ T cells stimulate NK cell-mediated killing

CD4⁺ T cells represent an important source for many cytokines and their presence could provide a supporting microenvironment for NK/NKT cells. I was interested to see if autologous CD4⁺ T cells would influence effector functions. Therefore, I included them in one set of experiments to assess their contribution to NK cell-mediated killing of EBV-infected cells. Indeed, NK/NKT cells elicited stronger cytotoxic activity in the presence of CD4⁺ T cells (figure 2.8B, right panel). In the samples that were infected with BCRF1-negative EBVs, this difference was markedly strong (30% increase of killing), but absent in B cells infected with recombinant wildtype and Δ BNLF2a virus. Subpopulations of CD4⁺ T cells can show cytotoxic activity (Martorelli et al., 2010), but lysis did not exceed background levels when exclusively CD4⁺ T cells were added in absence of NK/NKT cells (figure 2.8B, left panel).

An even more prominent picture of the beneficial effects of CD4⁺ T cells on NK/NKT cell mediated killing was obtained at lower effector/target ratios, however only when BCRF1 deficient virus was used for infection (figure 2.8C).

Exogenous administration of viral and human IL-10 hardly affected NK/NKT cell-mediated killing at effector/target rates of 10:1 nor did it completely rescue the Δ BCRF1 phenotype (figure 2.9A).

In contrast, exogenous IL-10 abrogated the supportive effects of CD4⁺ T cells on NK/NKT cell-mediated killing. These findings show that CD4⁺ T cells stimulate NK/NKT cell-mediated killing of EBV infected B cells (figure 2.9B). In wildtype EBV infected cells, vIL-10 counteracts CD4⁺ T cell help and prevents NK/NKT-mediated killing.

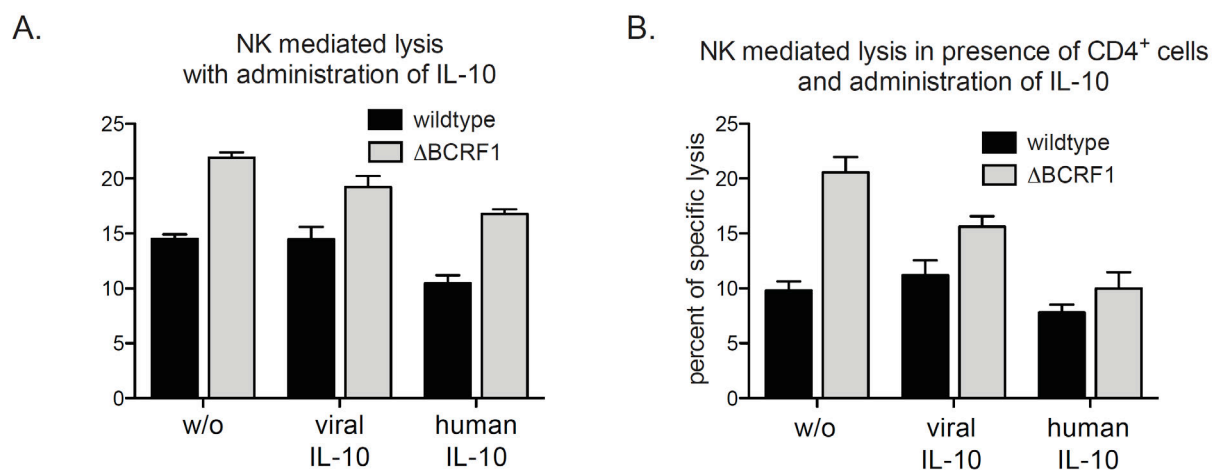


Figure 2.9: NK mediated killing is partly rescued, CD4 effects are fully reverted by exogenous administration of IL-10. Killing assays were performed with an effector:target ratio of 10:1 (A) and CD4⁺ assisted killing assays were performed with an effector:helper:target ratio of 2:1:1 (B). His-tag purified viral or human IL-10 was administered at 1000pg/ml where indicated.

3. Effects on long-term immune control

The previous experiments revealed that BNL2a promotes the escape from the CD8+ T cell response and BCRF1 impairs NK/NKT cell-mediated killing and Th1 cytokine shedding. I could find that both factors are active already during the early days of EBV infection and wondered whether these early effects exert any impact on virus establishment in the presence of immune control.

In vitro, such effects can be assayed in so-called regression assays (Wilson and May, 2001), *i.e.* serial dilutions of EBV-infected PBMCs that are plated in statistically sufficient number of replicates and cultured for six weeks. During this time, infected B cells are either eliminated in case of sufficient numbers of effectors (dense cultures), grow out because the numbers of effectors are too low (medium dense cultures) or simply do not grow because the initial numbers of B cells are too low to support proliferation of EBV infected B cells at all (low density cultures). The number of wells with proliferating cells correlates with initial numbers of cells per well. This correlation follows a Gaussian distribution (figure 2.10A). A prerequisite for regression assays are both identical virus titers and identical transformation capacities of the viruses allowing for comparison of the results obtained with different viruses. Limiting dilutions of virus stocks revealed that the viruses used in this study showed similar characteristics of growth transformation of B cells (figure 2.10B).

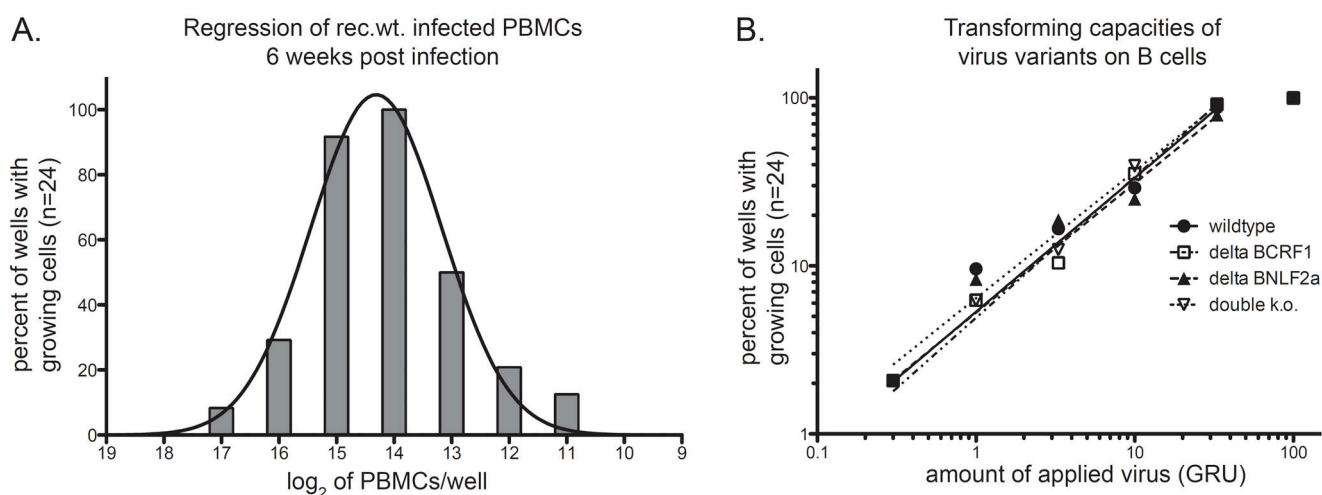


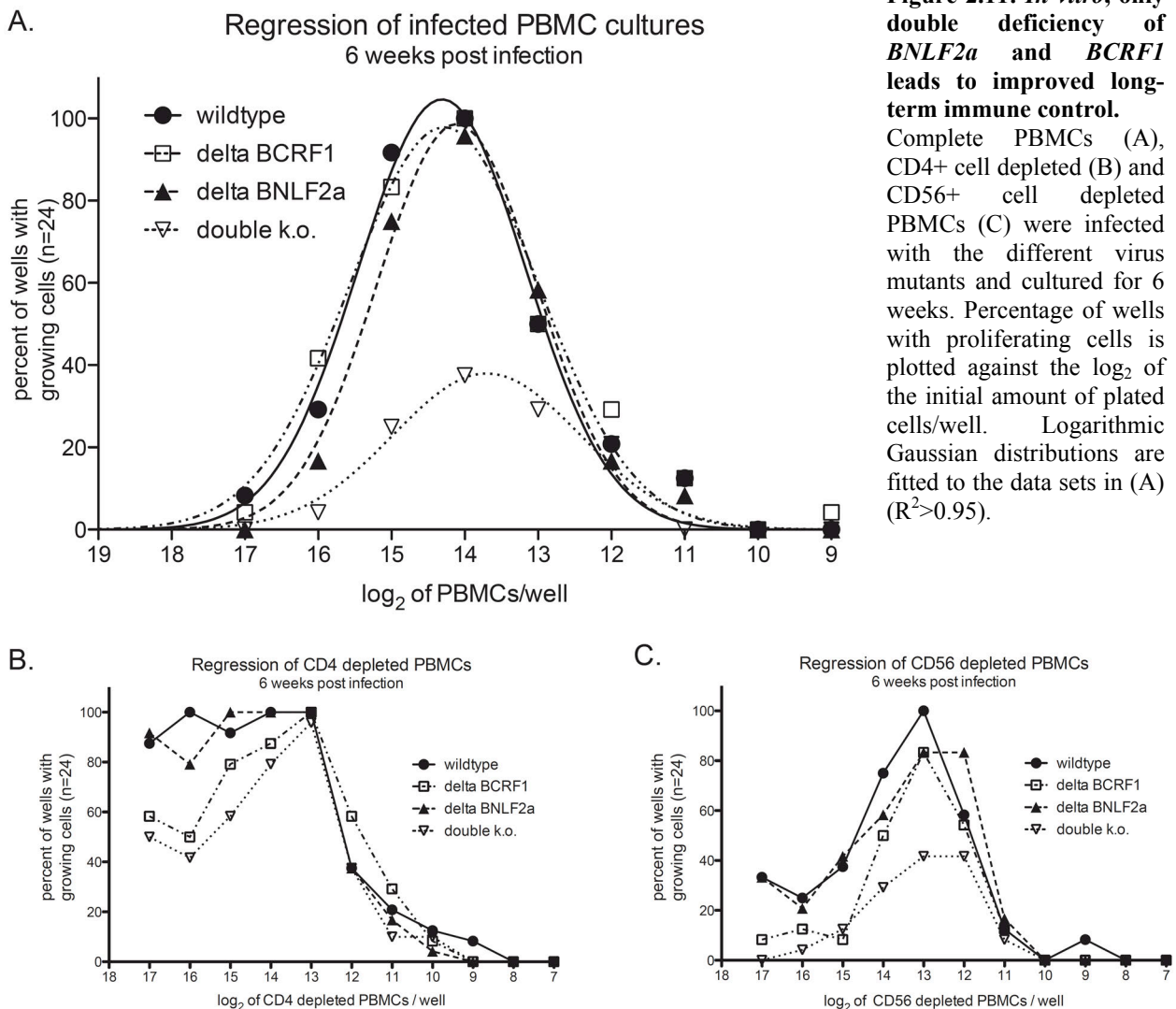
Figure 2.10:

A. Regression assays follow a Gaussian distribution. PBMCs of a seropositive donor were EBV infected and plated at serial dilutions with 24 replicates. After 6 weeks of culture, the number of wells with proliferating cells was assessed, following a bell-shaped distribution. Solid line: approximated logarithmic Gaussian distribution.

B. Limiting dilution of the viruses showed comparable transformation characteristics. After overnight infection with indicated dilutions of the virus stocks, primary B cells were seeded on 96-well flat bottom plates with 1×10^5 cells/well and 48 replicates per virus dilution. After six weeks of culture, the number of wells with proliferating cells was assessed and plotted against the number of green Raji units (GRU) per well.

The results of the regression assays demonstrated that only the growth of B-cells infected with double k.o. virus was significantly impaired, whereas $\Delta BCRF1$ - and $\Delta BNL2a$ - infected cells escaped from immune control as efficiently as wildtype virus (figure 2.11A).

Subsequent analyses with PBMCs that had been depleted of CD4+ cells indicated that T cell help is critical for efficient immune control (figure 2.11B), as expected (Janssen et al., 2003; Shedlock and Shen, 2003; Janeway, 2005). I observed a weak impairment of growth in samples with $\Delta BCRF1$ - and double k.o.-infected B cells in the CD4 depleted assay, presumably reflecting increased NK/NKT cell-mediated killing in case of BCRF1-deficiency (see chapter 2.5). Depletion of CD56+ cells from PBMCs affected the outcome of the regression assays only to a minor extent. Again, $\Delta BCRF1$ and double k.o. infections resulted in slightly impaired outgrowth, but here CD4+ T cell activity was presumably increased and resulted in a stronger immune response. This might reflect a consequence of stronger Th1 activity in case of BCRF1-deficiency (figure 2.11C). However, the effects on CD56+ and CD4+ cells are weak and thus are not detected in regression assays with complete PBMCs (compare figure 2.11A).



RESULTS II

- Packaged virion RNAs trigger initial events in EBV infection -

1. The origin of early transcripts in EBV-infected B cells

It has been described previously that EBV transcripts are detectable in infected B cells very early after infection and drive the initial lytic phase (Cheung et al., 1993; Miyazaki et al., 1993; Kalla et al., 2010). The expression analysis performed in the first part of this work revealed the presence of BNL2a transcripts in infected B cells as soon as 2 hpi (figure 2.3). Initially, the transcript levels of BNL2a stayed constant for six to eight hours and increased subsequently.

Interestingly, certain Herpes viruses incorporate RNA into their virions, among them the closely EBV related Kaposi sarcoma Herpes virus (KSHV) (Bresnahan and Shenk, 2000; Sciortino et al., 2001; Bechtel et al., 2005). I wondered if EBV virions also contain packaged RNAs and if they drive detectable functions in the target cell immediately after infection.

1.1 Several EBV transcripts are present in B cells immediately upon infection

I wanted to address the question whether transcripts other than BNL2a were also present in B cells early after infection. In order to cover transcripts from different functional subfamilies, I established qPCRs for viral transcripts that represent the following classes of viral genes:

- a. Immediate early (IE) and early (E) transcripts of the lytic cycle,
BZLF1 and BRLF1 encode transcription factors that are essential for the switch to the lytic cycle (Countryman et al., 1987; Ragoczy et al., 1998), BMRF1 encodes a DNA polymerase processivity factor with essential function during genomic DNA replication and early induction in the lytic cycle (Bayliss and Wolf, 1981; Neuhierl and Delecluse, 2006; Nakayama et al., 2009).
- b. Immune evasins
BNL2a inhibits TAP function (shown in this study and in Hislop et al., 2007), BCRF1 interferes with NK effector functions and the Th1 cytokine response (shown in this study), and BGLF5, a host shutoff factor (Rowe et al., 2007).
- c. Apoptosis antagonists
BHRF1 and BALF1 are redundant genes, which encode homologues to Bcl-2 and are important for the initial survival of infected B cells (Altmann and Hammerschmidt, 2005)

d. Latent genes

LMP1 and LMP2A/B, which trigger CD40-like and BCR-like signals in infected B cells, respectively (Busch and Bishop, 1999; Mancao et al., 2005), EBNA2 encodes a transcriptional regulator which is critical for cell-cycle regulation and essential for EBV-mediated growth-transformation (Hammerschmidt and Sugden, 1989; Pan et al., 2009).

e. non-coding RNAs

EBER 1 and 2 were shown to induce TLR3 and RIG-I signaling and contribute to B cell transformation (Iwakiri and Takada, 2010; Samanta and Takada, 2010).

I infected B cells from adenoids with recombinant wildtype EBV (p2089), prepared total RNA 2 hours post infection (hpi) and assessed the presence of viral transcripts by quantitative PCR (qPCR). Similar to BNLF2a, a number of these transcripts could be detected as early as 2hpi (figure 3.1). BMRF1 and EBER1 showed the highest prevalence and only BALF1 RNA was not reliably detectable. All data were reproducible with peripheral B cells as well as B cells from adenoids of different donors (not shown).

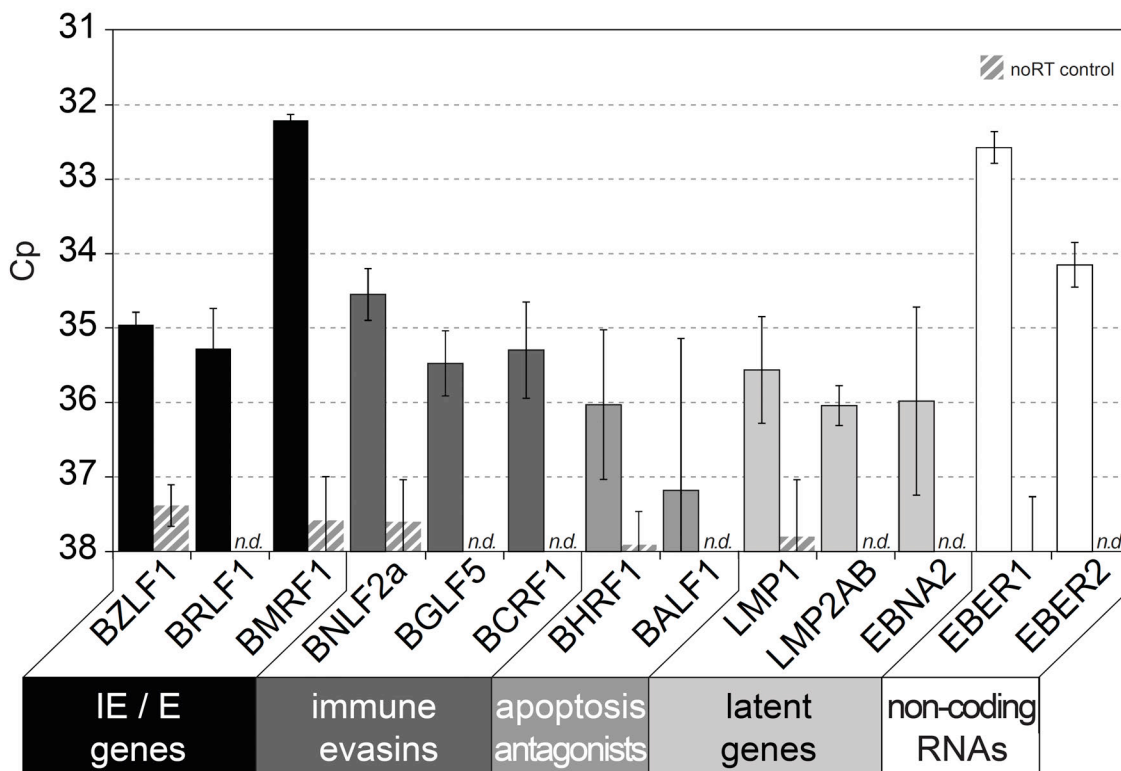


Figure 3.1: EBV transcripts are detectable in B cells as early as two hours post infection.

RNA was prepared from EBV-infected adenoid B cells two hours post infection, 1µg RNA was reversely transcribed into cDNA and analyzed by qPCR for various EBV transcripts. Reactions were run in triplicates and error bars represent the obtained standard deviations. PCR was additionally performed with controls that had not been reversely transcribed (noRT) and signals were not detected (n.d.) or shown as striped bars. Cp, crossing point (equivalent to the second derivative maximum of the sigmoid function of fluorescence intensity in qPCR); IE, immediate early; E, early.

The analysis of later time points provided the kinetics of single transcripts. The level of most genes rapidly inclined within 2-4 hours following infection (figure 3.2, lower and mid panel). The strongest induction was observed for transcripts of EBNA2, one of the essential factors for EBV-mediated transformation of B cells (Hammerschmidt and Sugden, 1989). In contrast, the transcripts of BNLF2a, LMP1, LMP2AB and EBER1 were stable during the first 8 hours of infection and increased steadily thereafter (figure 3.2 upper panel).

The biphasic kinetics of several transcripts (BNLF2a, LMP1, LMP2AB, EBER1, and less pronounced also BZLF1 and BRLF1) appeared interesting. The transcripts were detectable at stable levels for about 6 to 8 hpi, followed by a substantial increase over time. The biphasic nature suggests that virion-delivered transcripts are responsible for the initial phase, which is followed by a second phase of active transcription from the viral genome. Moreover, it might be virion-delivered messenger of BZLF1 and BRLF1 that triggers the early lytic phase.

2. EBV particles contain RNAs

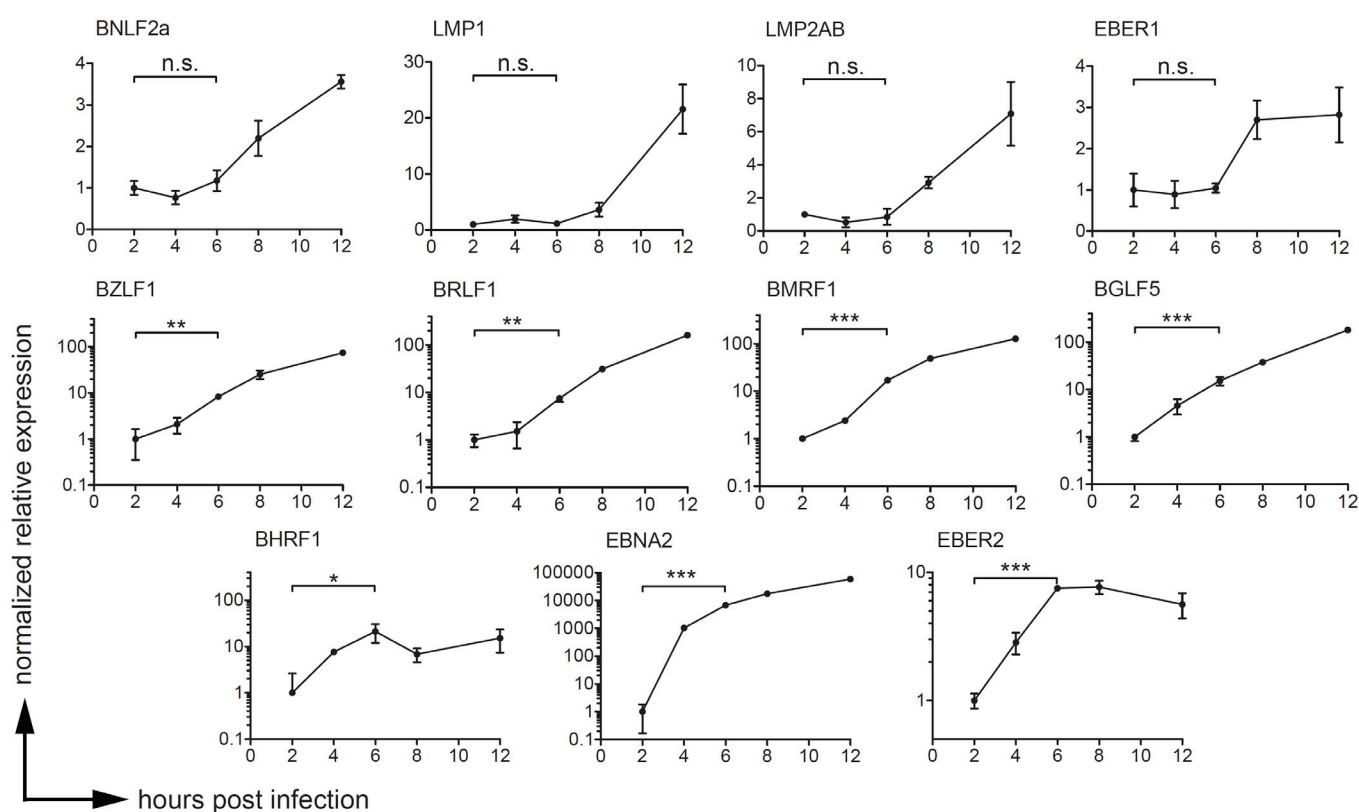


Figure 3.2: Several transcripts are immediately detectable and remain stable in the first hours of infection. RNA was prepared from EBV-infected adenoid B cells at the indicated time points after infection and 1 µg was reversely transcribed into cDNA. qPCR was performed, the values were corrected for the PCR efficiency of the given primer pair and put into relation to GUSB signals (housekeeper). The ratios were set to one at the first time point (2 hpi). Unpaired, two-tailed Student's T tests were performed to analyze the significances of differences. ***/**/*: $p < 0.001/0.01/0.05$, n.s.: not significant.

EBV virion-incorporated RNA might become transferred to recipient cells and could account for the observed transcript presence in cells immediately after infection. This assumption seemed promising because similar observations have already been made for other members of the herpes virus family (Bresnahan and Shenk, 2000; Greijer et al., 2000; Sciortino et al., 2001; Bechtel et al., 2005). Thus, I sought to determine whether viral RNAs are packaged within EBV virions.

2.1 Preparation and validation of RNA from viral particles

The analysis of packaged RNAs is challenging because these RNAs might be unstable, scarce and contaminating viral DNA genomes could be the source of false positive signals. EBV is particularly difficult to study as only a very limited number of cell lines are known, which release infectious particles. Besides, the EBV-titers released from these cell lines are far lower than those of other herpes viruses. To cope with these difficulties, I established a protocol as detailed in the section “Material and Methods”, chapter 2.3.8f, which uses concentrated virions from the supernatant of B95.8 cultures. In brief, EBV virions were concentrated, enzymatically treated to eliminate free RNA and DNA, pelleted by ultracentrifugation and subjected to standard RNA preparation. Based on this protocol, I could successfully isolate up to 2 μ g virion RNA from virion particles present in one liter of B95.8 cell culture supernatant.

Reverse transcription and subsequent qPCR analyses were performed on the RNA samples to detect BNLF2a as exemplary viral transcript. In parallel, quality controls were included at different steps of the preparation to verify the elimination of contaminating free RNAs or viral DNA genomes. Figure 3.3 displays the preparative workflow after the first step of supernatant concentration and the qPCR results obtained with samples from the different preparative steps. RNA samples were either subjected to reverse transcription (RT), or left untreated (noRT). Strong qPCR signals for the viral transcripts of BNLF2a were obtained in reversely transcribed samples, whereas noRT samples did not show any signals above background level. Hence, signals were derived from RNA and indicated that EBV virions contained BNLF2a transcripts protected from initial RNase-treatment (figure 3.3). Strong signals were observed whenever DNase treatment was omitted (panels B and C). The particle preparations were spiked with RNA from the human EBV negative cell line BJAB representing the only source of PCR signals for human glucuronidase beta (GUSB). The B95.8 cell line is of marmoset origin and primers did not amplify marmoset GUSB. External DNase and RNase treatment did not affect the detection of viral transcripts, but eliminated

human GUSB RNA efficiently that had previously been spiked in (panels A and B) indicating the successful degradation of any free RNA.

The applied protocol proved appropriate for the analysis of packaged RNAs because it efficiently removed contaminating DNA or RNA. The following set of experiments is based on this method of preparation.

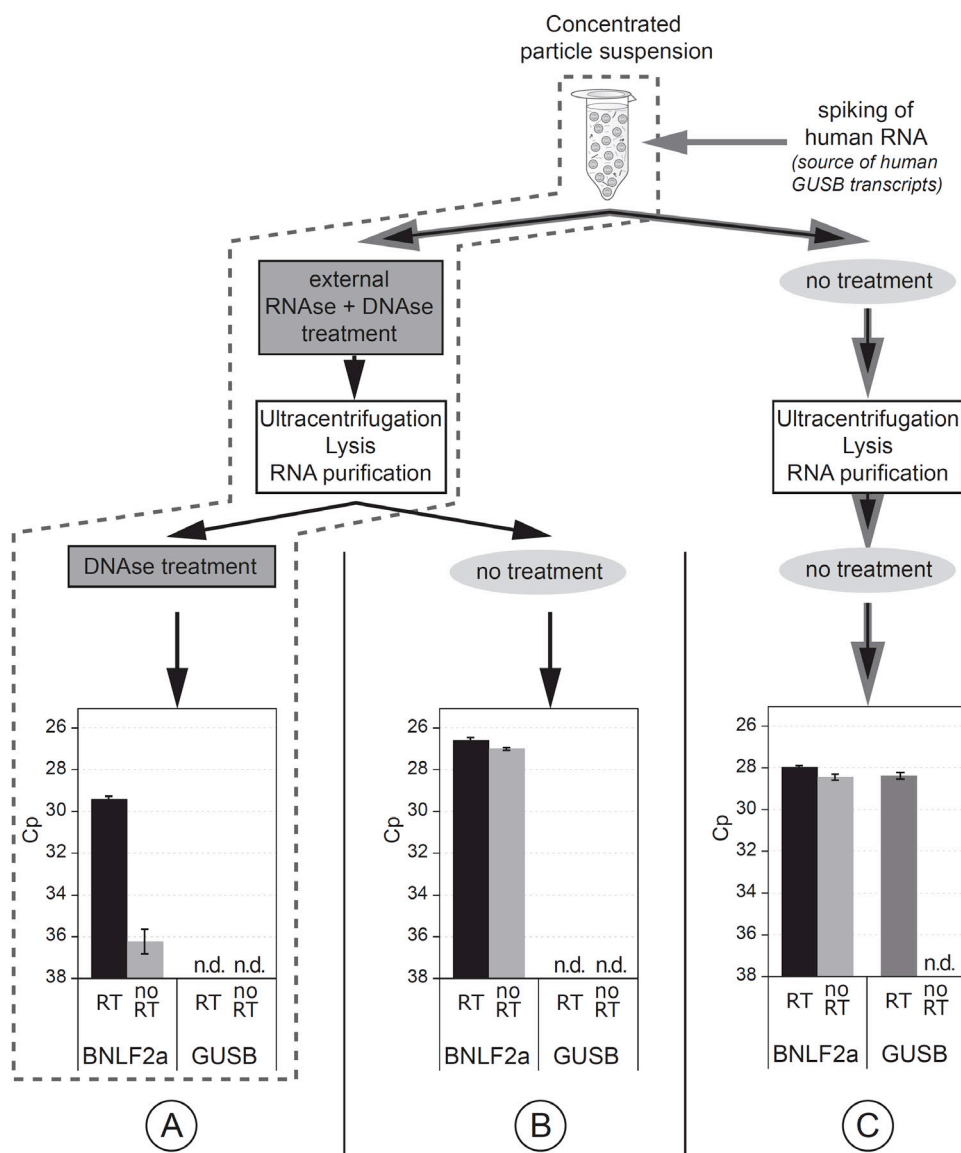


Figure 3.3: Viral transcripts are located inside EBV particles. EBV particles were enriched by sequential centrifugation steps from B95.8 cell culture supernatant. Human RNA was spiked into the preparation and represented the exclusive source of PCR signals for human GUSB (primers did not amplify GUSB from the marmoset cell line B95.8). Successful RNase and DNase treatment eliminated human GUSB signals (panels A and B). Genomic EBV DNA was removed in a second step of DNase treatment after capsid lysis. RT samples showed strong signals for BNLF2a (panel A), indicating that RNA was contained in viral particles and was protected from RNase treatment. n.d., not detected.

2.2 Assessment of different transcript categories in viral particles

Following the established protocol, I prepared EBV particles from two liters of B95.8 supernatant and analyzed selected viral transcripts in virions by qPCR after cDNA synthesis. I obtained clear signals for all RNAs analyzed (figure 3.4A). Again, the highest levels were obtained for BMRF1 and EBER1 transcripts, but in contrast to B cells infected B95.8 virus stocks, BNLF2a, BHRF1 and LMP1 transcripts were also readily detectable.

In the next step, I addressed the question whether EBV particles might also contain viral microRNAs. I prepared B95.8 particles as described above and applied a protocol for microRNA preparation. In EBV B95.8 infected cells, 13 mature microRNAs have been identified so far. They are derived from 9 pre-microRNAs that are encoded in the BART and BHRF1 transcripts. Three stem-loop structures are part of the BHRF1 transcript and are processed to pre-microRNAs (miR-BHRF1-1, miR-BHRF1-2, miR-BHRF1-3). BART microRNAs are organized in a cluster comprising 4 pre-microRNAs (miR-BART 3, 4, 1 and 15) and the single, more distally located miR BART-2 (Pfeffer et al., 2004; Grundhoff et al., 2006). Each pre-microRNA stem-loop is processed to mature microRNAs that can arise from the 5' or 3' end of the stem structure or both. Based on a protocol as detailed in Material and Methods I prepared cDNA from selected mature microRNAs from all loci but miR BART4, which could not be efficiently amplified by PCR. All microRNAs could be detected at high levels (figure 3.4B).

With the help of the TR⁻ 2/293 packaging cell line (Delecluse et al., 1999) it is possible to generate non-infectious virus-like particles (VLPs), termed TR⁻ VLP in this study. TR⁻ VLPs do not contain viral DNA, are not transforming but still fuse with B cells – a process termed pseudo-infection in this study. I analyzed VLP preparations for the presence of incorporated viral RNAs. I prepared RNA from one liter of supernatant from TR⁻ 2/293 cells, which had been induced for particle production. In analogy to B95.8 virion preparations, TR⁻ VLPs contained detectable amounts of viral RNAs (figure 3.4C) and microRNAs (figure 3.4D). BZLF1 transcripts were present in TR⁻ VLPs at much higher concentrations than in B95.8 virions, presumably because BZLF1 is expressed at very high levels in TR⁻ 2/293 cells after transient transfection of a BZLF1 expression plasmid to induce VLP production. My findings indicate that VLP are a useful tool to investigate the function of transferred RNA in the absence of virion DNA in infected B cells.

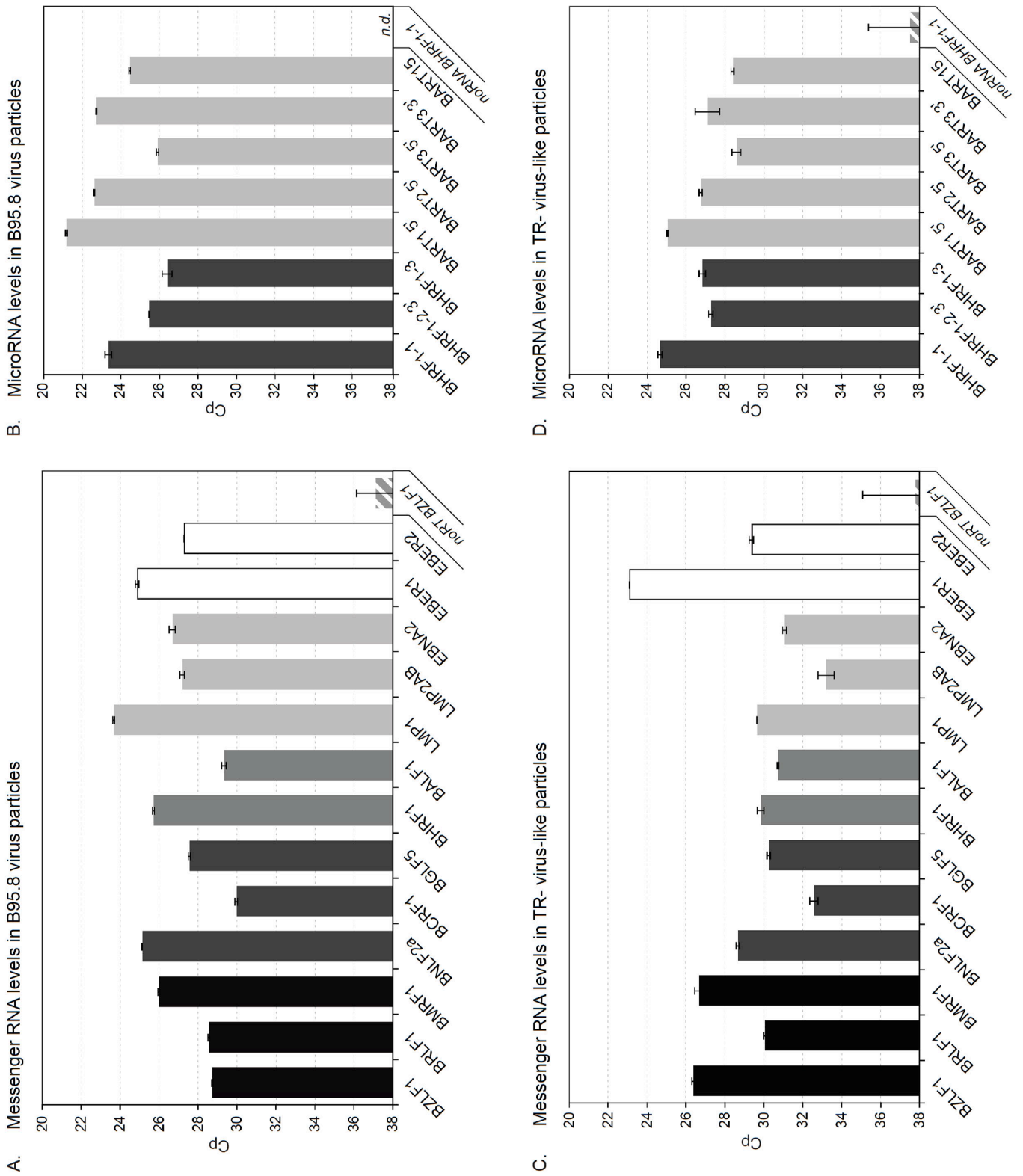


Figure 3.4: B95.8 particles and TR⁻ particles contain viral RNAs. Following the protocol depicted in Figure 3.3, RNAs (A,C) and microRNAs (B,D) were prepared from B95.8 super-natants or recombinantly produced TR⁻ VLP and reversely transcribed. The presence of transcripts from different categories and microRNAs from each known locus in B95.8 was assessed by qPCR. The analysis included RNA preparations without reverse transcription (noRT) or mock controls without RNA (noRNA). All controls led to Cp ≤ 36 and are shown for BZLF1 and miR-BHRF1-1 analyses.

2.3 Levels of selected transcripts differ between virus producers and viral particles

Levels of virion-incorporated RNA can reflect those of their source cells suggesting a random integration (hCMV, Terhune et al., 2004), or are enriched in virus particles as in the case of HSV1 (Sciortino et al., 2002). To analyze the situation with EBV, I compared the transcript levels in B95.8 cells and viral particles that these cells release.

EBV producing cells express the viral glycoprotein gp350 on their surface (Flamand et al., 1993; Yuan et al., 2006). The fraction of gp350+ cells in the B95.8 cell line depends on culture conditions and ranges between 1-10%. I enriched the gp350+ fraction of B95.8 cells by FACS-sorting and obtained an almost pure population (figure 3.5A) that was subjected to RNA preparation and reverse transcription for subsequent qPCR analysis.

Transcript levels in two different samples can be compared by normalization to a housekeeping transcript that is expressed at equal levels in both samples. This requirement could not be assured in my approach addressing producer cells and viral particles. I chose the BMRF1 transcript as reference, which showed high abundance in both B95.8 cells and B95.8 virus particles. Relative levels of several transcripts in sorted gp350+ cells and viral particles were calculated and plotted as shown in figure 3.5B.

Based on this calculation, none of the transcripts showed equal levels in lytic cells and particles. The ratio between gp350+ B95.8 cells and viral particles shown in figure 3.5C suggested that most transcripts were contained in lower relative amounts in viral particles than in gp350+ cells, with exception of LMP1, LMP2AB and EBER transcripts. This finding might reflect their preferential packaging together with transcripts of the *BMRF1* gene pointing to a preferential incorporation of certain transcripts.

Whether the observed differences resulted from a selective packaging of BMRF1, LMP1, LMP2AB and EBER transcripts to virions is currently unclear. It will be essential to verify a reliable reference transcript for relative transcript comparisons. Analyses on the basis of absolute transcript levels remain error-prone because of a different compositions of cellular and particle RNAs, as 1µg of cellular RNA contains more than 90% of ribosomal and transfer RNA that is unlikely to be present to the same extent in viral particles.

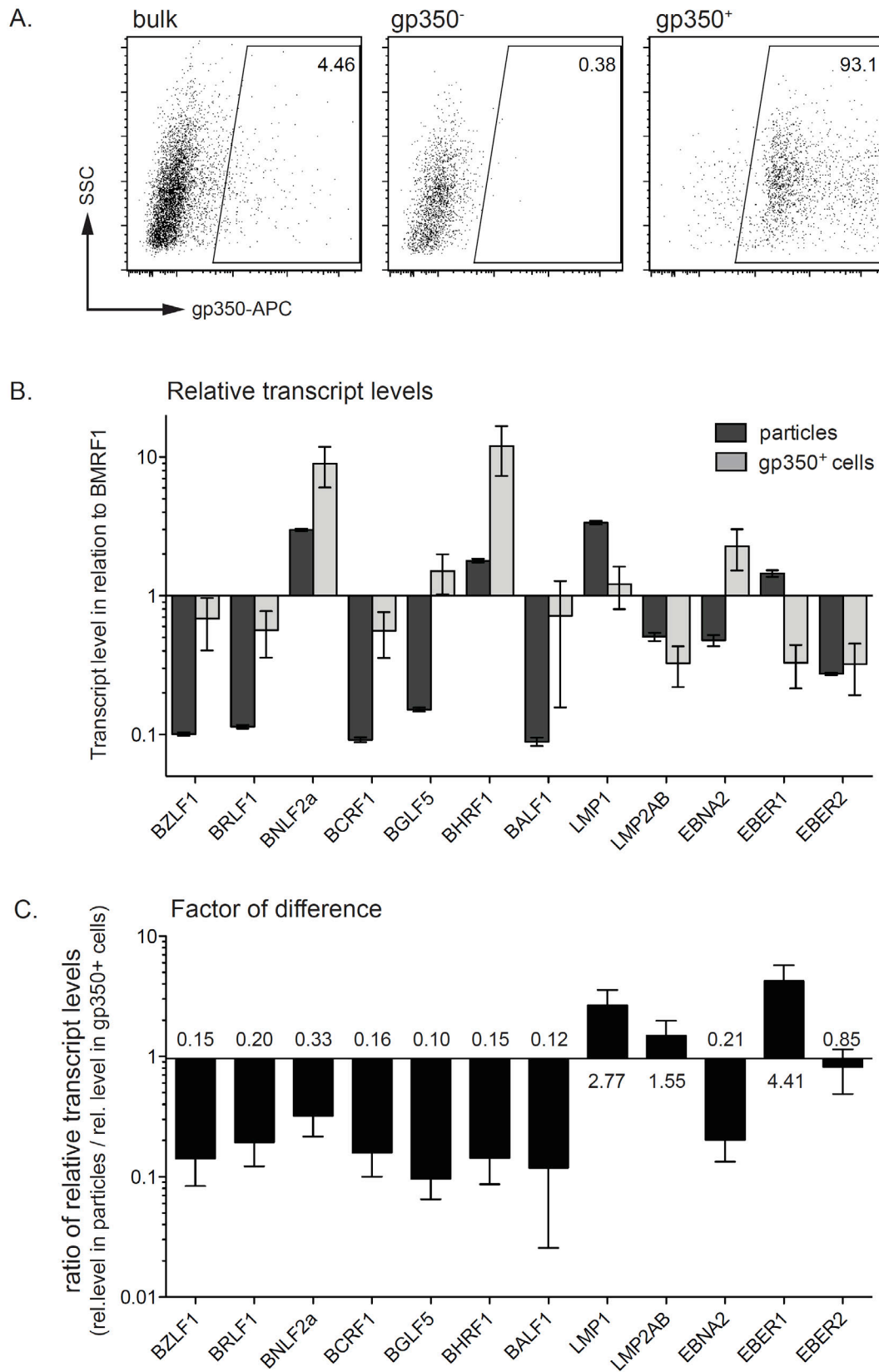


Figure 3.5:
Viral particles and producer cells differ in their transcript levels.

A. The fraction of spontaneously virus-producing B95.8 cells was assessed by FACS analysis. Gp350⁺ and gp350⁻ cells were separated by FACS sorting. B. Levels of different transcripts were normalized to BMRF1 and compared for viral particles and gp350⁺ cells. C. The ratio of the transcript levels was calculated from data in B.

2.4 The RNA shuttle-protein EB2 of EBV is present in virions

The *BMLF1/BSLF1*-encoded EBV protein EB2 is a candidate for the selective packaging of RNAs into viral particles. This hypothesis builds on previous analyses of capsid assembly and particle function (Gruffat et al., 2002; Batisse et al., 2005), and the *in vitro* interaction of EB2 with RNA (Hiriart et al., 2003a). EB2 has been shown to be essential for the formation of progeny virus in producer cells and mediates the export of non-spliced transcripts during the lytic phase. If EB2 is a mediator of the selective packaging of RNAs, it might become incorporated and be itself part of virions. I addressed the presence of EB2 in virions in the recombinant system for EBV production. Because an EB2 antibody is not available, I took use of a FLAG-tagged wildtype EB2 (wtEB2-FLAG) and FLAG-tagged mutant EB2 (mutEB2-FLAG), with mutEB2 being incapable of RNA binding (Hiriart et al., 2003b). Expression plasmids for these constructs were transfected into the EBV producer cells 293/2089 (rec.wt.) (Delecluse et al., 1998) together with an expression plasmid for BZLF1, which induces the lytic phase and the synthesis of progeny virus. The supernatants were harvested and parts of them used to infect Raji cells. The number of infected GFP+ Raji cells was assessed by FACS on day three after infection. The virus titers in the supernatants generated with the FLAG-tagged wildtype EB2 or mutant EB2 were comparable (figure 3.6A).

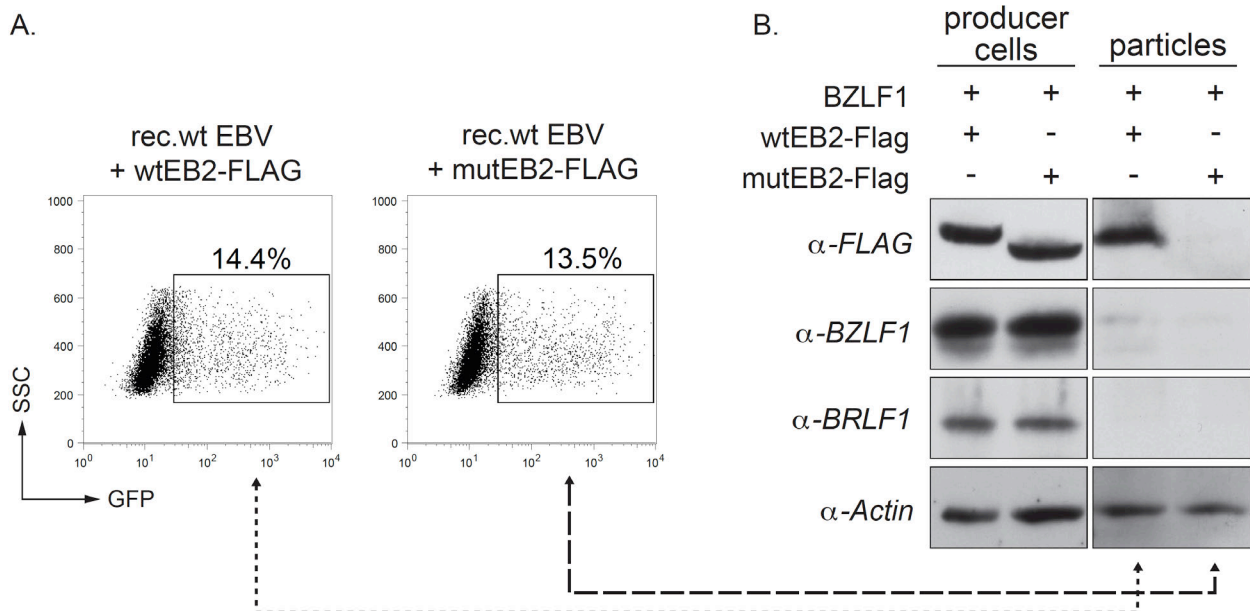


Figure 3.6: EB2 protein is packaged into virions.

Wildtype recombinant EBV producer cells (293/2089) were induced for virus production by transfecting a BZLF1 expression plasmid. WtEB2-FLAG or mutEB2-FLAG expression vectors were co-transfected. A. Raji cells were infected with the respective supernatant. Equal percentages of GFP+ Raji cells in FACS analyses 3dpi confirmed equal virus production for both samples. B. Lysates from producer cells (left) and produced particles (right) were assessed by Western blot for FLAG-tagged EB2 proteins, BZLF1 and BRLF1. Actin signals served as loading control.

Lysates from the producer cells were analyzed by Western blot immunodetection and confirmed successful transfection of wtEB2-FLAG, mutEB2-FLAG as well as BZLF1. BRLF1, a viral gene downstream of BZLF1 was also readily induced and indicated the initiation of the lytic cycle in the cells (Amon et al., 2004; Yuan et al., 2006). Viral particles were purified and the protein lysates analyzed for the presence of wtEB2-FLAG and mutEB2-FLAG protein by Western blot immunodetection. Distinct signals for wtEB2-FLAG, but not EB2mut, indicated that EB2 is contained within EBV particles suggesting that it might mediate RNA incorporation. The binding motif must be essential for incorporation, ARM-motif deleted “mutEB2” protein could not be detected in viral particles (figure 3.6B).

In analogy to findings with HSV1 (Sciortino et al., 2002), the incorporation of EB2 into viral particles points to its role as a mediator of transcript selection serving as a transfer matrix. The general presence of EB2 in particles gives room to speculate on its role as a mediator of directed transcript incorporation into particles.

3. Virion-transferred transcripts are translated in recipient cells

3.1 Virion-incorporated transcripts are translated immediately in infected cells

Two publications claim that mRNAs packaged into viral particles are translated in infected cells directly after virus entry (Bresnahan and Shenk, 2000; Bechtel et al., 2005). To address the translation of incorporated RNA in virus particles of EBV, I used EBV-negative Daudi cells (Nanbo et al., 2002) as indicators because Daudi cells are highly susceptible to EBV infection (own observations). In order to analyze the translation of virion-transferred RNAs, it is mandatory to discriminate this class of RNAs from those that are *de novo* transcribed in infected cells. Treatment of cells with ActinomycinD (ActD) efficiently inhibits transcription (Sobell, 1985) and copes with this issue. Additionally, a transfer of virion-borne protein also had to be considered. Control samples were treated with cycloheximide (CHX) prior to infection to block translation (Siegel and Sisler, 1963) evaluating the contribution of direct protein delivery by viral particles. ActD-treated and CHX-treated samples then provided the necessary controls in this experiment.

First, I confirmed that ActD completely blocked transcription - the decrease of short-lived c-MYC mRNA (Marcu et al., 1992) served to measure inhibition. The concentration of 5 μ g ActD per ml medium entirely blocked *de novo* transcription in Daudi cells because c-MYC mRNA levels declined rapidly within 240 min (figure 3.7A).

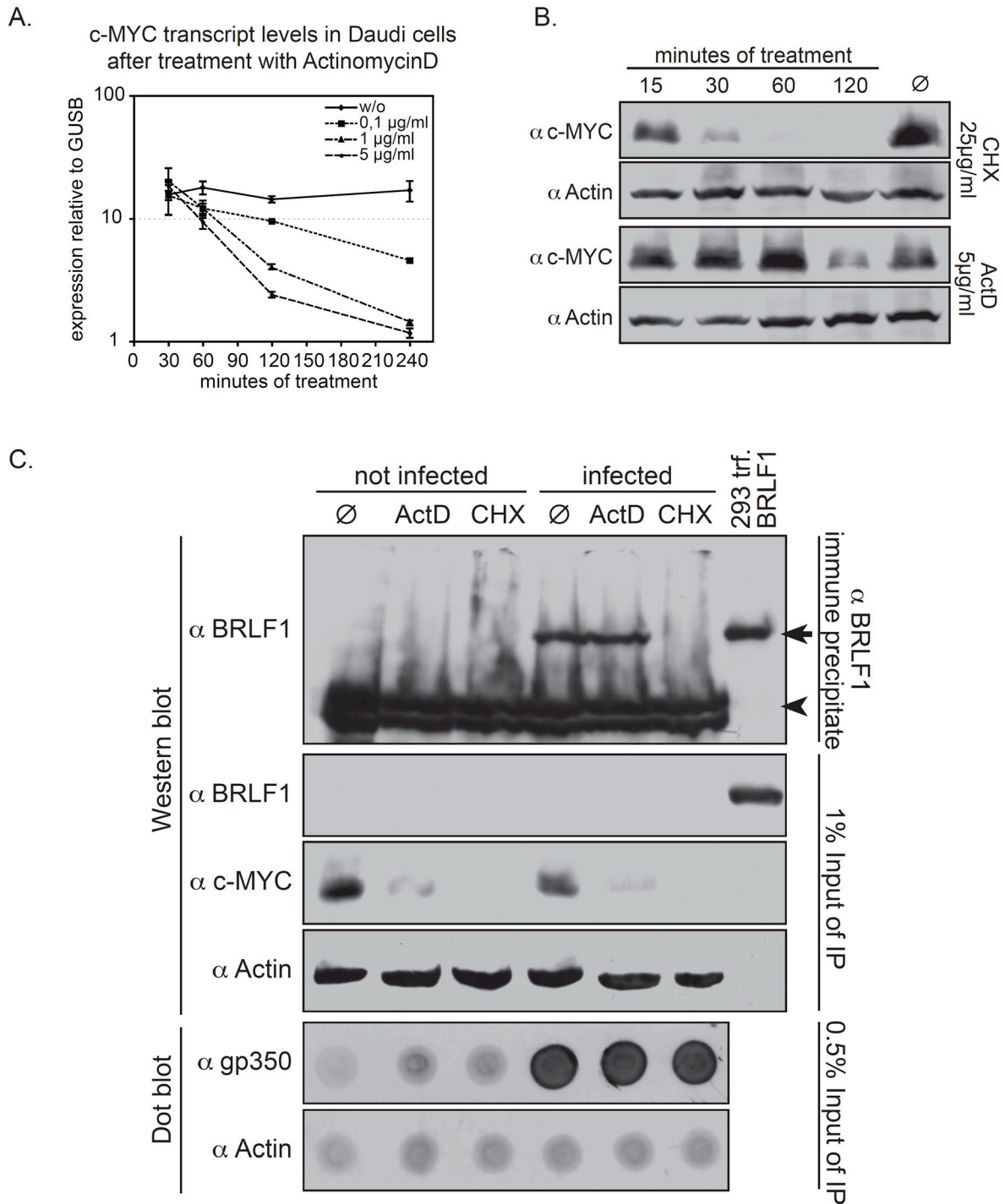


Figure 3.7: Particle transcripts are translated in newly infected cells.

A. Daudi cells were treated with indicated doses of ActinomycinD and transcript levels of c-MYC mRNA were measured in relation to GUSB by qPCR at indicated timepoints.

B. Cycloheximide (CHX) at a concentration of 25 $\mu\text{g/ml}$ inhibited translation of c-MYC at the indicated timepoints (upper panels). Actinomycin D (ActD) inhibited transcription and indirectly prevented *de novo* synthesis of c-MYC protein in a delayed manner (lower panels).

C. 1×10^8 Daudi cells were treated with inhibitors as indicated and infected with concentrated B95.8 virions or left uninfected. Two hours post infection, cells were lysed, BRLF1 protein was immunoprecipitated and analyzed by Western Blot immunodetection. 1% of the input lysate was included to control for BRLF1 enrichment and successful inhibitor treatment. Infection of the respective samples was verified by dot blot analysis of 5 μl input lysate with a gp350-specific antibody. Actin signals served as loading control. Total cell lysates of BRLF1 transfected 293 cells served as positive control for BRLF1 signals (arrow), signals for the heavy chain of the IP-antibody indicate equal treatment during immunoprecipitation (arrowhead).

Translation was efficiently blocked in Daudi cells at a concentration of 25 μ g CHX per ml because c-MYC protein decreased with the reported half-life of about 15min (Luscher and Eisenman, 1988) and became undetectable after 60min of treatment (figure 3.7B).

Next, virus particles were prepared from two liters of cell-free B95.8 supernatant and concentrated approximately 100-fold as described in Material and Methods. Daudi cells were pre-treated with ActD or CHX or left untreated and then incubated with concentrated B95.8 particles for 2 hours at 37°C. Whole cell lysates were prepared and subjected to immunoprecipitation with an antibody specific for the viral BRLF1 protein. The precipitates were separated on SDS PAGE and the same anti-BRLF1 antibody was used to detect the protein. A clear signal of the expected size (105kD) was present in lysates from infected cells that had been pre-treated with ActD or left untreated. Moreover, untreated and ActD-treated cells displayed similar levels of BRLF1 protein, indicating that delivered mRNAs constitute the predominant source for BRLF1 protein within the first hours following infection. No signal could be detected in CHX-treated cells, hence BRLF1 protein levels in infected Daudi cells originated from *de novo* translation (figure 2.5C). The control experiments excluded the simple transfer of BRLF1 protein through viral particles.

My experiments clearly demonstrated that EBV virions transfer RNAs that are translated in recipient cells immediately after infection.

3.2 The translation of transferred RNAs leads to antigen presentation

EBV antigen-specific CD8⁺ T cell clones constitute an alternative sensitive tool for the detection of viral proteins in infected cells because endogenously translated proteins are degraded in the proteasome and subsequently presented in association with MHC I molecules (Janeway, 2005).

My experiments suggested that viral proteins could be translated from virion-packaged mRNAs. It appeared as a likely consequence that viral peptides are presented to antigen-specific CD8⁺ T cells after RNA transfer. I used CD8⁺ T-cell clones specific for the immediate early EBV proteins BZLF1 (epitope RAK) and BRLF1 (epitope YVL), for the early protein BMLF1 (epitope GLC) and the latent protein EBNA3a (epitope QAK). These T cells were co-incubated with HLA-matched B cells that had been pseudo-infected with TR⁻ VLP, which contain viral RNAs (figure 3.4) but are devoid of EBV DNA genomes. As a negative control, a fraction of the B cells had been pre-treated with CHX to block translation and also uninfected, untreated B cells were included. After 18 hours of co-culture, I assessed Ifn- γ levels in the supernatants released by antigen-activated effector T cells.

The results in figure 3.8 clearly indicate that T cells recognized MHC I associated epitopes on primary B cells that had been pseudo-infected with TR⁻ VLPs. The levels of Ifn- γ were much lower than those obtained with LCLs as positive control, but differences between not infected and TR⁻ VLP pseudo-infected cells were evident. CD8⁺ T cells specific for the lytic epitopes YVL of BRLF1, RAK of BZLF1 and GLC of BMLF1 released Ifn- γ , but T cells specific for the epitope QAK of EBNA3a did not. EBNA3a is a latent gene and its transcriptional activity is very low suggesting that EBNA3a RNA molecules are not incorporated into virions or translated at a level that is below detection in this assay.

This experiment revealed that TR⁻ VLP-transferred RNA is translated in the recipient cells, resulting in antigen presentation that is sufficient to trigger CD8⁺ T cell activity. This effect was clearly dependent on functional translation in the infected cells.

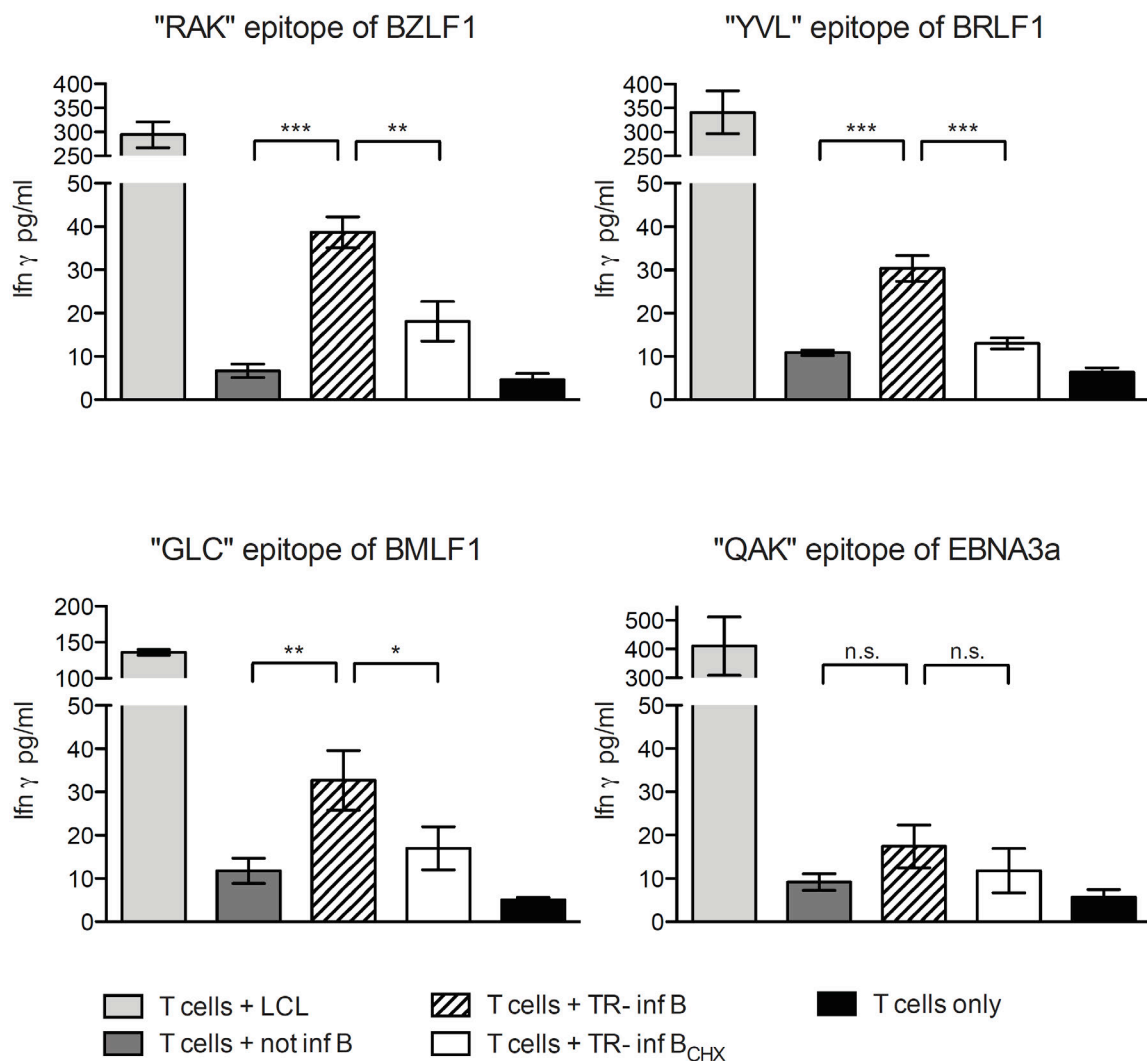


Figure 3.8: CD8 T cell clones specific for lytic EBV epitopes recognize TR⁻ VLP infected B cells.

Peripheral B cells of matching HLA allotype were infected overnight with concentrated TR⁻ virus like particles (VLP) and treated with cycloheximide (CHX) as indicated. Cells were washed, counted and incubated for 18h with T cells specific for the indicated epitope at an effector target ratio of 1:2. Ifn- γ levels in the supernatant of the co-culture were assessed by low-range ELISA. Error bars indicate standard deviations of three biological replicates, significance was analyzed by Student's T test, */**/**: $p \leq 0.05/0.01/0.001$; n.s., not significant.

4. Virion-transferred RNAs modulate the immune response

4.1 Packaged BNLF2a-RNA decreases the recognition of infected B cells by CD8⁺ T cells

BNLF2a is an important immune evasin that inhibits TAP-dependent antigen presentation and exerts important function within the first days of infection, as described in the first part of this work. Transcripts of BNLF2a were detected in viral particles as well as in freshly infected cells (figures 3.1 and 3.4).

I addressed the immediate impact of transferred BNLF2a-RNA on T cell recognition. To this end, I infected primary B cells with either recombinant wildtype EBV (Delecluse et al., 1998) or the *BNLF2a*-deficient EBV mutant that was generated in the first part of this work (Δ *BNLF2a*, section "Results I", chapter 1). Both are infectious viruses and induce de novo transcription upon infection. This was prevented in Actinomycin D (ActD) treated samples, delineating remaining effects to transferred RNA. The inhibition of translation in

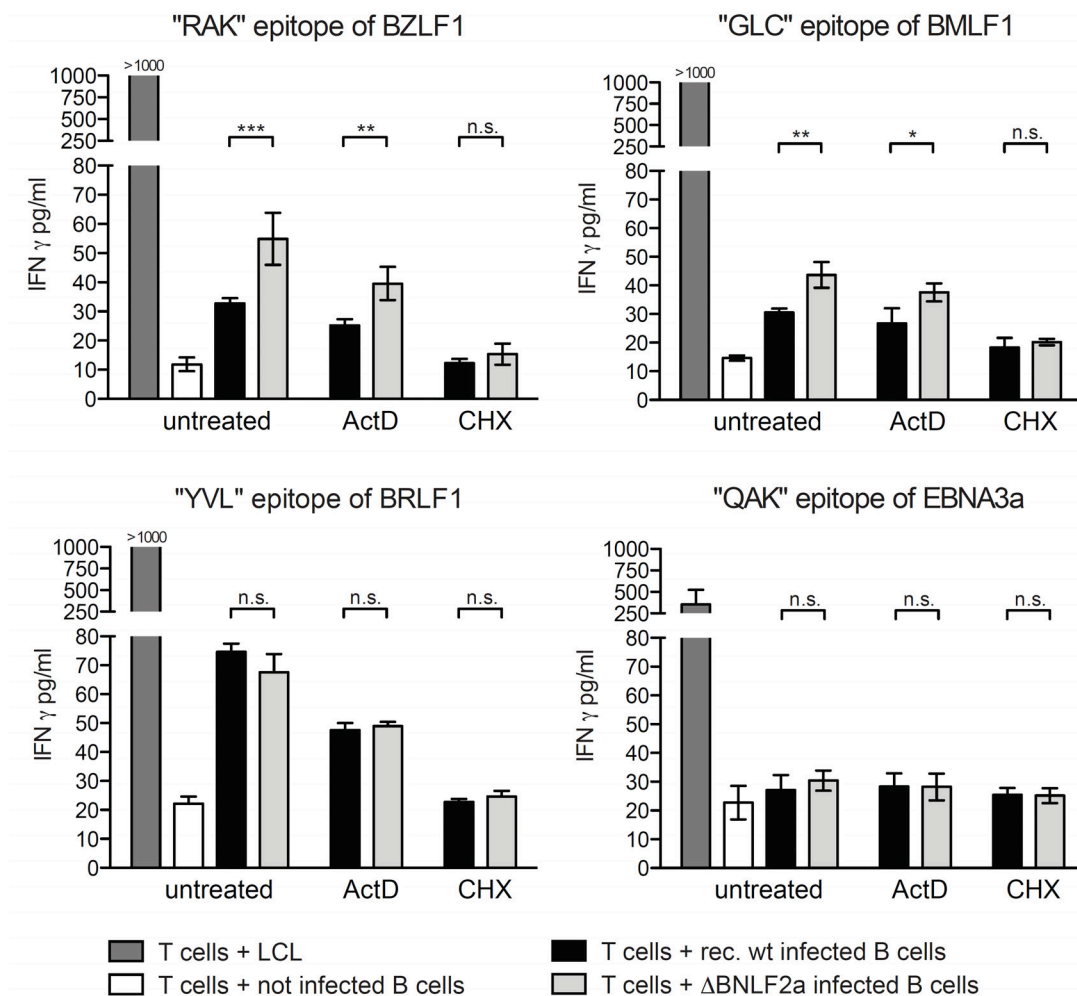


Figure 3.9: The transfer of BNLF2a transcripts impairs immune recognition of infected cells immediately after infection. Untreated, ActD-treated or CHX-treated B cells were infected overnight with recombinant wildtype (rec. wt) virus or Δ *BNLF2a* virus. The cells were co-incubated with EBV-specific clonal CD8⁺ T cells at an effector:target ratio of 1:2 for the following 18hrs. Ifn- γ levels in the supernatants of the co-culture were assessed by low-range ELISA. Error bars indicate standard deviations of three biological replicates, significance was analyzed by Student's T test, ***/**/*: p \leq 0.05/0.01/0.001; n.s., not significant.

Cycloheximide (CHX) treated control samples resolved the putative contribution of virion-mediated protein transfer to functional differences.

As expected, RAK-epitope specific T cells recognized primary B cells infected with the Δ *BNLF2a* mutant EBV better than cells infected with recombinant wild-type EBV one day after infection. However, ActinomycinD treated B cells were also recognized by T cells and the difference in recognition of wild-type and Δ *BNLF2a* infected B cells samples remained significant. Cycloheximide treated cells did not present the epitope (figure 3.9, upper left panel). Similar observations were obtained for the GLC epitope of BMLF1, reflecting however an overall weaker recognition (figure 3.9, upper right panel).

Thus, transfer of BNLF2a transcripts but not BNLF2a protein contributed to impaired recognition of newly infected B cells. Besides, these results expanded the findings from the previous chapter: Also upon infection with functional virus transferred RNA is translated, which leads to the presentation of viral peptides on MHC I.

Rather strong T cell responses were also obtained with the YVL-epitope (derived from the viral BRLF1 protein), but BNLF2a did not show any effect here (figure 3.9, lower left panel). This resulted from TAP-independent loading of the hydrophobic YVL peptide to MHC I (Lautscham et al., 2003) that is not affected by BNLF2a-mediated interference with antigen presentation (BNLF2a inhibits TAP, Horst et al., 2009). The equal T cell response to this epitope in samples with and without ActD however showed that ActD treatment did not affect antigen presentation. The QAK epitope was not recognized one day after infection and reflected previous findings with TR⁻ VLP pseudo-infections (figure 3.9., lower right panel).

This experiment assigned a first functional advantage to virion-mediated RNA transfer, as EBV uses this strategy to immediately impair epitope presentation by the transfer of BNLF2a RNA that is translated to act as an immune evasin.

4.2 Packaged EBERs induce *Ifn- α* production in infected cells

The non-coding RNAs EBER-1 and -2 of EBV are among the most abundant viral transcripts in infected cells. EBERs form secondary structures with double-strand character that bind to cellular PAMP recognition receptors (PRR), including retinoic acid-inducible gene (RIG)-I (Samanta et al., 2006) and toll-like receptor (TLR)-3 (Iwakiri et al., 2009). Binding activates their downstream signaling cascade (Kawai and Akira, 2008; Iwakiri and Takada, 2010). As EBER-1 and -2 transcripts are abundantly present in EBV particles (figure 3.4), I asked whether they might function immediately upon infection. The most prominent

effect ascribed to EBERs is the induction of type I interferons in EBV infected cells upon binding to RIG-I or TLR-3 (Samanta and Takada, 2010).

For this analysis I generated two EBV mutants that lack the genes for both *EBER-1* and *-2*. The first mutant, termed $\Delta EBER$, is derived from the recombinant wildtype EBV genome p2089 (Delecluse et al., 1998). The second mutant, termed $\Delta EBER TR^-$, is derived from the recombinant EBV genome that lacks the terminal repeats (p2114, “TR⁻”, (Delecluse et al., 1999). Accordingly, $\Delta EBER$ virions contain viral genomes and viral RNAs, whereas $\Delta EBER TR^-$ virus-like particles (VLP) are devoid of viral genomes, but still contain viral RNAs. Both efficiently transduce the co-packaged RNAs to target cells, however only the infection with genome-containing virions stably establishes the virus in the cell.

I infected primary B cells from adenoids with (i) recombinant wildtype virus, (ii) $\Delta EBER$ virus, (iii) TR^- VLPs or (iv) $\Delta EBER TR^-$ VLPs and measured *Ifn- α* synthesis. In order to exclude free EBERs in the supernatant, which are sufficient to induce *Ifn- α* (Iwakiri et al., 2009), one subset of EBER containing virus supernatants was additionally treated with RNase prior to infection. *Ifn- α* levels in the supernatant were assessed by ELISA three days after infection.

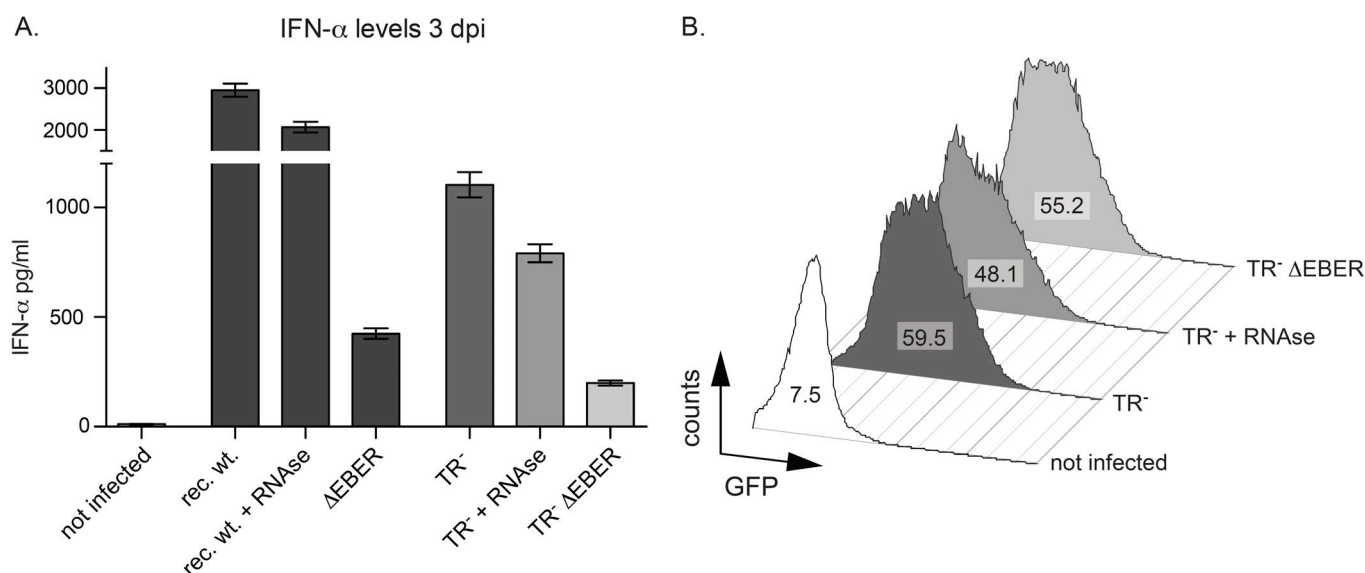


Figure 3.10: The virus particle-mediated transfer of EBERs induces *Ifn- α* synthesis in infected B cells. B cells were infected with recombinant wild-type EBV (rec.wt.), *EBER*-deficient recombinant EBV ($\Delta EBER$), TR^- VLP or *EBER*-deficient TR^- VLP ($TR^- \Delta EBER$). To control for effects of free EBERs, an RNase treated sample was included. A. *Ifn- α* levels in the supernatant were determined by ELISA, errors bars indicate the standard deviation of three biological replicates. B. Equal infection rates of VLP-infected samples were confirmed by FACS analysis, numbers in histograms indicate the mean GFP-fluorescence intensity of the samples. The same control was applied for virus-infected samples (not shown).

As shown in Figure 3.10, recombinant wild-type infected B cells produced high levels of Ifn- α within the first three days of infection as did B cells pseudo-infected with TR⁻ VLPs. In sharp contrast, cells incubated with Δ EBER virus or Δ EBER TR⁻ VLPs released significantly less Ifn- α . Treatment of the supernatants with RNase reduced the Ifn- α production only slightly. These results indicate that EBER transfer through virus particles is already sufficient to trigger RIG-I signaling. Moreover, free EBERs in the supernatant contribute only little to Ifn- α induction, but the majority of EBERs is obviously contained in particles and during infection.

These data demonstrate that packaged EBERs are functional in infected cells as they are sufficient to induce the synthesis of Ifn- α .

4.3 Virion-transferred microRNAs decrease MICB surface levels on infected B cells

Since their discovery, a large number of miRNAs have been described and many of them deploy important regulatory function. miRNAs have by now been proven to be potential regulators in nearly every aspect of cellular biology (He and Hannon, 2004). So far, also 235 miRNA-encoding stem-loops have been discovered in viruses, which of 146 are encoded by Herpes viruses. EBV field strains encode 25 miRNA stem-loops whereas the laboratory strain B95.8 has only 13 miRNAs stem-loops left due to a 10.5kb deletion in its genome (Grundhoff et al., 2006; Swaminathan, 2008). So far, two B95.8 miRNAs are known to target cellular transcripts: miR BHRF1-3 decreases messenger levels of CXCL11, a chemoattractant for B cells, and miR BART2-5' targets transcripts of MICB, a NK cell activating surface ligand (Xia et al., 2008; Nachmani et al., 2009). Hence, both miRNAs are immune modulatory and support EBVs immune escape.

As viral particles contain relatively high levels of miR BART2-5' (figure 3.3), I evaluated whether a downregulation of MICB surface levels is detectable on B cells and associated with the virion-mediated transfer of miR BART2-5'.

To address this question, I infected primary B cells from adenoids with either recombinant wildtype EBV, or an EBV mutant deficient for all known miRNAs (Δ miRall, Seto et al., 2010), or TR⁻ VLPs. Three days after infection, I assessed MICB surface levels of GFP⁺ infected cells by FACS analysis.

The infection with Δ miRall virus led to a 50% increase in MICB surface expression on infected cells 3dpi, compared to infection with recombinant wildtype EBV. Infection of B cells with virus-like particles (VLP) also reduced the surface levels of MICB, indicating that

miRNAs are transferred and target messenger RNAs immediately after infection and delivery (figure 3.11). Additionally, these data provide first evidence that miR BART2-5' targets MICB also in B cells. The early timing and magnitude of this effect suggests a high importance of this molecule for the immune escape of EBV-infected primary B cells.

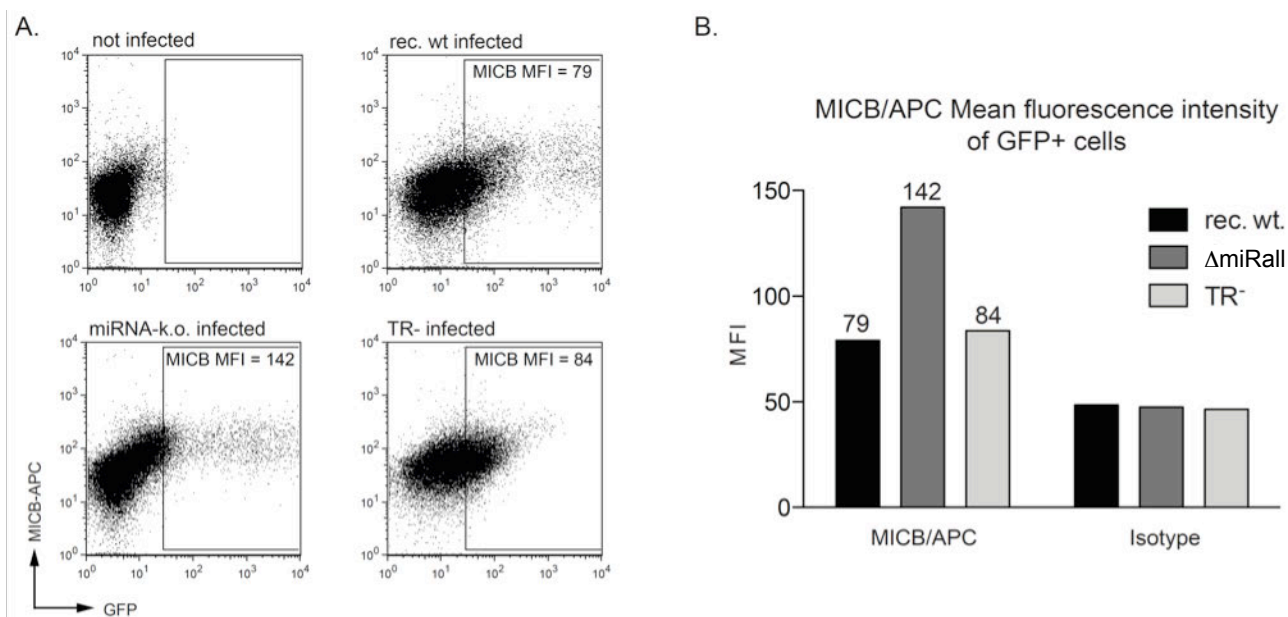


Figure 3.11: Within the first days of infection, TR⁻ VLP pseudo-infection results in comparable MICB surface levels as on wildtype infected-B cells, indicating functional microRNA transduction.

B cells were infected with recombinant wildtype EBV or microRNA deficient recombinant EBV (Δ miRNA) or pseudo-infected with TR⁻ VLP, cultured for three days and analyzed by FACS for MICB surface levels. A. Dot blots of FACS analyses. Virion-infected cells are GFP+, TR⁻ VLP pseudo-infected cells are GFP shifted, mean fluorescence intensities (MFI) of the MICB signal are shown in gates. B. Bar chart of MICB MFI and Isotype MFI of GFP+ cells, numbers indicate APC-MFIs (compare to A).

4.4 Packaged RNAs enhance EBV's capacity to transform B cells

Growth transformation of human B-cells *in vitro* is a hallmark of EBV. Following an initial lytic transcription program, EBV eventually establishes a latent infection in B cells. The latency-associated expression of viral genes is the reason for growth-transformation of EBV infected cells *in vitro* (Rickinson and Kieff, 2007). EBV-transformed B cells start to proliferate in culture and give rise to permanently proliferating lymphoblastoid cell lines (LCL). The transformation capacity of EBV preparations can be quantified in limiting dilution assays that are analyzed for the amount of proliferating cells several weeks after infection (Wilson and May, 2001). I used a modified limiting dilution assay to analyze whether the particle-associated transfer of RNAs enhance EBV's transforming capacities.

I compared the transformation capacity of B95.8 particles either alone, in combination with TR⁻ VLPs, or in combination with gp350+/GFP+ exosomes derived from transiently transfected HEK293 cells. Gp350+/GFP+ exosomes were included as a control because the binding of gp350 to CD21 might result in a stimulus sufficient to reactivate B cells (Bouillie et al., 1995) and also promote successful infection. I plated primary B-cells on 96-well cluster plates at a density of 10.000 cells/well and infected them with serial dilutions (5 - 0.1 µl/well) of B95.8 virus stocks, including 24 replicates per dilution step. In a preliminary experiment, 5µl/well of the B95.8 virus stock caused the outgrowth of infected cells in approximately 50% of the cultures. Three sets of plates were prepared and cells were infected with B95.8 virus. One of these plates was additionally pseudo-infected with TR⁻ VLPs, the second one treated with gp350+/GFP+ exosomes and the third one left as it was. Cells on additional sets of plates were only pseudo-infected with TR⁻ VLP or treated with gp350+/GFP exosomes and controlled for direct effects of these particles on B cell outgrowth without addition of B95.8 virus. The infection of the donor with field-strain EBV can be sufficient to lead to outgrowth of B cells. An additional plate with untreated cells controlled for this putative spontaneous outgrowth. Six weeks post infection, I assessed the number of wells with proliferating cells by an MTT-assay.

TR⁻ VLPs, but not gp350+/GFP exosomes, significantly fostered the outgrowth of B95.8-infected cells. At limiting doses of B95.8 virus (0.5µl/well), the additional infection with TR⁻ VLP boosted the outgrowth most prominently (figure 3.12A). Control plates did not show any proliferating cells after 6 weeks of culture. The supportive effect of TR⁻ VLPs at low concentrations of B95.8 particles considerably illustrated the relevance of packaged RNAs for the establishment of latency. The particle concentration of TR⁻ VLP and gp350+/GFP+

exosome preparations were adjusted by infection of Raji cells and FACS analysis of GFP fluorescence (figure 3.12B).

Taken together, this assay provided evidence that particle-mediated transfer of viral RNAs to target cells significantly increased EBV's capacity to transform primary B-cells. These findings support the hypothesis that transcription-independent translation of viral proteins enhances the success of EBV to infect primary B cells and to establish a latent infection.

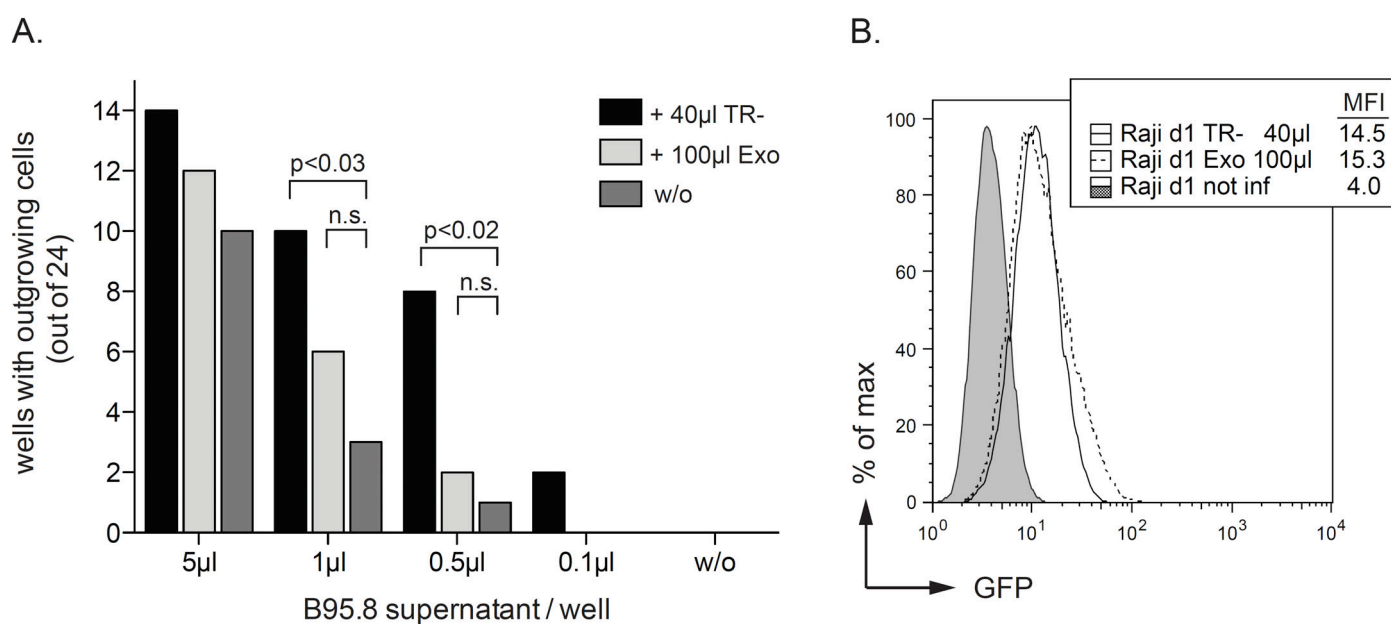


Figure 3.12: Co-infection of primary B cells with EBV and TR⁻ VLP enhances the transformation potential of B95.8 virus stocks.

A. Limiting dilution assays were performed with B95.8 supernatant. Either TR⁻ VLPs (TR⁻), gp350+GFP+ exosomes (Exo) or no additives (w/o) were included to the infection. After six weeks of culture, the number of wells with proliferating cells was determined by an MTT assay. Significances of differences were calculated by Fisher's exact test, n.s.: not significant ($p > 0.05$).

B. The particle concentration of TR⁻ VLP and gp350+/GFP+ exosome preparations were adjusted by infection of Raji cells and FACS analysis of GFP fluorescence 1dpi.

DISCUSSION

1. EBV balances immune evasion to prevent counter-mechanisms

1.1 Unraveling viral immune evasin mechanisms by reverse genetics

Extensive investigations led to detailed knowledge on the latent and the lytic phase of EBV. A variety of sophisticated viral mechanisms have been unraveled including principles of virus-mediated growth transformation of B cells, different types of latency and efficient immune evasion strategies (Cohen, 1999; Rensing et al., 2008). However, much of this knowledge results from model systems, which rely on ectopic expression of single viral genes at high levels. These studies revealed dedicated protein functions, but the models did not reflect viral function during the process of infection. In a seminal work, Hammerschmidt and colleagues (Delecluse et al., 1998) established a recombinant system to produce infectious EBV from an engineered viral BAC genome, which made the virus amenable to reverse genetics. Based on this work and further optimization of BAC modifications (Warming et al., 2005), straight-forward investigations can now be performed on loss-of-function situations. This option provides the possibility to study the contribution of single viral factors during infection of primary human B cells (Delecluse et al., 2008).

I applied reverse genetics to study BNLF2a and its contribution to the evasion of CD8+ T cell recognition. In general, my observations are in line with data from previous overexpression experiments (Hislop et al., 2007; Horst et al., 2009), but my data additionally show that BNLF2a is of high importance during the initial phase of infection. It became evident that no other viral gene complements BNLF2a's function. Its deletion causes strongly increased immunogenicity of EBV-infected cells, which is most apparent early after infection.

In contrast to previous publications (Zeidler et al., 1997), my experiments with *BCRF1*-negative EBV indicated that the endogenous expression level of BCRF1 hardly influences TAP levels and antigen presentation on MHC I molecules. After viral infection of primary B cells the amounts of vIL-10 are insufficient to decrease TAP2 levels, but I observed systemic effects on cytokine orchestration and impaired NK cell function. My findings rank vIL-10 as an important immune evasin, addressing however a different compartment of immune effectors than BNLF2a.

These data emphasize the importance of loss-of-function approaches to interpret gene functions. The outcome of loss of endogenous gene expression can be significantly different from overexpression or artificial administration, as shown here for BCRF1.

However, loss-of-function analyses can also be misleading when gene deletions interfere with the expression of neighboring genes or cis-acting promoter elements. Depending on the genomic structure, modifications of the EBV genome were thus realized by different approaches of mutagenesis in this study.

BCRF1 was replaced by a prokaryotic selection marker. The open reading frame (ORF) of *BCRF1* did not overlap with adjacent genes or promoters and thus allowed for complete replacement. A similar strategy could be applied for the replacement of the *EBER* genes in the second part of this work.

The *BNLF2a* ORF shares the transcript with *BNLF2b*. Therefore, I mutated the methionine1-codon to prevent translation. No information is available on the regulation of translation for *BNLF2b*, but considering other bicistronic transcripts, a collateral effect of increased *BNLF2b* translation in case of mutated *BNLF2a* could not be ruled out. The observed *BNLF2a* phenotype could theoretically also result from upregulated *BNLF2b* translation. However, such effects seem unlikely because overexpression of monocistronic cDNA of *BNLF2a* (Hislop et al., 2007) led to a complementary phenotype to that observed with loss of *BNLF2a* function in my experiments.

1.2 **BNLF2a – a dedicated antagonist of antigen presentation**

BNLF2a has important function for the evasion of infected B cells from CD8⁺ T cell responses, in particular during the early phase of infection. Deletion of *BNLF2a* increased TAP-dependent antigen presentation starting as early as one day after infection. However, neither MHC I surface levels nor NK cell-mediated killing were altered by the loss of *BNLF2a*.

1.2.1 **The early phase of infection reveals phenotypes of early lytic genes**

The increased CD8⁺ T cell response to B cells that were infected with *BNLF2a* mutant EBV was expected from previous studies (Hislop et al., 2007; Croft et al., 2009; Horst et al., 2009). These reports, however, dealt with results from artificial expression or induced and spontaneously lytic cells. The very early manifestation of a *BNLF2a* phenotype in the present study illustrates its relevance during the establishment of infection for the first time. The physiological expression levels of *BNLF2a* during the initial phase of infection are obviously sufficient to exert strong function. These findings are in line with reports of an incomplete lytic phase following EBV infection and *BNLF2a* as an early lytic gene (Yuan et al., 2006). My results suggest that this early phase of infection is suitable to reveal phenotypes of early

lytic genes. Simultaneous infection of nearly all cells triggers the synchronized initiation of the initial lytic phase. This circumvents the need for separate considerations of lytic and latent subfractions of an infected LCL culture or even the artificial induction of the lytic phase to obtain enough lytic cells for analyses. Additionally, investigations on the initial phase of infection provide insights into events that are of importance for the success of the virus, but are still only poorly understood. But, comparisons of samples immediately after infection depend on the premise of equal infection and transformation rates. To this end, thorough evaluation of recombinant virus supernatants represent a mandatory requirement.

1.2.2 TAP-dependent antigen presentation represents a vulnerable bottleneck

The observed BNLF2a effects were limited to TAP-dependent epitopes and thus in line with the postulated molecular mechanism of BNLF2a-mediated interference with antigen presentation: BNLF2a binds to the ATP-binding pocket of TAP1 and also blocks interaction of TAP1 with peptides, inhibiting their translocation to the ER (Hislop et al., 2007; Horst et al., 2009).

In analogy, interference strategies of other viruses also aim at the bottleneck of TAP-dependent peptide translocation. Many of them prevent ATP- and peptide-binding to TAP similar to BNLF2a (US6 of hCMV, UL49.5 of HHVX, ICP47 of HSV1), but certain viruses also prevent TAP expression (UL 41 in pseudorabies) or target TAP for degradation (MK3 in mHV68)(Hill et al., 1995; Ambagala et al., 2003; Boname et al., 2004). Hence, TAP interference represents a highly exploited strategy to diminish the presentation of antigens. The advantage for the virus is evident: One viral factor is sufficient to inhibit the presentation of the majority of viral epitopes.

Highly hydrophobic peptides do not rely on TAP translocation but presumably diffuse passively to the ER, where they are loaded onto MHC I molecules (Lautscham et al., 2003). BNLF2a does not affect this mechanism. For EBV, eight TAP-independent epitopes have been characterized so far (Lautscham et al., 2003). Their contribution to the elimination of infected cells is difficult to judge, as the prevalence of these epitopes is variable as well as the frequency of HLA alleles that enable their presentation. The TAP-independent pathway enables antigen presentation although infecting pathogens interfere with TAP-dependent epitope presentation. Hence, interference with TAP severely reduces antigen presentation, but never prevents it completely.

1.2.3 Endogenous BNLF2a expression leaves MHC I levels unaffected

The interference with MHC I antigen presentation usually results in decreased MHC I surface levels, as only epitope loaded MHC I molecules show sufficient stability to dissociate from chaperones and migrate to the cell surface (Purcell and Elliott, 2008). Reduced MHC I surface levels can result from impaired epitope loading, as observed with BNLF2a overexpression (Hislop et al., 2007). In turn, extremely low surface levels of MHC I molecules are recognized as a signal of infection and trigger NK cell cytotoxicity (Long, 1999).

In my experiments, BNLF2a did neither decrease MHC I surface levels nor increased NK cell-mediated killing of EBV-infected cells (figures 2.4 and 2.8). BNLF2a expression levels are obviously tightly balanced to achieve impaired antigen presentation without altering the MHC I surface levels that would evoke NK cell activation. This equilibrium points to a perfect adaptation of immune evasin levels to the host's counter-acting defense mechanisms.

Still, the complete lack of influence of BNLF2a on MHC I surface levels comes to a surprise. Besides the assumed balanced expression of BNLF2a, other viral factors could also be responsible for steady levels of MHC I despite impaired antigen presentation. For hCMV, UL18 and UL142 were identified to mimic MHC I molecules and both were shown to inhibit NK cell-mediated lysis (Beck and Barrell, 1988; Wills et al., 2005; Wagner et al., 2008). Homologous proteins have not been described for EBV, however a similar mechanism might have evolved independently, as observed for the development of various analogous TAP inhibitors in different virus species (Hansen and Bouvier, 2009; Griffin et al., 2010). If such molecules were indeed present on EBV infected cells, they would share at least those domains with human MHC-I molecules that interact with NK cells and that are bound by the MHC-I specific antibody used in FACS analyses (Figure 2.4A, pan-specific HLA-A/B/C antibody).

1.3 *BCRF1*/vIL10 – a secreted immune evasin with differences to hIL-10

The performed experiments on the immune evasive functions of *BCRF1*/vIL-10 pointed to an involvement in cytokine orchestration and the prevention of NK cell-mediated killing of infected cells. The elimination of Δ *BCRF1*- or double k.o.-infected B cells by NK cells was found to be enhanced. At low effector/target rates CD4⁺ T cells improved NK cell-mediated killing in Δ *BCRF1*-infected samples. *BCRF1* deficiency was associated with a more pronounced Th1 cytokine response that presumably accounted for the boost of NK cell activity when CD4⁺ T cells were present.

1.3.1 Endogenous *BCRF1* expression does not influence specific T cell recognition *in vitro*

The observation that *BCRF1* deficiency did not influence MHC I levels or T cell activity (figures 2.4A, 2.5 and 2.6) contrasted with experiments on vIL-10 effects of previous studies (Zeidler et al., 1997; Bejarano and Masucci, 1998; Salek-Ardakani et al., 2002). Presumably, levels of vIL-10 differed significantly between these studies. Levels of different cytokines, and those of IL-10 in particular, are known to be critical for function (Moore et al., 2001). Inappropriate timing and dosage may even evoke opposing effects (Mocellin et al., 2004).

In general, the ad-hoc recognition of targets by activated T cells is independent of secondary signals in case of a strong TCR trigger (Akdis and Blaser, 2001). The conditions to generate and raise T cell clones enrich exactly those T cells with high TCR affinity to EBV targets (Rickinson and Moss, 1997). This experimental setting might have simply masked the direct impact of secreted vIL-10 on T cells. Nevertheless, physiological vIL-10 levels apparently did not affect MHC-I levels and antigen presentation.

1.3.2 vIL-10 and Th1 cytokines

In experiments with PBMC derived effector cells *ex vivo*, *BCRF1* deletion resulted in an immune phenotype. One of the assays revealed a dampening effect of vIL-10 on the Th1 cytokine response. This observation is in line with the known feature of IL-10 to promote Th2 responses and to impair Th1 cytokine secretion (Moore et al., 2001). Interestingly, production of human IL-10 did not complement *BCRF1* deficiency and did not rescue the phenotype. In contrast, IL-10 reached highest levels when cells had been infected with virus that lacked *BCRF1*, but still did not prevent high Th1 levels (figure 2.7). Apparently, vIL-10 impairs Th1 cytokine production with a higher specificity than human IL-10, which at first glance contrasts the described low affinity of vIL-10 to the IL-10R (Liu et al., 1997). However, a number of reports have associated high IL-10 levels with effector activation (Mocellin et al.,

2004). The suboptimal binding of vIL-10 probably induces an intermediate signaling of that might rather induce anergy and prevent Th1 cytokine shedding.

CD4⁺ T cells represent the major source of Th1 and Th2 cytokines, but other cells can also secrete these factors. Dedicated effects of BCRF1 on CD4⁺ T cells were however observed in experiments that investigated the supportive role of CD4⁺ T cells in NK cell mediated killing of infected B cells. This observation strongly contributed to the model that vIL-10 indirectly hampers the induction of cellular immune responses via the inhibition of Th1 cytokine synthesis by CD4⁺ T cells.

Taken together, vIL-10 appears to be of defined inhibitory function for Th1 cytokine responses and might fulfill this task to a larger extent than human IL-10. Hypothetically, the IL10-R induces a weak signaling cascade in case of low affinity binding of viral IL-10 and a strong signal upon high affinity binding of human IL-10. Whether this is indeed the case and why CD4⁺ T cells react on vIL-10 in a particularly sensitive way remains to be elucidated.

1.3.3 vIL-10 impairs NK cells

NK cells can be a source of IL-10 and have regulatory potential on dendritic cells (Vivier and Ugolini, 2009). However, I observed that NK cells can also be inhibited themselves by vIL-10, representing a remarkable advantage for EBV and presumably also for other IL-10 encoding viruses (Rode et al., 1993; Fleming et al., 1997; Kotenko et al., 2000). For human IL-10 in contrast, several publications postulate stimulating effects on NK cell activity (Petersson et al., 1998; Lauw et al., 2000; Parato et al., 2002). The reason that NK cells react differently to hIL-10 and vIL-10 remains elusive and mechanistic reasons are unclear. Generally speaking, the artificial administration of high concentrations of IL-10 probably leads to different outcomes than cellular secretion.

Interestingly, CD8⁺ T cells were shown to recruit cytokine receptors to the immunological synapse upon target recognition, which was shown by fluorescent labeling and time lapse analysis (Maldonado et al., 2004; Maldonado et al., 2009). Hence, sensitivity to cytokines can be regulated by the recipient cell and might also be realized by NK cells. The visualization of such processes at the immunological synapse is technically demanding, but would probably bear interesting insight on the general behavior of NK cells during target recognition.

Patients with X-linked lymphoproliferative disease (XLD), a rare disease with abrogated NK and NKT cell development (Hislop et al., 2010), suffer from symptoms highly similar to infectious mononucleosis in case of EBV infection. This observation represents the link that NK cells importantly contribute to the control of an EBV infection *in vivo*. The EBV microRNA BART2-5' targets the NK cell activating ligand MICB which implies NK cell

mediated immunity (Nachmani et al., 2009). My experiments could contribute the aspect that synthesis of EBV-encoded vIL-10 reduces NK cell killing of infected B cells *in vitro*. To which extent this observation differs for NK cell subsets that are comprised in CD56+ cells (Cooper et al., 2001; Godfrey et al., 2004) could not be derived from this data, but remains to be addressed in future investigations.

1.3.4 vIL-10 and hIL-10 – homologues with different posttranscriptional regulation

Viral IL-10 has apparently acquired distinct features that distinguish it from human IL-10. In addition, expression analyses revealed different transcript levels: Human IL-10 messengers are abundant in primary B cells and not affected by EBV infection. *BCRF1* transcripts, in contrast, were barely detectable and relative levels *per se* suggested a minor contribution compared to hIL-10.

Regulation of human *IL-10* has been intensively studied and occurs on both transcriptional and post-transcriptional level (Mosser and Zhang, 2008). No comprehensive data exist for *BCRF1*. The prediction of promoter binding sites 800 bp upstream of the *BCRF1* ORF by the PROMO algorithm identified binding sites for many of those transcription factors that also regulate *hIL-10* expression (http://algggen.lsi.upc.es/cgi-bin/promo_v3/promo/promoinit.cgi?dirDB=TF_8.3, Messeguer et al., 2002). Apparently, also the *cis*-acting promoter elements of *hIL-10* have been integrated in the viral genome within gene uptake (figure 4.1A). The same regulatory elements can hence drive both *hIL-10* and *BCRF1* expression. Moreover, four BZLF1 binding sites were identified for *hIL-10* and presumably also exist for *BCRF1*, despite they differ in relative distance to the start site of gene transcription (Mahot et al., 2003; Bergbauer et al., 2010). Thus, both genes appear to be also similarly regulated by the viral transactivator BZLF1.

Nevertheless, significant differences in transcript prevalence were detected in this work. In general, cytokine transcripts are highly regulated also at the post-transcriptional level. Tristetraprolin (TTP) represents an important regulator of transcript half-life, as it targets messengers for accelerated decay by binding to an AU-rich element (ARE) (Carballo et al., 1998; Blackshear, 2002). TTP also affects hIL-10 due to its six AUUUA pentamer motifs in the 3' untranslated region (UTR) (Stoecklin et al., 2008). TTP is induced upon EBV-infection and is of presumable importance for this method of transcript regulation during infection (own observations).

Human IL-10 mRNA is targeted by microRNA hsa-miR106a, which is expressed in all cells of lymphoid origin (Sharma et al., 2009). In total, the 5'UTR of 60bp and the 3'UTR of

1032bp flank the 537bp of coding sequence in the transcript of human *IL-10*, rendering it highly prone to additional post-transcriptional regulation mechanisms.

In sharp contrast, EBV genes generally have short UTRs - presumably driven by the evolutionary pressure to reduce the risk of unintended cellular regulation to a minimum. Accordingly, *BCRF1* transcripts comprise a 5'UTR of 44bp and a 3'UTR of just 73 bp. The entire transcript lacks both ARE motifs and a consensus sequence for hsa-miR106a.

Hence, the post-transcriptional regulation of hIL-10 and *BCRF1* differs fundamentally (figure 4.1B). The low abundance of *BCRF1* transcripts might be compensated by a high transcript longevity resulting in levels of vIL-10 protein that are obviously sufficient to cause the distinct phenotypes.

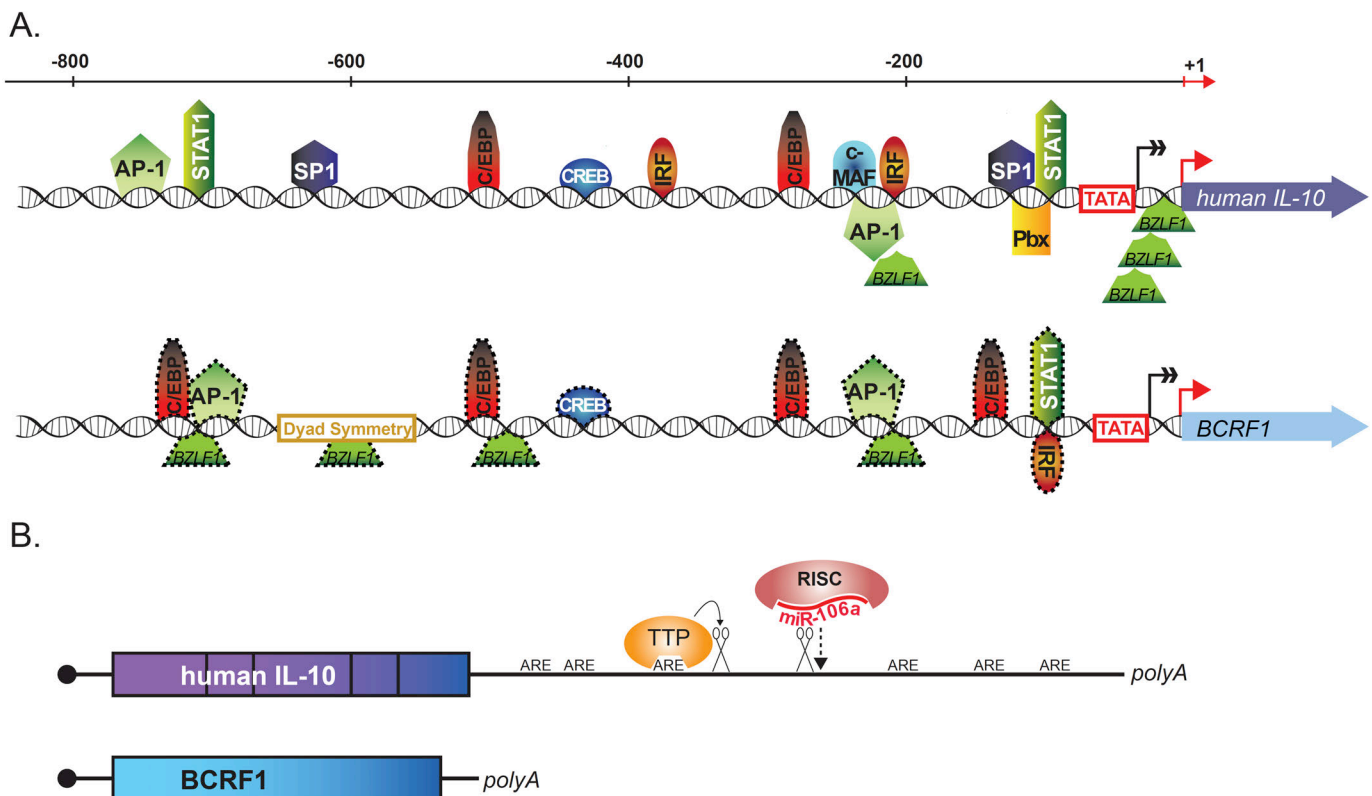


Figure 4.1: Transcriptional and post-transcriptional regulation of *hIL-10* and *BCRF1*. A. Known promoter binding sites for *hIL-10* (Mahot et al., 2003; Mosser and Zhang, 2008) and predicted binding sites for *BCRF1* (symbols with dotted outlines, prediction by the PROMO algorithm, Messeguer et al., 2002, and Bergbauer et al., 2010). Black arrow: transcriptional start, red arrow: translational start, the scale indicates the approximate distance in nucleotides relative to the translational start.

B. Transcript structure of hIL-10 and *BCRF1*, boxes indicate translated sequence with black bars representing exon-exon junctions. Known sites of posttranscriptional regulation are indicated (Stoecklin et al., 2008; Sharma et al., 2009). ARE, AU rich element.

1.4 EBV copes with innate and adaptive immunity

The results of the first part of this study pointed to effective viral mechanisms to evade both the innate and adaptive immune response of NK cells and CD8+ T cells, respectively. In addition, EBV also impairs the Th1 cytokine secretion of CD4+ T cells. Hence, EBV encodes potential modulators of both major arms of the immune system.

The long-term effects of the immune evasive genes *BCRF1* and *BNLF2a* were analyzed in regression assays. This *in vitro* model revealed an impaired outgrowth of cells infected with the double k.o. mutant virus. The impact of deficiency in either *BCRF1* or *BNLF2a* was too weak to lead to a detectable effect *in vitro*. Apparently, only the impairment of both the innate and the adaptive arm of the immune system at the same time led to a more efficient immune control in this *in vitro* setting. The immune control was completely lost when CD4+ T cells were depleted, but depletion of CD56+ NK cells had a minor effect, only. These findings emphasized the importance of CD4+ T cells for in anti-viral immune responses and confirmed the role of NK cells in containment of viral infections but minor contribution to the effective elimination.

Both *BCRF1* and *BNLF2a* are classified as early lytic genes (Yuan et al., 2006). *In vitro*, their pronounced effects during the early lytic phase after infection are sufficient to influence the overall success of LCL outgrowth in the presence of immune effectors. This observation emphasizes the importance of immune evasion during the early lytic phase, which is crucial for the establishment of an EBV infection and for the persistence in sero-positive hosts.

The artificial milieu and technical detection limits of regression experiments *in vitro* might mask additional effects. The obtained results will therefore readily reveal strong effects, but not necessarily reflect the same characteristics that regression *in vivo* would have. Thus, regression assays point out a tendency but hardly ever reflect a complete picture.

1.5 Concluding remarks

With a reverse genetics approach, I was able to discover the physiological impact of BNLF2a and BCRF1 expression on the immune evasion of EBV during the establishment of an infection. I found that BNLF2a is of high importance for infected cells in the early lytic phase to evade the CD8⁺ T cell response. Viral IL-10 was assigned to impair Th1 cytokine secretion by CD4⁺ T cells and to prevent NK cells from eliminating EBV infected B cells, contributing a new aspect to the involvement of NK cells to the immune control of EBV infection. Furthermore, effects of viral IL-10 could be analogous in other IL-10 encoding viruses.

With regard to BCRF1, obtained data shed new light on the function of this viral cytokine, but the mechanism of transcriptional regulation and its perception by effectors demand further investigation. The functional redundancy of vIL-10 and hIL-10 could only be partially confirmed. How different conformations of vIL-10 and hIL-10 lead to different function remains an interesting topic for future investigations.

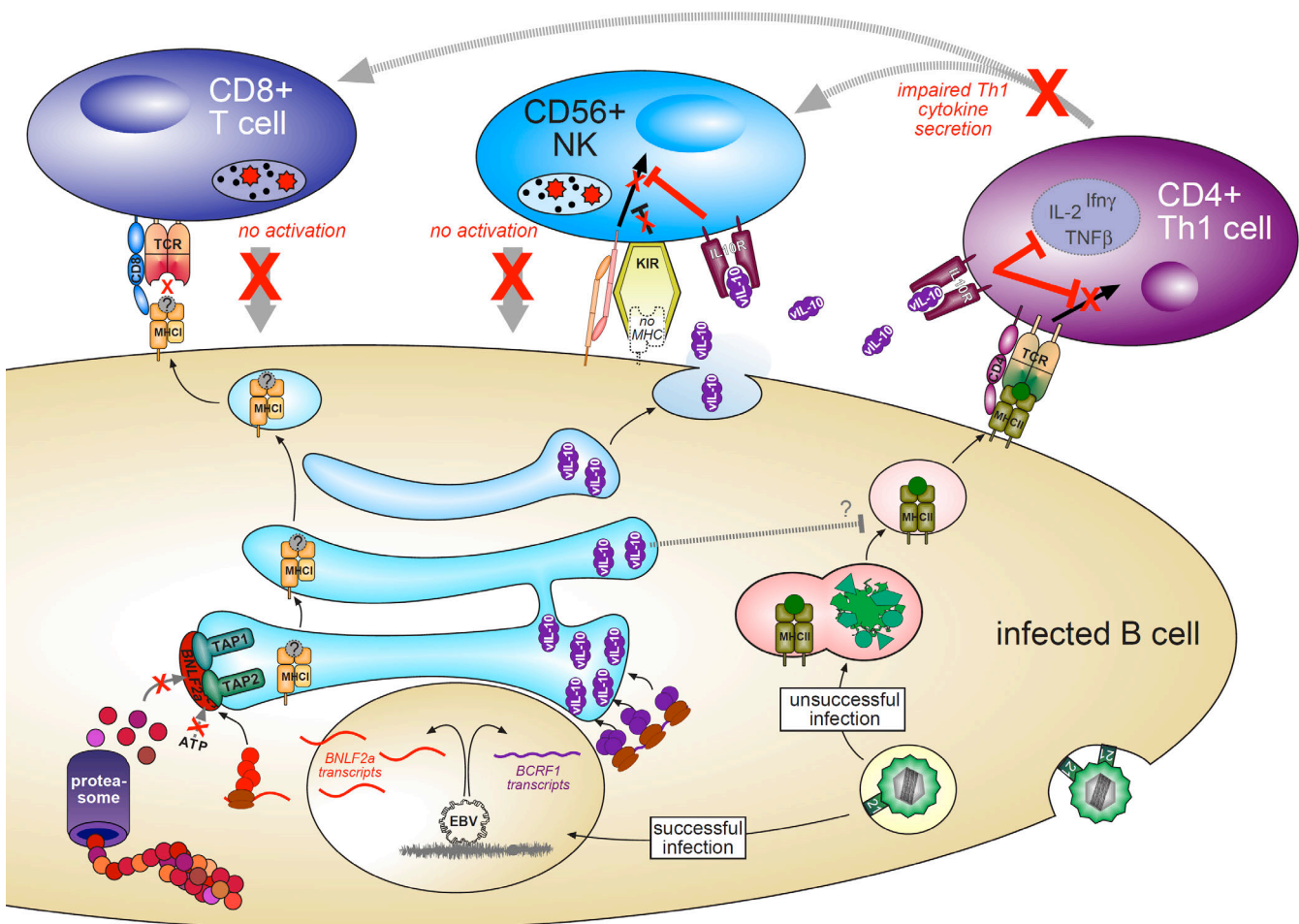


Fig. 4.2: Scheme of BNLF2a and BCRF1 mediated immune evasion. BNLF2a impairs epitope loading onto MHC I, preventing CD8⁺ T cell-activity. vIL-10 impairs NK cell- and Th1 CD4⁺ T cell-activity, presumably by attenuated IL10R signaling. TCR, T cell receptor; KIR, killing inhibitory receptor; NK, natural killer cell; IL10R, IL-10 receptor; 21, CD21.

2. Viron packaged RNAs trigger early events in EBV infection

The second part of this work focused on events that occur concomitantly to infection but influence longterm viral establishment. I could show that EBV particles contain viral RNAs and transfer them to their target cells. During the first few hours of infection, this transfer renders the virus independent from *de novo* transcription. In addition, I could demonstrate the functionality of transferred viral RNAs in different experiments and their contribution to successful establishment of latent infections of B cells.

2.1 Which events trigger the initial lytic phase of EBV?

The classical view of EBV's life cycle in B cells consisted of the primary establishment of latency and eventual reactivation of the lytic phase to give rise to progeny virus. Both phases are associated with distinct expression patterns of viral gene subsets. This biphasic life cycle has recently been revised, as an initial lytic phase was discovered that follows infection and precedes the establishment of latency. In contrast to productively lytic cells, this initial lytic phase does not give rise to progeny virus but enhances the establishment of EBV infection (Kalla et al., 2010).

Kalla and colleagues observed the presence of lytic transcripts 1dpi, *i.e.* the earliest time point assessed. I expanded these findings and could demonstrate that these transcripts were already present in infected cells as early as 2hpi. Although the kinetics of intracellular capsid transport and DNA decapsidation are not known for EBV, it can be deduced from other herpes viruses that these RNAs are most likely co-transferred by the virion and do not require *de novo* transcription (Sodeik et al., 1997; Ojala et al., 2000).

This observation led me to investigate EBV particles for the presence of viral RNAs. The first report on viral transcripts in Herpes viruses dates from Breshnahan and Shenk for human cytomegalovirus (hCMV), followed by similar observations for HSV (Bresnahan and Shenk, 2000; Sciortino et al., 2001). These findings reshaped the established concept of the infection with these viruses, as RNA-transfer had so far not been considered (Roizman, 2000). I could find that RNA is also packaged in EBV virions and that it is transferred during the process of infection.

An initial lytic phenotype comparable to that of EBV has also been described for Kaposi sarcoma associated Herpes virus (KSHV). Interestingly, also KSHV was found to carry RNAs in its virions. These virion transcripts correspond to transcripts that drive KSHV's initial lytic cycle (Krishnan et al., 2004; Bechtel et al., 2005). This renders transferred RNA a likely

trigger of the initial program in KSHV and identical conclusions can be drawn from the data I obtained for EBV in this study. The presence of transcripts for the transactivators of the lytic switch (BZLF1 and BRLF1) is fundamental in this context. Known to create positive feedback loops and to transactivate each other (Miller et al., 2007), the immediate translation of BZLF1 and BRLF1 represents the prerequisite to launch the lytic program. Although the subsequent onset of this phase during the first few days of infection relies on *de novo* transcription from the viral genome, the initiation likely arises from the translation of transferred transcripts of these factors.

2.2 Translation of transferred RNA proves the concept

The presence of messenger, non-coding and microRNA in EBV particles is a new aspect in EBV biology. An effective transfer of mRNA by virus particles however implies their translation within infected cells. Previous studies demonstrated the translation of virally transferred transcripts for selected examples. Along this line, I could immunoprecipitate BRLF1 protein from freshly infected, transcription-inhibited cells and provide first biochemical evidence for the translation of transferred RNAs after EBV infection (figure 3.7).

Additionally, T cell responses constitute a very sensitive assay to detect cellular protein synthesis. Misfolding during translation and natural protein turnover leads to protein degradation. This process generates peptide fragments of any cellular protein and certain peptides from this pool are loaded onto MHC I molecules and presented to cytotoxic CD8⁺ T cells. A presentation of phagocytotically acquired material on MHC I, called “cross-presentation”, is common for dendritic cells but does not occur in B cells (Rock and Shen, 2005). Thus, the epitopes that were detected by clonal T cells in my experiments were derived from viral protein that had been translated endogenously within the presenting B cell. T cells also recognized epitopes from viral proteins on TR⁻ VLP pseudo-infected B cells, which indirectly proved the translation of transferred RNA. Epitope presentation was omitted when translation was inhibited and further substantiates this interpretation.

2.3 Linking RNA transfer to function

The translation of packaged mRNAs in the recipient cell raised the question whether the immediate presence of protein influences any process in the infected cell to a measurable extent. In this study, I could directly link the transferred virion RNAs to function and thus associate them with distinct effects for the first time.

2.3.1 Counteracting RNA induced immunogenicity

The immediate translation of viral RNA in newly infected B cells goes along with immediate presentation of foreign peptides. This puts newly infected B cells at risk to become eliminated by effector T cells. The presence of several transcripts that give rise to immune evasins however points to a viral strategy how to cope with this issue. Indeed, the transfer of BNLF2a transcripts led to a detectable impairment of CD8⁺ T cell responses. The differences reached statistical significant levels, though the recognition of infected, but transcription inhibited cells was of low. With regard to BNLF2a, the levels of transferred RNA are hence far from replacing de novo transcription one day post infection, but do exert function. However, faint effects might already be of importance during the first hours of infection – but this period cannot be precisely addressed with T cell recognition assays. As BNLF2a was among those transcripts that are not de novo transcribed until 8hpi (figure 3.2), the transfer of transcripts circumvents this gap and enables BNLF2a function immediately following infection.

Experiments with TR⁻ VLP pseudo-infected cells illustrated that immune responses were reduced by BNLF2a albeit not completely prevented. A certain immunological challenge due to immediate RNA translation is hence inevitable. To which extent this challenge results in the induction of an adaptive immune response and the elimination of freshly infected cells *in vivo* could not be delineated from these data. Apparently, the remaining risk to raise an immune response is largely compensated by benefits of RNA transfer for successful infection.

2.4 Effects of non-coding RNA

In functional analyses of transferred RNAs the experimental settings usually had to control for putative protein co-transfer by virions. Non-coding transcripts do not give rise to protein and represent the ideal target to analyze functional effects of transferred RNA. EBV encodes several forms of non-coding RNAs that include numerous microRNAs and two non-coding EBV-encoded RNAs (EBER) (Swaminathan, 2008).

2.4.1 EBERs and their functions

EBER1 and EBER2 are two non-coding RNAs of similar length (around 170 nt). They are transcribed by polymerase II and III, lack a poly-A tail and are abundantly expressed in all EBV infected cells.

Their presence has been known for decades (Lerner et al., 1981; Rosa et al., 1981) but their function is still not fully understood. Several approaches to analyze their role with the help of *EBER*-negative EBV did not result in a defined phenotype and led to controversial results (Swaminathan et al., 1991; Komano et al., 1998; Ruf et al., 1999; Gregorovic et al., 2011).

However, EBERs induce defined signaling events in infected cells: EBERs form stem loop structures that bind to toll-like receptor 3 (TLR3) or retinoid acid inducible gene I (RIG-I) (Samanta et al., 2006; Iwakiri et al., 2009). Downstream signaling cascades induce IL-10, which promotes B cell survival, and type I Interferons (Ifn- α and Ifn- β). Many events can induce IL-10 (Moore et al., 2001) and do not necessarily correlate with EBV infection (own observations). In contrast, Ifn- α induction in B cells depends almost exclusively on induction by EBERs in the context of an EBV infection. EBERs themselves prevent autocrine Ifn- α effects by inhibiting RNA-activated protein kinase (PKR) activation that interrupts Ifn- α induced apoptosis signaling (McKenna et al., 2007).

Hence, the secretion of Ifn- α provided a precise indicator for EBER-induced signaling. Accordingly, the generated *EBER*-deficient virus mutants showed strongly impaired Ifn- α induction. These effects were also observed in pseudo-infections with TR⁻ VLP and proved that particle packaged EBERs function in the recipient cell. This observation provided strong evidence that RNA transfer of Herpes viruses is intended to immediately modulate the cellular phenotype.

2.4.2 MicroRNA regulated immune escape

Pfeffer and colleagues discovered that EBV encodes microRNAs (miRs) (Pfeffer et al., 2004), which was followed by analyses on their expression patterns and putative viral and cellular targets (Grundhoff et al., 2006; Dolken et al., 2010). The viral transcripts of LMP1 and BALF5 are targeted by miRs encoded in the BamH1A rightward transcript (BART) region (Lo et al., 2007; Barth et al., 2008). Also two cellular targets have been described, which interestingly belong to the class of immune stimulatory molecules: CXCL11, a T cell attractant, which is targeted by miR BHRF1-3 (Xia et al., 2008), and MICB, an NK cell activating membrane molecule, which is targeted by miR BART2-5' (Nachmani et al., 2009). Whereas most investigations of MICB were performed in epithelial cells, I could show that

MICB is induced in B cells upon EBV infection (figure 3.11). The comparison of MICB levels on B cells that had been infected with recombinant wildtype EBV or microRNA deficient EBV showed notably higher levels when microRNAs were absent. This experiment illustrated that the described effects of EBV microRNAs in HeLa cells (Nachmani et al., 2009) were detectable in EBV infected B cells. Furthermore, this data confirmed functional transfer of microRNAs during the process of particle fusion with infected cells. The influence of virion incorporated microRNAs on immune responses of the infected cells is an important feature, but presumably represents only one aspect out of a multitude of potential effects. The observation that EBV miRNAs participate in the establishment of latency and counteract apoptosis is of special importance in this regard (Seto et al., 2010). The immediate counteraction of apoptosis might represent one of the major advantages that RNA transfer confers to the success of EBV infection.

2.5 RNA in particles: a coincidence or a selective mechanism?

The criteria for RNA packaging into virions can be difficult to analyze and the underlying mechanism may be different for each virus. Accordingly, Shenk and colleagues initially postulated selective packaging of RNA into CMV particles, but showed a few years later that particle transcript levels in virions mirror those of the virus-producing cells (Bresnahan and Shenk, 2000; Terhune et al., 2004). For HSV-I, an RNA-interacting protein was described that is a virion component and mediates RNA loading of particles and the transfer to the cytoplasm of the infected cell (Sciortino et al., 2002). In case of KSHV, exactly those transcripts were detected in viral particles that were subsequently responsible for the initiation of an early lytic phase comparable to EBV (Bechtel et al., 2005).

The comparison of transcript levels in viral particles and producer cells in this study was based on gp350 as a surface marker for virus producing cells. Gp350 presence on cells gives evidence for the completion of the lytic cycle (Al Tabaa et al., 2009) and these cells presumably contribute to the highest extent to particles in the supernatant, rendering them the model of best fit for EBV producing cells.

Assuming that viral particles contain a rather different RNA composition than cells, I consider comparisons of absolute transcript levels inappropriate as this technique relies on the use of equal amounts of RNA. The relative quantification of transcript levels require the identification of a housekeeper with stable levels in both particles and cells that could not be realized in this work.

The given data in figure 3.5 are thus preliminary but point to the following model:

In lytic cells the high prevalence of viral transcripts causes coincidental packaging into particles. In addition, transcripts for certain factors that are crucial for transformation are selectively enriched (here detected for LMP1, LMP2AB and EBER1). Upon fusion with a target cell, all transcripts are delivered and immediately translated in the cytoplasm of the infected cells. Due to the high prevalence of coincidentally packaged transcripts, the translational state of the lytic cell of origin is transferred to the new host cell. Within translation all factors become functional, including the transcription factors of the lytic switch, BZLF1 and BRLF1. The presence of BZLF1 and BRLF1 triggers the early lytic phase that, once initiated, is self-sustaining but excludes the expression of late lytic genes. This would require a certain pattern of genome methylation, which is missing early after infection (Bergbauer et al., 2010). Eventually, the lytic cycle is aborted and the virus switches to latency. Thus, the principal intention of transcript transfer might be the immediate provision of latency factors that accelerate the establishment of the virus – and result in enhanced transformation *in vitro*. The additional transfer of lytic transcripts might be coincidental, but still advantageous. The early lytic phase reactivates the B cell, which is equally essential for successful infection. It is likely that the virus has evolved the virion-mediated transfer of mRNAs to its advantage, because the immediate mRNA presence confers a robust advantage for the establishment of the virus in the cell: The transcripts support cell survival, activate the cell, mediate evasion of immune recognition and help to establish a latent infection.

Interestingly, the detected latent transcripts that are enriched in particles match those that are present at stable levels in the first hours of infection (LMP1, LMP2AB, EBER1; figures 3.2 and 3.5). It remains to be elucidated in which aspect their function is important in the first hours of infection. In contrast, BNLF2a also showed stable levels in the first hours after infection, but the applied method did not indicate BNLF2a transcript enrichment in particles. Hence, how and why viral transcripts are enriched in particles remains a topic for future investigation.

The involvement of the EBV protein EB2 (BMLF1/BSLF1) in the process of RNA selection is interesting. The interaction of EB2 with transcripts was allocated to an RNA binding “arginine rich motif” (ARM), that shuttles unspliced EBV transcripts from the nucleus to the cytoplasm. This function is not restricted to EBV transcripts (Hiriart et al., 2003a). The mutation of this motif abrogates RNA binding and prevents the incorporation of the protein into particles. MutEB2 proteins are still able to shuttle between the nucleus and the cytoplasm and the reason why mutEB2 is not incorporated into particles remains obscure. The

analysis of EB2-shuttling between sites of virion assembly and the cytoplasm might provide new insights to this issue.

If EB2 is present in spontaneously produced B95.8 virus particles and is indeed an important key player in RNA packaging to EBV virions, are challenging open questions for the future.

2.6 RNA transfer increases the chances of virus establishment

To investigate putative effects of RNA transfer on transformation, I applied a modified limiting dilution experiment. Doses of B95.8 virus stocks that barely led to transformation of primary B cells were supplemented with RNA-carrying, genome-free TR⁻ VLPs. This increased the outgrowth rates significantly. Controls did not show this effect and included gp350+ exosomes instead of TR⁻ VLP to assess B cell activation that occurs upon CD21 stimulation (Rock and Shen, 2005). Co-stimulatory signals can increase transformation rates in EBV infection (Iskra et al., 2010) and these samples were reliable controls to assign effects to TR⁻ VLP contents. As the exosome controls did not change outgrowth rates, TR⁻ VLP-transferred RNAs are the most likely reason for improved transformation. This improvement in successful infection provides the virus with an important advantage that obviously compensates for the concomitant hazard of potential immune responses.

In general, virion assembly is always accompanied by the synthesis and release of virus-like particles (VLP). VLPs may still be able to fuse with target cells, but lack a viral genome and do not establish the virus in the cell. So far considered as an inevitable bystander product during virus synthesis, they acquire a functional quality with the observation that VLPs contain RNA (here observed for TR⁻ VLP). The virus probably benefits from their presence: co-infection of the same cell with virion and VLP increases initial transcript amounts and thus promote a faster establishment of infection.

2.7 Concluding remarks

My data represent the first report of RNA in EBV particles. The function of selected transcripts and one microRNA for the process of infection could be demonstrated, such as immediate immune evasion. Moreover, RNA transfer most likely represents the so-far unknown trigger for the initial lytic cycle in freshly infected B cells (Kalla et al., 2010).

Despite the fact that EBV is a DNA virus, it also depends on RNA transfer during infection, which is surprising but in line with other members of this virus family (Bresnahan

and Shenk, 2000; Sciortino et al., 2001; Bechtel et al., 2005). Herpes viruses seem to use this strategy to their benefit.

First experiments support the notion that several transcripts are selectively enriched in the virus particles. It remains a challenging task to analyze the underlying molecular mechanisms and purpose of this selection.

Taken together, the presence of RNA in EBV particles sheds new light on the biology of the Epstein Barr virus and will probably influence future investigations on this topic.

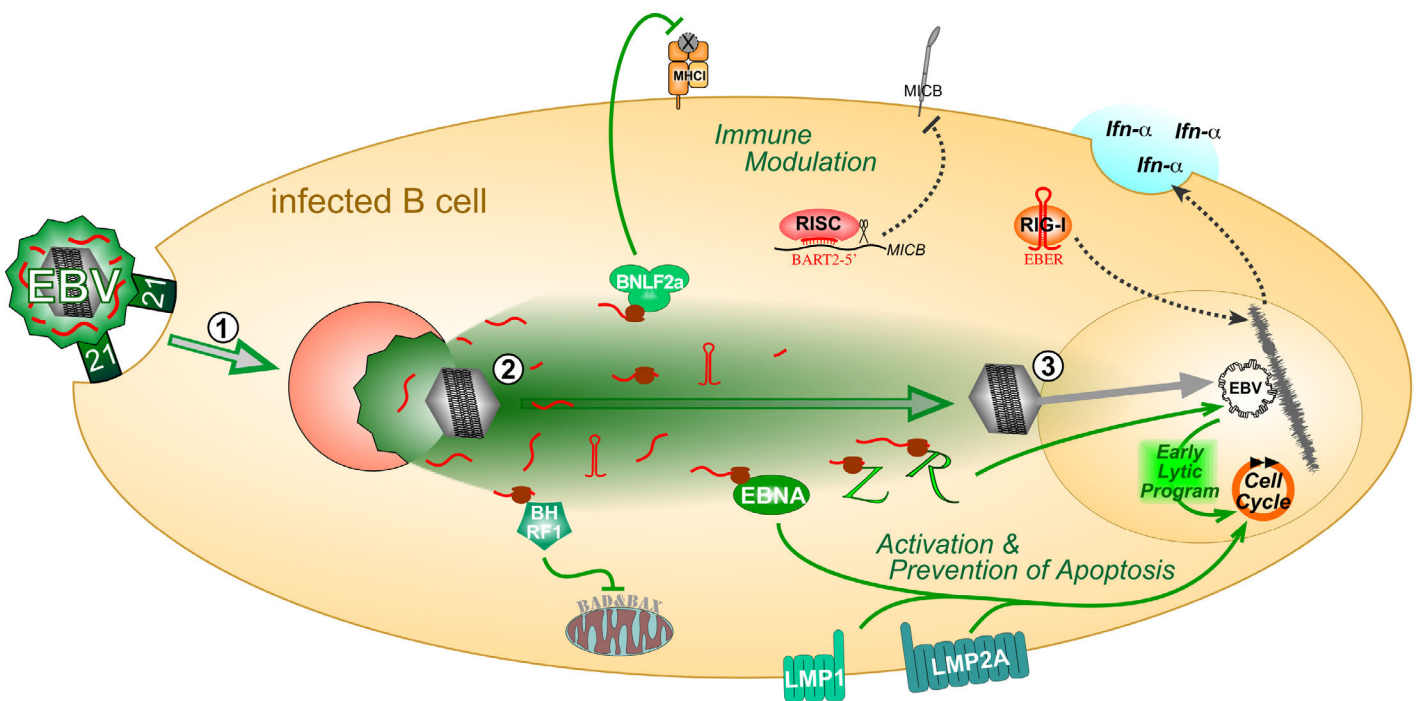


Figure 4.3: Immediate effects of transferred RNA provide a supportive environment for EBV establishment. (1) The virus binds to the B cell and is internalized. The acidic milieu of the endosome induces the fusion of the virion envelope with the vesicle membrane. (2) The virus capsid and the packaged RNAs are released to the cytosol. The immediate translation of messengers and function of non-coding RNAs prevent apoptosis, modulate the immune response of the infected cell and trigger cell activating signaling. (3) The capsid unloads the viral genome into the nucleus and immediately present viral factors initiate the early lytic phase. Effects of transferred RNAs shape an environment that promotes virus establishment independently of *de novo* transcription. Red: packaged viral RNA, green: viral proteins and

MATERIAL & METHODS

1. Material

1.1 General equipment

Agarose gel chamber	Peqlab, Erlangen
Bacteria incubator	Thermo Fisher, Waltham, USA
Blotting apparatus	Trans-Blot SD, Bio-Rad, München
Centrifuges	Avanti J-26 XP, Beckman Coulter, Krefeld Multifuge 3L-R, Heraeus, Hanau 5415R, Eppendorf AG, Hamburg
Electroporation device	GenePulser II, BioRad, München
ELISA plate reader	EL-800, BIO-TEK Instruments, Bad Friedrichshall
FACS machine	FACSCalibur, BD, Franklin-Lakes, USA
FACS sorter	FACSAria, BD, Franklin-Lakes, USA
Film developing machine	CP100, AGFA, Mortsels, Belgium
Fluorescence plate reader	Wallac Victor2 1420, PerkinElmer, Rodgau-Jügesheim
Heating blocks	Eppendorf AG, Hamburg
Hybridization oven	Kendro, Langenselbold
Light Cycler	LC480, Roche, Basel, Switzerland
PCR Cycler	Biometra, Göttingen
pH meter	WTW, Weilheim
Pipets	Gilson, Limburg-Offheim Brand, Wertheim Integra Biosciences, Zizers, Switzerland
Quantification of nucleic acids	nanodrop, PeqLab, Erlangen DanaQuant 200, Hoefer, Holliston, USA
Rotors for ultracentrifuges	70Ti, TFT 75.13, SW28, SW30, TL-100, Beckman Coulter, Brea, USA
SDS PAGE device	Hoefer MightySmall, Amersham, Freiburg
Ultracentrifuges	Optima XL70, Beckman Coulter, Brea, USA TL-100, Beckman Coulter, Brea, USA
UV-transilluminator	Peqlab, Erlangen

1.2 General consumables

Dialysis membrane	Spectra/Por, Spectrumlabs, Breda, Netherlands
ELISA plates	Nunc, Wiesbaden
Films (autoradiography)	Hyperfilm ECL, GE Healthcare, Freiburg Hyperfilm MP, GE Healthcare, Freiburg
NiNTA agarose and columns	Qiagen, Hilden
Nitrocellulose membrane	Hybond ECL, GE Healthcare, Freiburg
Nylon mebrane for nucleic acids	Immobilon-NY+, Millipore, Zug, Switzerland
PCR tubes	ThermoStrips, Thermo Scientific
Pipet tips	Gilson, Limburg-Offheim
Pipet tips with filter	Greiner Bio-One, Kremsmünster, Austria
Polystyrene tubes 15ml, 50ml	BD Falcon, Heidelberg
qPCR 96 well plates for LC480	Roche, Basel, Switzerland
Reaction vials 1.5ml, 2ml	Eppendorf AG, Hamburg
Sephadex columns	NICK columns G50, GE Healthcare, Freiburg
Tubes for ultracentrifugation	Microfuge Tubes 1.5ml, Beckman Coulter, Brea, USA Quickseal Tubes, Beckman Coulter, Brea, USA UZ PA 38.5, Kisker Biotech, Steinfurt

1.3 Cell culture equipment

Fluorescence microscope	Axiovert200M, Carl Zeiss, Jena
Incubator (5% CO ₂)	UniEquip, Martinsried
Irradiation unit	Gammacell 40 (Cs ¹³⁷ , t _{1/2} = 30y), calibration date 15.06.1979, 125,8 R/min, Atomic Energy of Canada Ltd., Ottawa, Canada
Laminar flow hood (S2)	BDK, Sonnenbühl-Genkingen
Microscope	Axiovert25, Carl Zeiss, Jena
Neubauer Counting chamber	Paul-Marienfeld, Königshofen

1.4 Cell culture consumables

96-well round bottom plates	Nunc, Wiesbaden
96-well V-bottom plates	Hartenstein, Würzburg
Cryo tubes	Nunc, Wiesbaden
Culture dishes (ø 10cm,14cm)	BD Falcon, Heidelberg
FACS tubes	BD Falcon, Heidelberg
Filter mesh for 50ml Tube	BD Falcon, Heidelberg
Filter units, 0.8µm pore size	Schleicher&Schuell, Dassel
Flat-bottom plates (6-/12-/24-/48-/96-well)	BD Falcon, Heidelberg
Needle for BAC extraction (CsCl gradient)	2.1x38mm, Bovivet, Henry Schein Vet, Hamburg
Roller bottles	BD Falcon, Heidelberg
Serological pipets	Greiner, Kremsmünster, Austria
Syringes, needles and butterflies	Dispomed, Gelnhausen

1.5 Media and solutions for cell culture

Actinomycin D	Merck, Darmstadt
Calcein AM	Invitrogen, Karlsruhe
Cycloheximide	Sigma-Aldrich, St.Louis, USA
Defibrinated sheep blood	Hemostat, Dixon, USA
Fetal calf serum (FCS)	Biochrom, Berlin
Ficoll ("Biocoll")	Biochrom, Berlin
HygromycinB	Invitrogen, Karlsruhe
IL-2 (Proleukin® S)	Novartis, Basel, Switzerland
MTT	Invitrogen, Karlsruhe
OptiMEM	Invitrogen, Karlsruhe
Polyethylenimine (PEI) (MW=25000)	Sigma-Aldrich, St.Louis, USA
Penicillin/streptomycin	Invitrogen, Karlsruhe
RPMI 1640	Invitrogen, Karlsruhe
Trypsin/0.5% EDTA	Invitrogen, Karlsruhe
Türk's solution	Merck, Darmstadt

1.6 Enzymes for molecular biology

Restriction enzymes and other DNA modifying enzymes that are not listed below were purchased from New England Biolabs, Ipswich, USA, or MBI Fermentas, St.Leon-Rot. All enzymes were used with buffers recommended by the supplier.

DNase I (bovine pancreas)	Roche, Basel, Switzerland
DNase I, RNase free (amp. grade)	Invitrogen, Karlsruhe
Klenow fragment	MBI Fermentas, St. Leon-Rot
Klenow fragment for radioactive labeling	High Prime DNA Labeling Kit, Roche, Basel, Switzerland
Lysozyme	Sigma-Aldrich, St. Louis, USA
Pfu PCR	Stratagene, Amsterdam, Netherlands
Proteinase K	Carl Roth GmbH, Karlsruhe
qPCR reaction Mix	LightCycler® 480 SYBR Green Master I, Roche, Basel, Switzerland
reverse transcriptase	SuperScriptIII Kit, Invitrogen, Karlsruhe
RNase A	Applichem, Darmstadt
RNasin	Promega, Mannheim
taq PCR	goTaq, Promega, Mannheim

1.7 Kits for molecular biology and biochemistry

Purpose	Product
Determination of protein content	BCA assay, ThermoScientific, Waltham, USA
ELISA	human Ifn- γ ELISA Kit, human IL-10 ELISA Kit, Mabtech, Nacka Strand, Sweden
ELISA	human Ifn- α lpha Kit (multi-subtype), PBL, Piscataway, USA
Magnetic cell sorting	human B cell isolation Kit II, CD56+ MicroBeads (human), CD4+ Microbeads (human), Miltenyi Biotec, Bergisch-Gladbach
Multiplex ELISA	11plex Th1/Th2 FlowCytomix, BenderMed Systems, Wien, Austria
Plasmid preparation (transfection grade)	EndoFree Plasmid Maxi Kit, Qiagen, Hilden

Preparation of genomic DNA	QIAamp DNA Blood Mini Kit, Qiagen, Hilden
Preparation of microRNA	mirVANA Kit, Ambion, Austin, USA
Preparation of total RNA	RNeasy Mini Kit, Qiagen, Hilden
Purification of DNA	NuceloSpin Extract II, Machery-Nagel, Düren

1.8 Chemicals and reagents

All chemicals and reagents that are not listed below were purchased from Carl Roth GmbH, Karlsruhe, or VWR, Darmstadt, or Sigma-Aldrich, St. Louis, USA.

Agarose	Biozym, Hess
Select Agar	Invitrogen, Karlsruhe
Ethidium bromide	Merck, Darmstadt
γ -P ³² dCTP, 3000Ci/mMol	Hartmann Analytik, Braunschweig
Cesium chloride	Merck, Darmstadt
dNTPs	Fermentas, St.Leon-Roth
Protease Inhibitor “completeMini”	Roche, Basel, Switzerland
BSA (crystalline)	Applichem, Darmstadt
MacConkey Agar	Invitrogen, Karlsruhe
HoechstDye 33258	Hoechst, Frankfurt

1.9 Media, solutions and buffers

Alkaline lysis solution I	50mM Glucose, 25mM Tris-HCl pH 8.0, 10mM EDTA in H ₂ O, store at RT, add RNase A (100µg/ml) before use
Alkaline lysis solution II	0.2M NaOH, 0.1% (w/v) SDS, do not store, prepare freshly
Alkaline lysis solution III	3M KAc, 11.5% (v/v) glacial acetic acid in H ₂ O, store at 4°C
Blocking buffer (WB)	5% (w/w) milk powder, 0.1% Tween 20 in 1x TBS
Church buffer	700ml 10% SDS, 89g Na ₂ HPO ₄ , 4ml H ₃ PO ₄ , 2ml 0.5M EDTA, 10g BSA (pre-dilute in 100ml H ₂ O), adjust pH to 7.2 with H ₃ PO ₄ , H ₂ O ad 1000ml, heat and keep at 40°C
DNA loading dye (5x)	50% glycerol, 0.1 M Tris-HCl pH 7.5, 0.1 M EDTA pH 8, 0.1% SDS, ca. 1% xylene cyanol, 5% bromphenol blue, in ddH ₂ O
DNA staining buffer (10x)	100mM Tris pH 7.4, 10mM EDTA, 1M NaCl
ELISA AP substrate (5x)	5mg/ml p-Nitrophenylphosphate (p-NPP), 0.5mM MgCl ₂ , 50% Diethanolamine, pH 9.5, store at -20°C
Laureth broth (LB)	10g tryptone, 5 g yeast extract, 5 g NaCl, H ₂ O ad 1000 ml, adjusted to pH 7.5 with NaOH, autoclaved
Lysis buffer "RIPA"	50 mM TrisHCl pH 7.4, 1% (v/v) NP-40, 0.5% DOC, 0.1% SDS, 137.5mM NaCl, 1% glycerol, 0.5mM EDTA pH 8.0, add protease inhibitor, do not stock
M63 agar (1 liter)	15g agar in 800mlH ₂ O (autoclave), 200ml M63 salt solution, 1ml 1M MgSO ₄ •7H ₂ O, 10ml 20% (w/v) galactose or 20%DOG+20% glycerol, 5ml biotin (0.2mg/ml), 4.5ml L-leucine (10mg/ml), antibiotic as selection marker
M63 salt solution (5x)	10g (NH ₄) ₂ SO ₄ , 68g KH ₂ PO ₄ , 2.5mg FeSO ₄ •7H ₂ O, adjust to pH 7.0 with KOH, add H ₂ O ad 1000ml and autoclave
M9 salt solution	6g Na ₂ HPO ₄ , 3g KH ₂ PO ₄ , 1g NH ₄ Cl, 0.5g NaCl, H ₂ O ad 1000ml, autoclave
PBS	138 mM NaCl, 2.7 mM KCl, 8.1 mM Na ₂ HPO ₄ • 2 H ₂ O, 1.76 mM KH ₂ PO ₄ in H ₂ O, ph=7.4
SDS PAGE running buffer	125mM Tris-HCl, 14.4% (w/v) glycine, 1% (w/v) SDS
SDS PAGE sample buffer (Laemmli)	62.5mM Tris/HCl (pH 7.4), 20% (v/v) glycerol, 2% (w/v) SDS, 5% β-mercaptoethanol, 0.0625% (w/v) bromphenol blue

SDS PAGE separating gel (12.5%, 4 mini-gels)	8ml separating gel buffer (4x), 10.7ml H ₂ O, 13.3ml 30%Acrylamid/8%Bisacrylamid, 200µl APS, 30µl TEMED
SDS PAGE stacking gel (5%, 4 mini-gels)	3.75ml stacking gel buffer (4x), 8.75ml H ₂ O, 2.5ml 30%Acrylamid/8%Bisacrylamid, 100µl APS, 15µl TEMED
Separating gel buffer (4x)	0.5M Tris-HCl (pH 6.8), 0.4% (w/v) SDS
Special TE	50mM Tris-HCl pH 8.0, 20mM EDTA
SSC (20x)	175.3g NaCl, 88.2g Sodium citrate dihydrate (M=294.1), 800ml H ₂ O, adjust to pH 7.0, add H ₂ O to 1000 ml
Stacking gel buffer (4x)	1,5M Tris-HCl (pH 8,8), 0,4% (w/v) SDS
Standard TE	10mM Tris-HCl pH 8.0, 0.1 mM EDTA
TAE (50x)	242 g Tris, 100 ml 0.5M Na ₂ EDTA pH 8.0, 57.1 ml glacial acetic acid, H ₂ O ad 1000 ml
TBE (5x)	54 g Tris, 27.5 g H ₃ BO ₃ , 3.72 g Na ₂ EDTA, H ₂ O ad 1000 ml
TBS (10x)	24.2 g Tris, 80g NaCl, H ₂ O ad 1000ml
TfB I (competent bacteria)	30mM KAc, 100mM RbCl, 25mM CaCl ₂ , 50mM MnCl ₂ , 15% glycerol, adjust pH to 5.8 (Ac) before adding glycerol
TfB II (competent bacteria)	25mM MOPS, 75mM CaCl ₂ , 25mM RbCl, 15% glycerol, adjust to pH 6.5 (KOH) before adding glycerol
Transfer buffer (semi-dry blotting)	39 mM glycine, 48 mM Tris, 0.0375% SDS, 20% MeOH
Washing buffer (WB)	0.1% Tween20 in TBS

1.10 Antibodies

1.10.1 Antibodies for FACS stainings

Specificity	Conjugate	Clone	Supplier	Dilution
CD3	PE.Cy5	HIT3a	BD Pharmingen, Heidelberg	1:50
CD4	PE	RPA-T4	BD Pharmingen, Heidelberg	1:50
CD8	APC	RPA-T8	BioLegend, SanDiego, USA	1:100
CD19	FITC	HIB19	BD Pharmingen, Heidelberg	1:50
CD56	PE	B159	BD Pharmingen, Heidelberg	1:100
MHC-I	PerCP	W6/32	BioLegend, SanDiego, USA	1:100
MHC-II	PerCP	TÜ39	BD Pharmingen, Heidelberg	1:100
MICB	none*	236511	R&D Systems, Minneapolis, USA	0.5µg/µl
gp350	none*	72A1	E.Kremmer, HelmholtzZentrum, München	not diluted (hybridoma SN)
mouse-Ig	APC	polyclonal	Invitrogen, Karlsruhe	1:500

* cells were counterstained by anti-mouse-Ig/APC

1.10.2 Antibodies for immune biochemistry

Specificity	Source	Clone	Supplier	Dilution (Western blot)
Rta / BRLF1	mouse	8C12	E.Kremmer, HelmholtzZentrum, München	1:100 (hybridoma SN)
Zta / BZLF1	mouse	BZ1	E.Kremmer, HelmholtzZentrum, München	1:50 (hybridoma SN)
gp350	mouse	72A1	E.Kremmer, HelmholtzZentrum, München	1:5 (hybridoma SN)
FLAG®	mouse	M2	M2, Sigma-Aldrich, St.Louis, USA	1:2000
c-MYC	mouse	9E10	E.Kremmer, HelmholtzZentrum, München	1:20 (hybridoma SN)
anti-mouse IgG, HRP coupled	goat	polyclonal	Promega, Madison, USA	1:10000

1.11 Oligonucleotides

Oligonucleotides were synthesized by Metabion GmbH, Martinsried.

1.11.1 Primers for standard PCR:

PCR	Primer name	Sequence (5'-3')	product size(bp)	Annealing (°C)
BCRF1	BCRF1 intern fw	TGGAGCGAAGGTTAGTGGTCAC	300	58
	BCRF1 intern rev	ATGGTCTTTGGCTTCAGGGTCC		
wtBNLF2a	common BNL2a fw	GAGCAGGCATAAAAAGTCCAA	188	58
	BNLF2a wt rev	GCCTCACTCTCGAGATGG		
ΔBNLF2a (M1STOP)	common BNL2a fw	GAGCAGGCATAAAAAGTCCAA	192	58
	BNLF2a ko rev	CTGTGCCCTCACTCTCGACTAGT		
oriP	oriP fw	GTCTTGGTCCCTGCCTGG	528	53
	oriP rev	GGTTAGTAAAAGGGTCCTAAGGAAC		
BNLF2b	BNLF2b fw	ACGATGGCGGAAACAACCTC	604	54
	BNLF2b rev	TCCAAAAGGTCAAAGAACAAGG		
EBV genotype	common EBV fw	ATCGACGTATCGCTGGAAAC	348	60
	wt/MABA EBV rev	ATCCTGTTCACAGTGGTGGT	489	
	B95.8 EBV rev	CAGTCCCTGATCGTCCCTCCTC	742	
	rec. EBV rev	CTTGTATGGAGCAGCAGACG		

1.11.2 Primers for maxiEBV cloning

Replacement	Primer name	Sequence (5'-3')
BNLF2aSTART → BNL2aGalK	BNLF2aGalK_fw	¹⁷⁷²⁶⁷ CCGCAGGCAGAGGACTGCTGCTCTAGCAAAGCACGCTCCAGG ACGTGTA ¹⁷⁷³¹⁶ <i>CCTGTTGACAATTAATCATCGGCA</i> _{pGalK}
	BNLF2aGalK_rev	¹⁷⁷³⁷² TGTCCTTACTGTATAAAAAGTCCACGAAAACAGCTGTGCCTCA CTCTCGA ¹⁷⁷³²² <i>TCAGCACTGTCCTGCTCCTT</i> _{pGalK}
BNLF2aGalk → BNL2aSTOP	BNLF2aSTOP_fw	¹⁷⁷²⁵⁸ GAAGAGCCGGGCAGGCCGAGGCAGAGGACTGCTGCTCTAGC AAAGCACGCTCCAGGACGTGTA ¹⁷⁷³¹⁶ <u>ACTAG</u> ¹⁷⁷³²² <u>TCGAGAGTG</u>
	BNLF2aSTOP_rev	¹⁷⁷³⁸⁵ CTGGCCTTCTTTCTTGTCTTACTGTATAAAAAGTCCACGAA AACAGCTGTGCCTCACTCTCGA ¹⁷⁷³²² <u>CTAGT</u> ¹⁷⁷³¹⁶ <u>TACACGTCCT</u>
EBER locus → GalK	EBERGalK_fw	⁵⁹³⁰ CATTAACCTCAACCACAAAATGGGGGTTGGAGAAAGTAACCAC ATATACT ⁵⁹⁷⁹ <i>CCTGTTGACAATTAATCATCGGCA</i> _{pGalK}
	EBERGalK_rev	⁷²⁵⁹ GAACTAAGACTGGGTGTCCAGGAAACCCTGTACAGAATTGAT TGGCAAAGG ⁷²⁰⁷ <i>TCAGCACTGTCCTGCTCCTT</i> _{pGalK}

bold letters: homology to the EBV genome; superscripted numbers: genomic position of homologous sequence in p2089; *italic letters:* matching sequence in PCR template; subscripted: template vector; underlined: complementary region of primer pair.

1.11.3 Primers for quantitative PCR

Target (transcript)	forward primer (5'-3')	reverse primer (5'-3')	product size(bp)
BZLF1	CTGGTGTCGGGGGATAAT	TCCGCAGGTGGCTGCT	107
BRLF1	CCTGTCTTGGACGAGACCAT	AAGGCCTCCTAAGCTCCAAG	100
BMRF1	CGTGCCAATCTTGAGGTTTT	CGGAGGCGTGGTTAAATAAA	116
BNLF2a	TGCTGACGTCTGGGTCCCT	TGCTTTGCTAGAGCAGCAGT	98
BCRF1	ACCTTAGGTATGGAGCGAAG	GGGAAAATTGTCACATTGGT	110
BGLF5	TTCGGCCGCTATTAGCTTAG	GACGGGGGAATAATCAACCT	75
BHRF1	CATCTGGAACGGCTTACCTC	CCCTTGTGAATAGGCCATC	82
BALF1	ACCGCAAACACCACTGTGTA	CGCAGTGTACAACGACCACT	75
LMP1	AGGCTAGGAAGAAGGCCAAA	CTGTTTCATCTTCGGGTGCTT	109
LMP2AB	ATCGCTGGTGGCAGTATTTT	GAGTATGCCAGCGACAATCA	105
EBNA2	ACATGAACCGGAGTCCCATA	TGCGGGGTCTATAGATGGAG	82
EBER1	GACCTACGCTGCCCTAGAGTTTTGC	CCAGCTGGTACTTGACCGAAGACG	150
EBER2	GGACAGCCGTTGCCCTAGTGG	AGCGGACAAGCCGAATACCCTTC	166
TAP1	CTCCCTCAGGGCTATGACAC	ACACGGTTTCCGGATCAAT	105
TAP2	AGCATATCGCCTCGACTCAC	GATCTCCCGAAGCACTTCCT	105
GUSB	CGCCCTGCCTATCTGTATTTC	TCCCCACAGGGAGTGTGTAG	91

1.11.4 Stem-loop primers and qPCR primers for microRNAs

Common stem-loop primer start sequence (5' terminus, 5'-3'):
GTTGGCTCTGGTGCAGGGTCCGAGGTATTTCGACCAGAGCCAACCTGTAC...

Target (microRNA)	Specific first strand primer terminus*(5'-3')	qPCR forward primer (5'-3')	product size(bp)**
BHRF1-1	...CAACTCC	AGAGTAACCTGATCAGCCCC	59
BHRF1-2 3'	...CTCAATT	GGCGTATCTTTTGCAGGAGCA	59
BHRF1-3	...CTGTGCT	GGCGTAACGGGAAGTGTGTA	59
BART1 5'	...CCACAGC	CGGTCTTAGTGGAAGTGACGT	60
BART2 5'	...CGCAAGG	GCCGGTATTTTCTGCATTTCGC	60
BART3 5'	...CAGCACA	GGCGGACCTAGTGTAGTGT	59
BART15	...CTCAAGG	GGCGGGTCAGTGGTTTTGTTT	60

Common miR-qPCR reverse primer (5'-3'): GTGCAGGGTCCGAGGT

* first strand synthesis was performed with miR specific stem-loop primers with a common part (5' terminus) forming the stem-loop and a specific part (3' terminus) annealing to the microRNA

** product sizes are related to qPCR products generated with the combination of miR-specific forward primer (see row) and common qPCR reverse primer

1.12 Plasmids

Plasmid No. (AGV database)	Description
p509	BZLF1 expression plasmid, lytic phase induction in recombinant producer cells
p2670	BALF4 expression plasmid, used for increased virus synthesis in induced producer cells
p2130	BRLF1 expression plasmid, overexpression in 293 cells (control lysates)
p2242	gp350 expression plasmid, used for gp350+ exosomes synthesis
p2104	GFP expression plasmid, used for GFP+ exosome synthesis
pGalK	GalK cassette encoding plasmid, PCR template for synthesis of recombination fragments
p3964	BCRF1-6xHis expression plasmid, generation of recombinant vIL-10
p3965	hIL-10-6xHis expression plasmid, generation of recombinant hIL-10
pAACFLAG EB2	EB2-FLAG, used for EB2 overexpression in virus producer cells (see also Hiriart et al., 2003a)
pAACFLAG EB2mut	EB2mutant-FLAG, used for EB2mut overexpression in virus producer cells (see also Hiriart et al., 2003a)
p3866	Cloning vector for prokaryotic kanamycin resistance cassette flanked by BCRF1-neighboring homology arms

1.13 maxiEBV BACs

Plasmid No. (AGV database)	Name	Description
p2089	recombinant wildtype	BAC encoding the EBV B95.8 genome, extended for CMV promoter driven expression of hygromycin resistance and GFP (Delecluse et al., 1998)
p2114	TR ⁻	like p2089, but with deletion of the terminal repeats (Delecluse et al., 1999)
p3912	Δ BCRF1	like p2089, but with the BCRF1-ORF replaced by a prokaryotic kanamycin resistance cassette
p4030	Δ BNLF2a	like p2089, but with transmutation of 5 nucleotides at the start of the BNLF2a-ORF to a STOP-codon
p4031	double k.o.	like p4030 with additional deletion of the BCRF1-ORF like in p3912
p4661	Δ EBER	like p2089 with replacement of both <i>EBER</i> genes by a prokaryotic GalK expression cassette
p4662	TR ⁻ Δ EBER	like p4661 with replacement of both <i>EBER</i> genes by a prokaryotic GalK expression cassette

For details on cloning and generation of producer clones with maxiEBV-BACs see Methods, chapter 2.1.4.

1.14 Bacterial strains

Escherichia coli DH5a	<i>F</i> -, <i>F80dlacZDM15</i> , <i>D(lacZYA-argF)</i> , <i>U169</i> , <i>deoR</i> , <i>recA1</i> , <i>endA1</i> , <i>hsdR17(rk-,mk)</i> , <i>supE44</i> , λ -, <i>thi-1</i> , <i>gyrA96</i> , <i>relA1</i>
Escherichia coli SW105	<i>F</i> - <i>mcrA</i> Δ (<i>mrr</i> - <i>hsdRMS</i> - <i>mcrBC</i>) Φ 80 <i>dlacZ</i> M15 Δ <i>lacX74</i> <i>deoR</i> <i>recA1</i> <i>endA1</i> <i>araD139</i> Δ (<i>ara</i> , <i>leu</i>) 7649 <i>galU</i> Δ <i>galK</i> <i>rspL</i> <i>nupG</i> [<i>λ</i> <i>cI857</i> (<i>cro</i> - <i>bioA</i>) $\langle \rangle$ <i>tet</i>], (from Warming et al., 2005)

1.15 Eukaryotic cell lines

B95.8	EBV B95.8 infected lymphoblastoid marmoset cell line	(Miller et al., 1972; Miller and Lipman, 1973)
Raji	EBV positive Burkitt lymphoma cell line	(Pulvertaft, 1964)
Daudi	Burkitt lymphoma cell line subcloned for EBV-loss	(Klein et al., 1968; Nanbo et al., 2002)
HEK-293	human embryonal kidney cells	(Graham et al., 1977)
293/TR ⁻ 2	HEK-293 stably transfected with p2114, recombinant TR ⁻ VLP producer cell line	(Delecluse et al., 1998)
293/2089	HEK-293 stably transfected with p2089, recombinant wildtype EBV producer cell line	(Delecluse et al., 1998)
293/3912.27	HEK-293 stably transfected with p3912, recombinant Δ <i>BCRF1</i> EBV producer cell line	established in this study
293/4030.J9F	HEK-293 stably transfected with p4030, recombinant Δ <i>BNLF2a</i> EBV producer cell line	established in this study
293/4031.J2	HEK-293 stably transfected with p4031, recombinant Δ <i>BCRF1</i> Δ <i>BNLF2a</i> (double k.o.) EBV producer cell line	established in this study
293/4661.36	HEK-293 stably transfected with p4661, recombinant Δ <i>EBER</i> EBV producer cell line	established in this study
293/TR ⁻ 4662.12	HEK-293 stably transfected with p4662, recombinant TR ⁻ Δ <i>EBER</i> VLP producer cell line	established in this study

1.16 EBV specific T cell clones

EBV specific T cell clones had been raised from PBMCs of EBV positive donors according to standard protocols (Moosmann et al., 2010) and were a kind gift from A. Moosmann. The following clones and their described epitopes were used:

short name	clone name	epitope	protein of epitope origin	HLA restriction	first identification
RAK	LSK-RAK#17	RAKFKQLL	BZLF1	B*0801	(Bogedain et al., 1995)
QAK	LSK-QAK#21	QAKWRLQTL	EBNA3a	B*0801	(Burrows et al., 1994)
IED	JN-IED#16	IEDPPFNSL	LMP2	B*4001	(Lee et al., 1996)
CLG	JG-CLG#18	CLGGLLTMV	LMP2	A*0201	(Lee et al., 1993)
GLC	MA-GLC#14	GLCTLVAML	BMLF1	A*0201	(Steven et al., 1996)
YVL	MA-YVL#1	YVLDHLIVV	BRLF1	A*0201	(Saulquin et al., 2000)

1.17 Primary cells

1.17.1 PBMCs

Peripheral blood mononuclear cells (PBMCs) of healthy donors were derived from voluntary blood donations of HLA-typed individuals in accordance to the Helsinki declaration of the World medical association on medical research with humans.

1.17.2 Adenoid tissue

Anonymized adenoid tissue samples from routine adenoidectomies were provided by the Department of Otorhinolaryngology, Klinikum Grosshadern, Ludwig-Maximilians-University of Munich. The institutional review board (Ethikkommission) of the Klinikum Grosshadern, approved of the study and did not require prior informed patient consent.

1.18 Software

FACS data	FlowJo 9, TreeStar, Ashland, USA
DNA analysis and vector maps	MacVector 10.0, MacVector Inc., Cary, USA
ELISA analysis	KC4, BioTek Inc., Winooski, USA FlowCytomixPro 2.3, BenderMedSystems, Wien, Austria
Image editing	Photoshop CS3, Adobe, San Jose, USA Illustrator CS3, Adobe, San Jose, USA Freehand MX, Macromedia, San Francisco, USA
Spreadsheet programs and statistical analyses	Excel 2008, Microsoft, Seattle, USA Prism 5, GraphPad Software, La Jolla, USA
qPCR analyses	LightCycler480 Software SP3, Roche, Basel, Switzerland
Word processor	Word 2008, Microsoft, Seattle, USA
Bibliography	EndNote X4, ThomsonReuters, San Francisco, USA

2. Methods

2.1 Molecular biology

2.1.1 Bacterial culture

Suspension cultures of bacteria were grown in LB medium at 37°C under aerobic conditions (shaking with 200rpm). Single cell clones were raised on LB-agar plates.

Bacteria were selected for resistance by addition of 100µg/ml ampicillin, 30µg/ml chloramphenicol or 100µg/ml kanamycin to the medium.

For long-term storage of bacteria, 500µl of a dense liquid culture were mixed with 500µl of 100% glycerol and stored at -80°C.

2.1.2 Generation and transformation of chemically competent bacteria

To generate stocks of chemically competent bacteria, 5ml of LB medium without antibiotics were inoculated with bacteria from a single clone and grown to a dense culture (o/n). This culture was expanded to two flasks with 400ml LB medium without antibiotics and grown at 30°C until the suspension reached an OD₆₀₀ of ~0.6. Bacteria were pelleted by centrifugation at 2000 g at 0°C for 10min and kept on ice. All following steps were performed on ice in the cold room and pre-chilled materials were used. The pellets were carefully resuspended in 80ml Tfb I buffer, pooled and centrifuged at 2000 g at 0°C for 10min. The supernatant was accurately removed and the pellet was resuspended in 20ml TfbII buffer followed by 15min of incubation on ice in the cold room. The suspension was aliquoted, shock-frozen on dry-ice and stored at -80°C. The competence in uptake of DNA was evaluated by transformation of 50µl competent bacteria with 10pg of plasmid DNA, that usually resulted in 50-100 colonies.

For transformation, competent bacteria were thawed on ice. For each sample, an aliquot of 50 µl was transferred into pre-chilled Eppendorf tubes and mixed gently with either 10 µl of a ligation mixture or 1-10 ng of plasmid DNA. After incubation on ice for 15 min the transformation reaction was heat shocked for 45 seconds at 42°C and subsequently placed on ice for additional 2 min. Following, the reaction mix was plated on agar plates and incubated o/n at 37°C.

2.1.3 Generation and electroporation of electro-competent bacteria

Competent bacteria were prepared by pelleting 40ml of liquid bacteria culture (OD₆₀₀ ≈ 0.6) at 2000 g for 10min at 0°C. The following steps were performed on ice and prechilled materials were used. Bacteria pellets were carefully resuspended in 1ml H₂O by

swirling the tubes in an ice-water slurry. 9ml of H₂O were added and the bacteria were pelleted again. This step was repeated once. After the final washing step, the supernatant was carefully removed by briefly inverting the tubes on a paper towel. The pellet was kept on ice and resuspended autonomously in the remaining supernatant.

For electroporation, 25µl of the electro-competent bacteria were mixed with approximately 50ng of DNA (5µl of a strong PCR product eluated in 50µl) and transferred to a 0.1cm pre-chilled electroporation cuvette. Electroporation was performed at 25µF, 1.75kV and 200 Ω, the cuvette was briefly chilled on ice (2min) and bacteria were resuspended in 1ml LB medium without antibiotics and left to recover and to express antibiotic resistance factors for 1h at 32°C in a shaking incubator. Finally, the cultures were pelleted, resuspended in 50-100µl and streaked on agar plates with appropriate selection.

2.1.4 Engineering of recombinant EBV

The use of recombinant EBV was established by Hammerschmidt and colleagues (Delecluse et al., 1998) and is based on an F-factor plasmid carrying the whole EBV genome of the B95.8 strain with additionally inserted CMV promoter driven expression cassettes for GFP and Hygromycin B phosphotransferase, providing phenotypic markers. A bacterial artificial chromosome (BAC) encoding an EBV genome that can give rise to progeny virus was termed “maxiEBV”.

The applied strategies to replace the *BCRF1* ORF and to prevent BNLF2a translation are depicted in figure 2.1. In analogy to *BCRF1*, the *EBER* genes do also not overlap with neighboring genes and allowed for a similar straight-forward gene replacement.

Genomic engineering was carried out by homologous recombination, based on the E.coli strain SW105 (Warming et al., 2005). This strain is RecA deficient but carries a λ prophage, that encodes RecA under the control of a heat inducible promoter, enabling homologous recombination upon heat shock. Furthermore, these bacteria are incompetent to galactose metabolism due to the lack of the *galK* gene, which provides an option for positive and negative selection.

The *BCRF1* gene was replaced by a prokaryotic expression cassette of Neomycin phosphotransferase II, conferring kanamycin resistance, with flanking arms of 200bp homologous to the EBV sequence up- and downstream of the *BCRF1* ORF. The whole construct of 1500 bp was cut out of the cloning vector p3866 and electroporated into recombination competent SW105 bacteria that contained the recombinant wildtype maxiEBV p2089. Successful recombination allowed for growth of resistant clones on kanamycin containing agar plates (100µg/ml).

The *EBER* genes represent a total fragment of 500bp and were replaced by a GalK expression cassette of 700 bp with an integrated BglIII restriction site. This product was generated by Pfu PCR and the use of the primer pair EBERGalK_fw/rev. The used forward primer consisted of the identical sequence as the 50 (non-priming) bases upstream of the targeted region and the initial 20 (priming) nucleotides of the galK cassette. The reverse primer consisted of the complementary sequence to the 50 (non-priming) bases downstream the targeted region and the terminating 20 (priming) nucleotides of the galK cassette. The PCR product was electroporated to SW105 bacteria that carried the recombinant wildtype EBV genome (p2089) or the TR⁻ genome (p2114) to generate EBV genomes that give rise to *EBER*-deficient EBV virions and *EBER*-deficient TR⁻ VLPs, respectively. After recovery from electroporation, residual amounts of medium were washed three times with M9 salt solution and subsequently plated on M63 minimal agar that contained galactose as exclusive carbon source. Bacteria were incubated for 5 days at 32°C, five colonies were picked and streaked on MacConkey/galactose agar. One bright pink colony from each plate was subjected to further analysis.

Due to a more complex genomic localization, the BNL2a ORF was not replaced, but instead prevented from translation by mutation of 5 nucleotides. The methionine-1 codon was replaced with a STOP-codon and a diagnostic SpeI site was inserted (see figure 2.1). This was realized by a two-step recombination strategy. First, a Pfu PCR product was generated with the primer pair BNL2aGalK_fw/rev from the template vector pGalK. As described above, the PCR product was electroporated to SW105/p2089 bacteria. The five targeted nucleotides were replaced with the galK expression cassette by homologous recombination. Positive clones were selected on minimal media plates with galactose as the exclusive carbon source, subcloned on MacConkey Agar and analyzed by restriction digests. In a next step, a forward primer with the identical 50 homologous bases used before, the desired 5 mutated nucleotides and 15 complementary bases to the reverse primer was used together with a similar reverse primer of opposing orientation. After annealing, these primers formed a 20bp double strand. 5'overhangs were blunted with Klenow polymerase (Fermentas), column purified (Nucleobond Kit, MacheryNagel) and quality checked on an agarose gel. The bacterial clone from the previous step was induced for recombination competence, the new fragment was electroporated and replaced the galK cassette by homologous recombination. Bacteria were in turn counter-selected for galactose metabolism by growth on minimal plates with 2-deoxy-galactose (DOG, toxic when metabolized) and glycerol as carbon sources.

For all engineered maxiEBVs, a restriction digest that generated a knockout specific band pattern due to the integrated additional restriction site during gene replacement indicated successful gene replacement. Overall BAC integrity was confirmed by uniform band patterns upon digestion with restriction enzymes that were not specific for the mutation. Sequencing confirmed the generation of the desired sequence at the intended region.

A detailed description on the procedure can be found in (Warming et al., 2005) and is available online at <http://web.ncifcrf.gov/research/brb/recombineeringInformation.aspx>.

2.1.5 Isolation of plasmid DNA from bacteria

Plasmid DNA for transfection was purified from bacteria by matrix-affinity kits (including endotoxin removal) in accordance to the manufacturers protocol (Qiagen).

For enzymatic screening, plasmid DNA was prepared by alkaline lysis (Sambrook and Russell, 2001). In brief, bacteria from dense 2ml cultures were pelleted at 6000 g for 5min and resuspended in 200µl alkaline lysis solution I (including 50µg RNase/ml). 200µl freshly prepared alkaline lysis solution II, containing 1% SDS and 0.1M NaOH, were added and induced lysis of bacteria. Samples were gently inverted several times and incubated for 5min at RT. The reaction was neutralized by addition of 200µl prechilled alkaline lysis solution III. Samples were shaken vigorously and incubated on ice for 20min. Cellular debris and chromosomal DNA were pelleted by centrifugation for 20min at 16000 g and 4°C. Plasmid DNA was precipitated from the supernatant by adding 500µl of isopropanol, shaking and 10min of incubation at RT. DNA was pelleted by centrifugation for 10min at 16000 g, washed with EtOH and air-dried for 10min at RT. The DNA was resuspended in H₂O or TE and subjected to restriction digests.

2.1.6 Phenol-chloroform precipitation of DNA

The volume of the DNA containing solution was defined and 2.5 volumes of a phenol-chloroform mix (ratio 3:1, Carl Roth GmbH) were added. Following 30 seconds of vortexing, aqueous and phenolic phases were separated by 15min of centrifugation at 20000 g. The upper phase was transferred into a new tube and the addition of an equal volume of ether precipitated residual amounts of phenol. Centrifugation at 16000 g for 5min separated phases again. This time, the upper phase was discarded and residual amounts of ether and phenol volatilized during incubation for 1min at RT with opened lid in the fume hood. The residual volume was determined again and 1/10 volume of 3 M potassium acetate was added. By further addition of 3 volumes of isopropanol and thorough mixing DNA began to precipitate. After 15min of incubation at RT, DNA was pelleted by centrifugation at 16000 g at 18°C for

15min. The supernatant was carefully removed and the pellet was washed with 70% Ethanol, centrifuged at 20000 g for 10min, the supernatant was removed and the obtained pellet was air-dried for 10min. The purified DNA was finally resuspended in H₂O or TE.

2.1.7 Preparation of high quality maxiEBV BAC DNA

The establishment of stable virus producer cell lines by transfection of EBV genome-encoding bacterial artificial chromosomes (maxiEBVs) to 293 cells required DNA of both high purity and high integrity. Therefore, a protocol for preparation of maxiEBVs from bacteria had been established previously that represents a modified form of alkaline lysis. A 6ml pre-culture was inoculated with a maxiEBV carrying bacterial clone and incubated o/n. Six conical flasks with 400ml LB medium, 24ml 5M NaCl and an antibiotic for selection each were prepared and the pre-culture was equally distributed to them. In dependence of the bacteria strain, cultures were raised for 18-20h at 37°C or 24-30h at 32°C and bacteria were pelleted by centrifugation for 15min at 5000 g at 4°C and subsequently kept on ice. Each pellet of the six cultures was carefully resuspended in 10ml of prechilled alkaline lysis solution I, before the volume of each tube was adjusted to 45ml by further addition of alkaline lysis solution I. 10mg of lysoszyme were added per tube, followed by an incubation on ice for 5-10min. The addition of 58ml alkaline lysis solution II induced lysis and brief and cautious turning without overhead rotation ensured equal distribution. After incubation for 5min on ice, lysis was stopped by addition of 70ml of alkaline lysis solution III to each tube. Suspensions were immediately homogenized by careful mixing, including overhead rotation. The tubes were again incubated on ice for 30min. Debris was pelleted by centrifugation for 45min at 4°C and 9000 g. Passaging through gauze and a fluted filter further cleared the supernatant. The volume of the solution was determined and equally distributed to 4 new centrifugation tubes of 500ml capacity. The DNA was precipitated by addition of 0.75 volumes of isopropanol followed by thorough shaking, 20min of incubation at RT and centrifugation at 9000rpm at 20°C for at least 20min. DNA pellets were washed with 200ml 70% Ethanol, centrifuged as before and subsequently air-dried for 10min. Each pellet was carefully resuspended in 10ml Special-TE by slow agitation on a shaking device. All solutions were pooled in one tube and incubated at 37° for 15min after 400µg of RNase had been added. Following, contaminating proteins were digested by treatment with 6mg proteinase K and incubation at 50°C for 45min.

In the next step, nicked and supercoiled DNA were separated on a CsCl gradient. Therefore, the weight of the DNA solution was determined and 1g of CsCl was added per gram of solution. To avoid precipitation, the stepwise addition of CsCl was accompanied by

heating in a waterbath. The sample was distributed on two 35ml tubes suitable for ultracentrifugation, 1.5ml of a 1% ethidiumbromide (EtBr) solution was added to each tube and the residual volume in the vials was filled and balanced for centrifugation with an aqueous CsCl solution ($\rho = 1.55\text{g/ml}$). The tubes were centrifuged at 100000 g (38000rpm in a 70Ti rotor) at 20°C for 3 days. After this step, UV light illuminated nicked (upper band) and supercoiled (lower band) DNA that had separated due to difference in density. The lower band was extracted from the tube by a syringe and needle (bovivet) and transferred to an 11.5ml tube for ultracentrifugation. 0.5ml EtBr were added and the residual tube volume was filled again with aqueous CsCl solution. After further centrifugation at 100000 g at 20°C for 3 days, the lower band containing supercoiled DNA was extracted as before. DNA was precipitated by addition of 5ml (at least 1.5 volumes) CsCl saturated isopropanol and centrifugation (4000 g, 30min, RT), which was repeated several times to extract residual EtBr at the same time. Finally, the DNA pellet was washed with 75% ethanol and briefly air-dried (5min). Depending on the pellet size, 50-200 μl of TE were added and left for resuspension for 2 days at 4°C.

2.1.8 Measurement of DNA concentration

DNA concentration was measured by the ratio of light absorption at 260nm and 280nm using the nanodrop device and software (Pqclab). To determine the precise amount of double stranded DNA, aliquots of the samples were diluted in DNA staining buffer (10x) and H₂O to 1ml and stained with HoechstDye 33258 (dilution 1:10000) that intercalated in DNA double strands and emitted fluorescence (450nm) upon excitation (350nm) measured in a fluorimeter (Dynaquant, Hoefer).

2.1.9 Enzymatic treatment of DNA and agarose gel electrophoresis

These methods were carried out exactly as previously described (Sambrook and Russell, 2001). Besides, enzymatic treatment was performed in buffers recommended by the supplier.

For control digestions of maxiEBVs, all DNA from one miniprep (2ml bacterial culture) was analyzed in one restriction digest, as BACs replicate only in low copy numbers. In order to distinctly resolve the number and size of fragments that result from restriction digests of BACs, gelelectrophoresis was carried out in gels of 25cm length containing 0.8% agarose and run overnight at 50V with continuous circulation of running buffer to avoid pH imbalance at the electrodes.

2.1.10 Southern blotting

For southern blotting, genomic DNA from eukaryotic cells was extracted using the QIAamp DNA Blood MiniKit according to the manufacturers instructions for culture cells. 3µg of genomic DNA were digested by standard procedures and resolved on a 25cm agarose gel in an overnight run to achieve best resolution. DNA ladder sizes were marked with dots of ink in the gel that were applied with a needle under UV transillumination. Subsequently, nucleic acids were depurinated by 20min of slowly agitated incubation of the gel in 0.75% HCl in H₂O . This was followed by denaturation in a 1.5M NaCl/0.5M NaOH solution for additional 20min. These steps assured single strand conformation of the DNA and improved the transfer to the blotting membrane.

Blotting of the DNA from the gel to a membrane was performed by capillary transfer. The agarose gel was placed upside down on impermeable film. A nylon membrane for transfer of nucleic acids (Millipore) was placed on the gel and potentially included air bubbles were removed. Two whatman filters were pre-wetted in the solution used for denaturation and placed on top of the membrane, again avoiding the inclusion of air-bubbles. Capillary transfer was induced by placing a 4cm layer of cellulose sheets on top of the filters, additionally carrying a uniformly distributed weight of approximately 1 kg. Cellulose was replaced whenever liquid reached the uppermost sheets of cellulose. After approximately 2 hours, any liquid had been soaked from the gel to the cellulose, indicated by the drastically reduced thickness of the gel.

To mark DNA sizes also on the membrane, ink dots were applied again. The membrane was briefly washed in 2xSSC, transferred to a hybridization tube and pre-hybridized with 10ml of Church buffer in an hybridization oven under rotation at 65°C for about 30min.

In the meantime of blotting, a suitable DNA probe (preferentially of 300-800bp) was radioactively labeled. The template was briefly denatured at 95°C, followed by incubation on ice. 50ng of template sequence were resuspended in a total volume of 11µl H₂O and incubated with 4µl of High Prime mix (Roche) and 5µl of γ-P³² labeled dCTP, corresponding to 50µCi. The mix was incubated for 1h at 37°C, before the labeled probe was purified by a Sephadex G-50 column (GE Healthcare). The column was equilibrated with 2ml of TE, the labeled probe mix was applied and free nucleic acids were washed away by application of 400µl of TE. Another 400µl of TE eluted the probe from the column matrix. The successful labeling of the probe was verified by measurement of radioactive decays per minute in the sample, which exceeded at least exceed 10 millions. Finally, the probe was denatured again by incubation for 10min at 95°C. A hole in the lid of the tube prevented unsnapping during heating. The

labeled probe was added to 25ml of Church buffer that replaced the pre-hybridization solution. The membrane was then incubated o/n at 65°C under continuous rotation. On the next day, the labeling solution was discarded and the membrane was washed with 0.2xSSC/0.1%SDS repeatedly for 10min at 60°C in a shaking water bath, until the membrane emitted less than 100 counts/second (Geiger counter). Finally, the membrane was wrapped into saran film and exposed to Hyperfilm MP (GE Healthcare) at -80°C with exposure time varying with signal intensity (1d-2weeks).

2.1.11 RNA extraction

Total RNA extraction was performed using the RNeasy MiniKit (Qiagen) according to the manufacturer's instructions. In time course analyses, cells were harvested, washed in ice-cold PBS and lysed using the lysis buffer of the kit supplied with β -mercaptoethanol to inhibit RNAses. Lysates were stored at -80°C until further preparation of all samples of the time course.

In infected samples, a final treatment with RNase-free DNase (Invitrogen) was mandatory to eliminate contaminations with genomic virus DNA. Thus, the yielded 30 μ l of RNA preparation were treated with 2.5 μ l of DNase accompanied by addition of 4 μ l of DNase buffer (10x, Invitrogen) and 1.5 μ l of RNasin (Promega, inhibits RNase activity) for 30min at 37°C and subsequently inactivated by incubation at 65°C for 10min.

MicroRNAs were extracted using the miRvana Kit (Ambion) in accordance to the manufacturer's protocol. Also for microRNA preparations from infected samples a final DNase digestion was mandatory and performed as described above.

2.1.12 Reverse Transcription

cDNA was prepared from RNA by SuperScriptIII reverse transcriptase and the accompanying kit (Invitrogen). Usually, 1 μ g of RNA was used for reverse transcription. Random hexamer oligonucleotides were used for priming, as EBERs do not carry a polyA-tail (polymerase III transcripts). With regards to other transcripts, efficiency of reverse transcription did not differ for oligo-dT and random-hexamer priming.

Reverse transcription of microRNAs relied on stem-loop PCR priming as described elsewhere (Chen et al., 2005). In brief, specific RT-primers for each addressed EBV microRNA were included in the reverse transcription mix at concentrations of approximately 1pmol per primer and sample. Each of these primers specifically annealed to 6 nucleotides of one mature EBV microRNA and primed reverse transcription. The primer itself formed a stem-loop structure, that comprised an identical sequence for all miRNA-primers and served

later on as annealing template during quantitative PCR (see also figure 5.1). By this means, quantitative PCR can be performed with sequence specificity for miRNAs, despite mature miRNA sequences are in principle too short to give rise to a PCR product.

miRNA-first strand synthesis was also performed with SuperScriptIII, but used a mix of specific first-strand primers (max. 10) and followed the depicted PCR cycles:

1. 16°C for 30min
 2. 30°C for 30sec
 3. 42°C for 30sec
 4. 50°C for 1sec
 5. 85°C for 5min
- ↪ 60 cycles of step 2 to 3

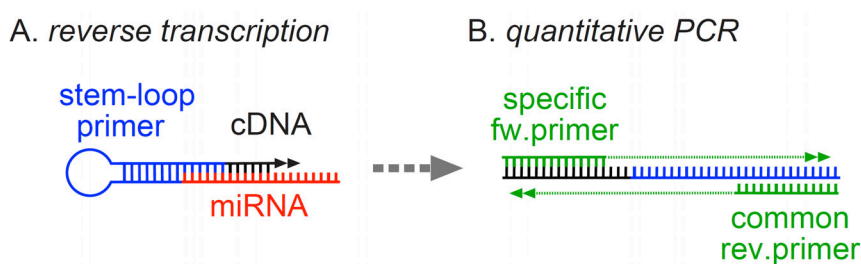


Fig. 5.1: Quantitative assessment of microRNAs. A. Reverse transcription of microRNAs is primed by stem-loop primers with specificity for 6 nucleotides of the microRNA. B. qPCR is performed with a microRNA specific forward primer and a reverse primer that anneals to the common stem-loop sequence.

2.1.13 quantitative PCR

Transcript prevalence was determined by real-time quantitative PCR on 96-well plates in a LightCycler®480 (Roche). PCR products were detected by intercalation of SYBRGreen into doublestrand DNA and resulting fluorescence. Three technical replicates were included for each sample as well as for the negative control that was free of template. The total reaction volume was 10µl, containing 5pmol of each primer, 2µl of diluted cDNA template and 5µl of 2x SYBRGreen Reaction Mix (Roche). Preceding use in qPCR, cDNA stocks had to be diluted at least 5-fold with H₂O in order to prevent influence of reverse transcription buffers on PCR efficiencies. qPCR efficiencies were determined for each primer pair with dilution series of LCL cDNA. Relative quantification was calculated with respect to PCR efficiencies using LC480 Software Service Pack 3 (Roche). Glutathione synthetase B was used as reference transcript for normalization, as it shows steady expression levels in B cells and LCLs (de Brouwer et al., 2006).

standard qPCR program:

1. 95°C 10min
 2. 95°C 10sec
 3. 60°C 10sec, acquisition of fluorescence
 4. 72°C 10sec
 5. 95°C 5sec
 6. 65°C 1sec
 7. continuous heating to 95°C with acquisition of fluorescence (melting curve)
- 
- 45 cycles of step 2 to 4

To increase specificity of qPCR on miR cDNA, a **touch-down program** was applied:

1. 95°C 10min
 2. 95°C 10sec
 3. touchdown annealing and combined elongation of 1min/cycle (including acquisition of fluorescence):
initial 5 cycles at 70°C
15 cycles with reduction of annealing temp. of 0.6°C/cycle
25 cycles with annealing at 60°C
 4. 95°C 15sec
 5. 65°C 10sec
 6. continuous heating to 95°C with acquisition of fluorescence (melting curve)
- 
- 45 cycles of step 2 to 3

2.1.14 Standard PCR

PCR was carried out using goTaq polymerase (Promega) with the supplied buffer. A standard mix comprised 20µl and contained 10-100ng template, 10pmol of each primer, 4µl goTaq buffer (5x), 0.5µl dNTPs (10mM, Fermentas) and 0.2 µl goTaq polymerase. Addition of 1µl DMSO prevented putative secondary structures in template or primers, H₂O was added to reach 20µl reaction volume.

A standard PCR program included initial denaturation at 95°C for 2min, annealing of primers at a primer-specific temperature for 20sec, product elongation at 72°C for a product-size dependent time (taq polymerase elongates ~1000bp in 1min) and denaturation at 95°C for 15sec. Restarting from the annealing step, up to 36 cycles were performed. A final step of 3min at 72°C enabled completion of abortive elongation reactions of all strands.

PCR for cloning purpose was performed using Pfu polymerase (Stratagene) that comprises a proof-reading feature and shows a drastically reduced error rate in sequence reproduction.

Pfu polymerase elongates approx. 500bp/min and requires extended elongation time in comparison to taq polymerase. Reaction conditions were similar but a special Pfu buffer had to be used (supplied by Stratagene).

2.1.15 EBV genotyping PCR

The generation of LCLs required the evaluation of the EBV genotype, as potentially also field-strain infected cells from EBV positive donors might give rise to growing cultures *in vitro*. To this end, a multiplex PCR was established, that generated PCR products of different sizes depending on the virus strain that was present in the cell. The assay included a common forward primer annealing in any EBV genome and strain-specific reverse primers. The PCR sample was prepared as follows:

- template of genomic LCL DNA 10-200ng
- Primer: EBV common fw 2.5pmol
- EBV wt/MABA rev 2.5pmol
- EBV B95.8 rev 2.5pmol
- EBV rec. rev 2.5pmol
- dNTPs (10mM) 0.5µl
- 5x goTaq Buffer 4µl
- goTaq 0.2µl
- MgCl₂ (25mM) 1µl
- DMSO 1µl
- H₂O ad 20µl

The PCR program included the following steps:

1. 95°C 2min
 2. 60°C 45sec
 3. 72°C 1min
 4. 95°C 30sec
 5. 72°C 3min
- ↻ 34 cycles of step 2 to 5



Fig. 5.2: Band patterns of the EBV genotyping PCR.

This led to products of 350bp in case of infection with field strain virus (*e.g.* MABA), of 500bp in case of infection with the laboratory strain B95.8 and of 750bp in case of infection with recombinant EBV (based on p2089). The assay takes use of the preferential formation of short products in PCR reactions to unravel contamination with wildtype-infected cells in predominantly recombinant EBV infected cultures.

2.2 Protein biochemistry

2.2.1 Cell lysis

Cells were washed in PBS and lysed by 20min of incubation on ice in RIPA buffer, containing a protease inhibitor (completeMini, Roche). Cellular debris was pelleted by centrifugation for 20min at 4°C and 16000 g, the supernatant was transferred to a new tube and protein content was determined using the BCA protein assay (Pierce). Lysates were stored at -20°C or directly subjected to immunoprecipitation or SDS-PAGE.

2.2.2 Immunoprecipitation of BRLF1 protein from infected cells 2hpi

Coupling of antibody to beads

250µl of SepharoseG bead slurry was centrifuged (1000 g, 1min) and liquid was discarded. Beads were washed with 1ml of PBS and subsequently incubated o/n with 5ml of anti-BRLF1 hybridoma supernatant (clone 8C12) on an orbital shaker at 4°C. Beads were pelleted by centrifugation, washed 5 times with PBS and finally resuspended in an equal volume of PBS, here 125µl.

Immunoprecipitation

2x10⁸ EBV negative Daudi cells were used per sample. Cells were pelleted by centrifugation at 300 g for 5min and washed with PBS. Whole cell lysates were prepared in RIPA buffer as described, however containing 0.2% SDS to improve results for BRLF1 protein precipitation and DNase (Roche, 100 µg/ml final) was added to digest large amounts of chromosomal DNA. 30µl of bead slurry that had previously been coupled to BRLF1-antibody were added to cleared lysates and incubated o/n at 4°C in an orbital shaker. Beads were settled by centrifugation and washed 3 times with RIPA Buffer. Finally, Laemmli sample buffer was diluted to 2x concentration with RIPA Buffer and 40µl were added to the beads. Boiling for 10min at 95°C eluted antibodies and precipitated protein from the beads, beads were settled again by centrifugation and the protein containing supernatant was subjected to SDS PAGE.

2.2.3 SDS polyacrylamide gel electrophoresis (SDS-PAGE)

In this study, electrophoretic separation of protein was performed under denaturing conditions by discontinuous SDS PAGE. For analysis, the protein content of all samples was adjusted to equal levels by addition of lysis buffer and Laemmli-sample buffer (4x). The intended denaturation of protein was achieved by the reducing conditions of the Laemmli buffer in combination with heating of the samples to 95°C for 10min.

Additionally, this led to homogenous coverage of proteins with SDS and provided a net negative charge in dependence of the protein's size. Hence, separation was driven by electric forces, but proteins were effectively separated in order to their size in denatured state and not due to their native charges (they are covered by SDS). In this work, separating Hoefer mini gels were prepared and consisted of a 12.5% acrylamide containing separating gel and an overlaying 5% acrylamide containing stacking gel. Gels were run in a Hoefer Mighty Small unit at a current per gel of initial 10mA (stacking gel) and subsequent 25mA (separating gel).

2.2.4 Immunoblotting

Protein Transfer to Membranes

For immunodetection of proteins that had been separated by SDS-PAGE, the proteins were transferred to nitrocellulose membranes by semi-dry blotting. Two sheets of whatman paper were soaked in blotting buffer and placed on the anode, the nitrocellulose membrane was also pre-wetted and placed onto the whatman papers. The gel was carefully positioned on top of the membrane and air bubbles were removed. Finally, two whatman papers were used to cover the gel and air bubbles were removed again. The cathode was placed on top and protein transfer was performed at 18V for 40min.

Immunodetection of Proteins on Membranes

Following the transfer of proteins, the membrane was incubated washing buffer containing 5% of milk powder for 1 h at RT under agitation. The blocking solution was removed and the membrane was rinsed with washing buffer. The blot was subsequently incubated with a primary antibody (diluted in washing buffer with 1% BSA and 0.01% azide) under gentle shaking for 3h at RT or o/n at 4°C. After washing 3 x 10min with washing buffer, the membrane was incubated with an idiotype-specific secondary antibody conjugated to horseradish peroxidase (diluted in washing buffer with 3% milkpowder) for 2h at RT. The membrane was washed 6 x 5min with washing buffer and incubated for 1min in chemiluminescence substrate (Roti®lumin, Carl Roth GmbH). Finally, the membrane was placed into a film cassette and bound secondary antibody was detectable by exposure to Hyperfilm ECL (GE Healthcare) due to chemiluminescence.

2.2.5 Purification of His-tagged protein

His-tagged human IL-10 and viral IL-10 were purified from serum free supernatants of transfected 293 cells by Ni-NTA agarose (Qiagen). Columns were loaded with 300µl Ni-NTA slurry and beads were allowed to settle down for 30min. Residual liquid was drained and the beads were equilibrated with 2ml of 10mM imidazole in RPMI. The supernatant was applied

in aliquots of 1ml, inducing a flow-through that supported efficient binding of His-tagged protein to the beads. The loaded columns were washed 3 times with 600 μ l (= two column volumes) 20mM imidazole in RPMI, followed by 2 elution steps with 600 μ l of 400mM imidazole in RPMI. Residual amounts of imidazole were removed by o/n dialysis of the eluate fractions against PBS through a membran of 10kD exclusion size (Spectrumlabs, Netherlands). Finally, protein contents were assessed by BCA assay (Pierce) and purity was evaluated by SDS PAGE with subsequent silver stain analysis according to standard protocols (Sambrook and Russell, 2001). The final acquisition of IL-10 concentrations was realized by pan-specific IL-10 ELISA (Mabtech).

2.2.6 ELISA

Kits with suitable antibodies for sandwich ELISA (enzyme-linked immunosorbent assay) were used in accordance to the manufacturer's instructions (Mabtech, Sweden). In brief, protein adsorbing plates (Nunc) were coated overnight at 4°C with primary antibody and blocked for 1h at RT with 10% FCS in RPMI before culture supernatants were applied (100 μ l/well). Standard concentrations of the cytokine of interest were included in duplicates following a $\sqrt{10}$ dilution: 146,3 μ l of the starting concentration were applied to the first well and 46.3 μ l thereof were transferred to the next well that already contained 100 μ l of sample matrix liquid, here 10% FCS in RPMI, resulting in a series of 10000-3333-1000-333-100-33-10-3.3-1 pg/ml. Samples and standards were incubated for 2h at RT, followed by 1h of incubation at RT with the second cytokine-specific antibody that was coupled to biotin. In a third step, streptavidin coupled alkaline phosphatase (AP) was bound to the biotin of the secondary antibody (45min at RT). Finally, the AP substrate p-Nitrophenylphosphate (p-NPP) was added and catalyzed to p-Nitrophenol. The intensity of the observed colorshift to yellow was photometrically assessed at 405nm wavelength by an ELISA-Reader and, based on the integrated standard, cytokine prevalences could be quantified. Between the incubation steps with antibody, the wells were washed with 0.05% Tween in PBS.

Low range ELISA on Ifn- γ was performed in analogy, but comprised blocking for 2h and development at 4°C in the dark for 24-48h. The ELISA Kit for multi-subtype human Ifn- α included pre-coated plates and was performed as recommended by the manufacturer (PBL, USA).

2.3 Cell culture

2.3.1 Culture of stable cell lines

Cells were cultured in GIBCO®RPMI 1640 medium (Invitrogen), supplemented with 10% FCS (PAA laboratories), penicillin (100U/ml) and streptomycin (100mg/ml) at 37°C in a 5% incubator, unless otherwise indicated.

Suspension cells were splitted by thorough resuspension and dilution with fresh medium. Adherent cells were splitted when plates reached confluency. Medium was soaked off and cells were washed with PBS. Trypsin was applied in amounts that were sufficient to form a covering liquid layer and incubated at 37°C for 5-10min to detach the cells. RPMI medium was added and repeated pipetting led to a single cells suspension, which of 1/10 was kept in culture and supplied with fresh medium.

2.3.2 Culture for EBV-specific CD8+ T cell clones

T cells clones had been generated from PBMCs of EBV positive donors as previously described (Moosmann et al., 2010) and were a kind gift of Dr. A. Moosmann. Cells were cultured on 96-well round-bottom plates (200µl/well) in medium supplied with IL-2 (1000U/ml) and 0.2nM selenium. Every two weeks, T cells were stimulated with a mix of feeder cells. Therefore, LCLs of matching HLA and not specified PBMCs of three different donors were irradiated (50 Gy). A feeder mix consisting of 1×10^5 irradiated LCLs and 1×10^6 irradiated PBMCs per ml medium (containing selenium and IL-2) was prepared, T cells were harvested, deprived of old medium and resuspended in the feeder mix. The suspensions were plated on 96-well plates. In parallel, the lack of growth of pure feeder mix cultures controlled for successful feeder inactivation.

Depending on the T cell growth, cells were splitted at a 1:2 ratio (max.) and/or supplied with fresh medium. The clonal specificity of the culture was regularly assessed by multimer-staining for the respective TCR and subsequent FACS analysis.

2.3.3 Freezing and thawing of eukaryotic cells

Cells were centrifuged for 5min at 300 g and resuspended in 500µl cold FCS (100%). During centrifugation, cryo-tubes (Nunc) were labeled and preloaded with 500µl of 20% DMSO in FCS (cold). The cells in FCS were mixed with the freezing solution in the tube, adjusting the final concentration of DMSO to 10%, the tubes were kept on ice and transferred to -80°C. For long-term storage, frozen cells were kept in the gaseous phase above liquid nitrogen (-192°C).

Cell stocks were thawed by brief incubation in a 37°C waterbath, followed by immediate transfer to 50ml of fresh medium or PBS. Cells were centrifuged at 300 g for 5min at RT, carefully resuspended in an appropriate amount of medium and plated in a suitable culture vial.

2.3.4 Transfection of 293 cells

For transfection, 293 cell cultures were cultured to ~70% density before medium was replaced with OptiMEM (Invitrogen). Polyethylenimine (PEI, MW=25000) diluted 1:1000 (w/v) in sterile H₂O was used for transfection. Depending on the culture size, the following parameters were applied:

culture dish	6-well (ø 3.5 cm)	14 cm dish
seeded cells	5x10 ⁵	1x10 ⁷
volume of OptiMEM on cells	1 ml	13 ml
amount of transfected DNA	1-1.5 µg	15-30 µg
dilution of DNA	100 µl OptiMEM	1 ml OptiMEM
amount of PEI (1:1000 dil.)	9 µl	120 µl
resuspension of PEI in	100 µl OptiMEM	1 ml OptiMEM
incubation	stir PEI/OptiMEM mix vigorously, incubate at RT for max. 5min, combine with DNA/OptiMEM, incubate for 20min, apply dropwise to cells, incubate overnight or at least 6h	
supply with full RPMI the following day	2.5 ml	20 ml

2.3.5 Generation of virus producer cells

1µg of high quality maxiEBV DNA was transfected to 293 cells as described. After 2 days, success of transfection was verified by GFP fluorescence, cells were trypsinized and plated on a 14cm culture dish. The addition of 80µg of hygromycin (Invitrogen) per ml medium selected for stably transfected clones and during the first week repeated change of medium removed large amounts of dead cells. After 3 weeks of culture, visible clones of growing cells formed. GFP+ clones were transferred by trypsin-soaked whatman snippets to 24-well plates and were further expanded. They were tested for virus production capacities by transfection as described in the next chapter. Frozen stocks were prepared for best virus producers and their respective genotypes were confirmed by southern blotting.

2.3.6 Induction of virus production in recombinant producer cell lines

For virus induction, producer cells were transfected by standard procedures as described in chapter 2.3.4. The transfection of a BZLF1 expression plasmid (p509, 1µg/6well) induced the lytic cycle in producer cells and was combined with the transfection of BALF4 (p2670, 0.3µg/6-well) that improved virus packaging and infectiousness (Delecluse et al., 1998; Neuhierl et al., 2002). Virus containing supernatant was harvested 3 days after transfection and centrifuged at 300 g for 5min to pellet accidentally transferred cells, followed by centrifugation at 2000 g for 10min to pellet cellular debris. Supernatants were stored at 4°C and did not show significant change in functional virus titers up to one year after production.

2.3.7 Virus titration

Recombinantly produced EBV encodes GFP as a phenotypic marker. Hence, cells express GFP upon infection with recombinant virus that serves to determine the titers of recombinant virus supernatants. To this end, 5×10^4 Raji cells were infected with 50, 100 and 200 µl of the recombinant supernatant and the percentage of GFP⁺ was assessed by FACS on day 3 after infection. The percentage of GFP⁺ cells was used to calculate how many of the Raji cells had turned green and thus how many infectious events, termed “green Raji units” (GRU), had been contained in the applied amount of supernatant. A certain variance of this method was kept to a minimum by subsequent back-titrations. Therein, the infection of 10% out of 5×10^4 Raji cells was intended and the calculated amount of supernatant was applied. The amount of infected cells was again assessed by FACS 3dpi and repetitions with empirical adjustment of applied virus supernatants were performed, until a certain volume of each assessed virus supernatant had been determined that led to the intended infection rate (tolerated variance: $\pm 10\%$ of the observed value). This represented the basis for the comparisons of virus functions in subsequent experiments.

A schematic workflow of the procedure to generate recombinant EBV is depicted in figure 5.3.

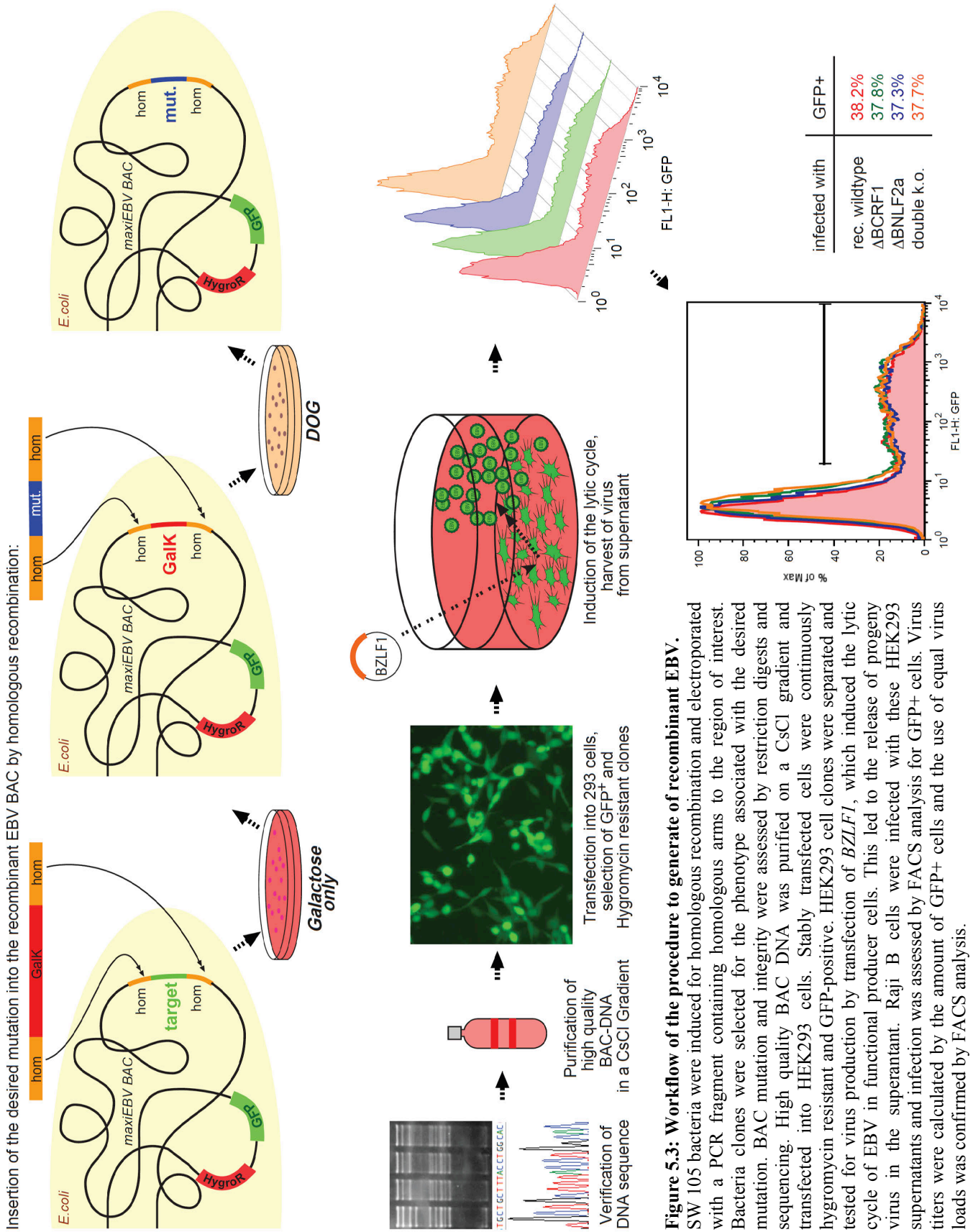


Figure 5.3: Workflow of the procedure to generate of recombinant EBV.

SW 105 bacteria were induced for homologous recombination and electroporated with a PCR fragment containing homologous arms to the region of interest. Bacteria clones were selected for the phenotype associated with the desired mutation. BAC mutation and integrity were assessed by restriction digests and sequencing. High quality BAC DNA was purified on a CsCl gradient and transfected into HEK293 cells. Stably transfected cells were continuously hygromycin resistant and GFP-positive. HEK293 cell clones were separated and tested for virus production by transfection of *BZLF1*, which induced the lytic cycle of EBV in functional producer cells. This led to the release of progeny virus in the supernatant. Raji B cells were infected with these HEK293 supernatants and infection was assessed by FACS analysis for GFP⁺ cells. Virus titers were calculated by the amount of GFP⁺ cells and the use of equal virus loads was confirmed by FACS analysis.

2.3.8 Harvest of virus from spontaneously lytic B95.8 cells

The marmoset derived lymphoblastoid cell line B95.8 was identified to spontaneously produce EBV in significant amounts and gave rise to the laboratory virus strain B95.8 (Miller et al., 1972). Virus production peaks when cultures are stressed due to high density, starvation and acidic medium, for example. Production of B95.8 supernatants was thus realized by raising dense cultures until splitting was indicated, but were incubated for another 8-10 days. Supernatants were harvested and disburdened from cells and debris by centrifugation as described in chapter 2.3.6. Titers of functional virus were assessed by limiting dilution assays as described in chapter 2.4.6.

2.3.9 Enrichment of virus particles by ultracentrifugation

For virus concentration, supernatants were harvested as described. Following pelleting of debris, the supernatants were filtered through a PVDF membrane of 0.8 μ m pore size to further eliminate fine debris. Fractions of 35ml per bucket were subjected to ultracentrifugation at 100000 g (25000rpm in SW28 rotor) for 2.5h, supernatants were soaked of and pellets were carefully resuspended. This technique allowed for approximately 50x enrichment of virus particle load. These concentrated supernatants were either used for infection or further processed for RNA preparation.

2.3.10 Preparation of particles for RNA purification

Particle concentrates were subjected to RNase (Sigma) and DNaseI (Roche) digestion (both at 10 μ g/ml final concentration) for 20min at RT to eliminate unprotected nucleic acids in the supernatant. Subsequently, the supernatant was distributed to 1.5ml tubes for ultracentrifugation and centrifuged at 48000 rpm at 4°C for 1h. Pelleted particles were then subjected to standard preparation of total RNA or microRNA using the RNeasy kit (Qiagen, see chapter 2.1.11).

A schematic workflow of particle concentration and RNA preparation is depicted in figure 5.4.

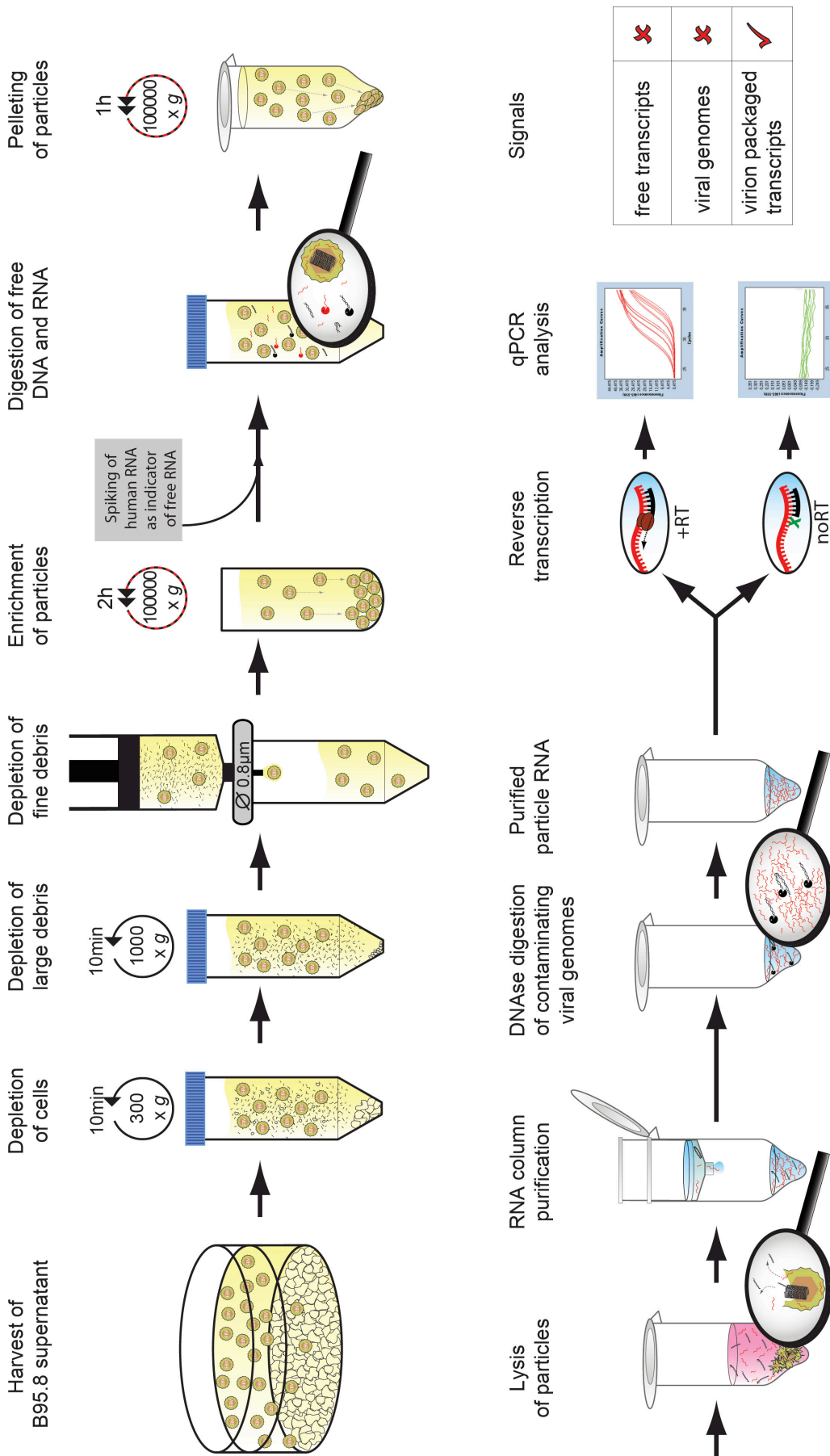


Figure 5.4: Workflow of virion-enrichment and preparation of packaged RNA. B95.8 cells are of marmoset origin and spontaneously produce EBV. Cell culture supernatant was harvested and contaminating cells and debris was pelleted by centrifugation. Fine debris was depleted by filtration (0.8µm pore size). Virions were enriched by ultracentrifugation. The concentrated supernatant was RNase and DNase treated to eliminate free nucleic acids. Previously spiked human RNA served to indicate successful treatment (see below). Particles were pelleted by ultracentrifugation, lysed and RNA was prepared by column purification. Contaminating viral genomic DNA was eliminated by DNase digestion. Samples were reversely transcribed and analyzed by quantitative PCR. Successful preparation of packaged RNAs was indicated by absent signals for free transcripts after reverse transcription (assessed by PCR specific for human *glutathione synthetase B*, *GUSB*), absent signals for viral genomic DNA (assessed in samples without reverse transcription) and strong signals for viral transcripts after reverse transcription.

2.3.11 Preparation of PBMCs from blood

Peripheral blood monocyctic cells (PBMCs) were derived from voluntary blood donations of healthy adults or from buffy coats purchased from the university clinics in Ulm, Germany. Buffy coats were diluted 1:1 with PBS prior to PBMC preparation. 35ml of blood or buffy coat dilution were underlaid by 12ml of Ficoll-Hypaque (“Biocoll”, Biochrom AG). PBMCs were enriched at the separating layer between Ficoll and blood plasma by centrifugation at 1000 g for 25min. PBMCs were transferred to a new tube, washed 4 times in PBS and used for experiments or subjected to cell sorting. PBMCs of an healthy individual contained among other cells 40-60% CD4+ T cells, 10-20% CD8+ T cells, 5-15% B cells and 10-25% NK cells.

2.3.12 Preparation of cells from human adenoids

Adenoids are tissue of lymphoid origin that eventually grows in the oropharynx and predominantly contains B cells. Adenoids eventually develop in young children, can hamper breathing and need to be surgically removed. Anonymized tissue samples were provided by the departments of orthorhinolaryngology of the Klinikum Grosshadern, Munich, and the Klinikum Dritter Orden, Munich. The tissue was mechanically dissected and passed through a mesh filter to obtain a single cell suspension. T cells were rosetted by addition of 1ml sheep blood. The volume was adjusted to 35ml by PBS and monocyctic cells were separated by a Ficoll-Hypaque gradient as described.

2.3.13 FACS analysis of cells

Size, granularity and fluorescence features of single cells can be assessed by fluorescence activated cell sorting (FACS). Endogenously expressed fluorescing molecules can be assessed directly, but surface molecules of the cell require staining with antibodies that are conjugated to or counterstained with fluorophores. For FACS analysis, up to 5×10^5 cells were washed in PBS and stained with 30 μ l of antibody diluted in PBS and incubated 15min on ice in the dark. Cells were washed with excess of PBS and either counterstained with a secondary antibody in the same manner or directly subjected to FACS analysis. In this study, FACS data were acquired on a FACSCalibur (BD, USA) featuring two lasers with 408nm and 633nm excitation wavelength, respectively, and a beam setup that allowed for 4 different fluorescence detection channels.

2.3.14 Specific TCR staining by multimers

T cell specificity was assessed by staining of the TCR with multimers (ProImmune, Oxford, UK) that mimic peptide loaded MHC complexes and bind specifically to T cells with

matching TCR. To this end, 3×10^5 cells were washed in PBS and stained in 30 μ l multimer dilution (1:100) in PBS at RT for 15min. The samples were washed again in PBS and counterstained with Pro5 Fluorotag R-PE (ProImmune, Oxford, UK) dilution (1:100) in PBS on ice for 10min. In parallel, samples were stained for CD8 as a pan-specific marker for cytotoxic T cells. These stainings confirmed T cell clonality by showing exclusively CD8+ multimer+ double stained cells and deficiency in CD8+ cells of non-multimer specificity.

2.3.15 Cell sorting

Fluorescence based – FACSAria

The term ‘fluorescence acquired cell sorting’ (FACS) refers to the acquisition of data on cell populations without recovering the cells after this process. It was then expanded for the option to recover these populations as purified fractions of living cells. Staining procedures are similar to normal FACS analysis, but require upscaling, as usually higher cell numbers are assessed, and mesh-filtration of the suspension to prevent clogging. The FACSAria cell sorter has a similar setup as the FACSCalibur, however extended for the option to sort cell containing drops into tubes or plates at defined positions. For reliable sorting, it is of essential importance to establish a stable stream with constant drop positions and to initially define the positions where these drops have to be sorted to. The desired cell populations need to be defined with regards to their fluorescence properties and are assigned to the tube they are sorted to. The detection of fluorescence and the applied pressure to the cells limits the sorting speed to some extent and, most importantly, also the cell types that support sorting (large cells or trypsinized cells are less suitable). In a final step, the result of sorting is evaluated by reanalysis of the fractions that should show highly enriched populations of the desired cell types.

Magnetic cell sorting – MACS

Magnetic cell sorting provides a convenient and gentle option to fractionize cells. However, it is limited to one parameter per sort. In this study, B cells were separated by the B cell isolation kit II (negative sort), NK and NKT cells were sorted by the CD56+ isolation kit and CD4+ T cells were sorted by the CD4+ isolation kit (Miltenyi Biotech). In brief, cells were stained with antibodies that were directly coupled to magnetic beads or biotin coupled and subsequently counterstained with streptavidin coupled magnetic beads. Cells were then applied to a matrix that was located in a magnetic field. Labeled cells (= positive sort) were retained in the field and separated from unlabeled cells (= negative sort) by repeated washing of the column. Retained cells were eluted after the column had been detached from the magnetic field. The purity of the obtained fractions was assessed by subsequent FACS

analysis. In this study, MACS separations with a purity of >90% were accepted for further experimentation.

2.3.16 Assessment of cell vitality by MTT

The vitality of cells can be assessed by an MTT assay (Mosmann, 1983). Living cells catalyze MTT (dimethyl-thiazolyl-diphenyl-tetrazolium-bromide, yellow) by mitochondrial reductases to formazan that precipitates as purple crystals in the cell. To test for the presence of living cells, 10 μ l of a MTT stock solution (5mg/ml in PBS) were added per 100 μ l of cell culture volume and incubated for 3 hours in a standard cell incubator. 10 μ l of 10%SDS were added per 100 μ l cell culture and incubated o/n at RT to dissolve cells and formazan crystals. Absorption of light at 595 nm was assessed and an OD₅₉₅ \geq 0.5 indicated a vital culture.

2.3.17 Cell counting

Cells were counted in a Neubauer counting chamber. 10 μ l of the cell suspension were mixed with 10 μ l of 0.2% (w/v) trypan blue in PBS to stain dead cells. Unstained cells of all quadrants were counted, the value divided by two and the resulting number multiplied with 1x10⁴ to obtain the amount of present living cells per ml. PBMCs and adenoid cells were counted after staining with Türk's solution (ready to use, Merck) that lysed contaminating erythrocytes.

2.4 Functional assays with living cells

2.4.1 Infection of B cells

B cells were infected with EBV at highest efficiency when a multiplicity of infection (MoI) of 0.1 GRU/B cell was applied. Primary B cells show an infection rate of approximately 80% at this MoI, due to a 10-fold less efficient infection of Raji cells with EBV. Infectious supernatant of defined GRU content were added to primary B cells and incubated overnight at 37°C and continuous rotation. On the next day, cells were centrifuged, supplied with fresh medium and plated in standard wells for continued culture in a standard cell incubator. This strategy resulted in less dead cells upon infection, equal infection even with low titer supernatants and provided the cells with completely fresh medium after several hours in virus containing supernatant of low nutritive quality.

2.4.2 Inhibition of transcription and translation.

The chemical compounds ActinomycinD (Calbiochem) and Cycloheximide (Sigma) were used to inhibit transcription or translation, respectively. The necessary concentrations were elucidated by titration and the assessment of c-MYC transcripts and protein. In this study, 5µg ActD/ml were determined to inhibit transcription and 25µg CHX/ml were determined to inhibit translation in 5×10^6 Daudi cells /ml. In infection experiments, the complete inhibition was ascertained by pre-incubation of the cells with the respective inhibitor 15min prior to addition of the virus.

2.4.3 T cell recognition assays

Recognition of EBV infected B cells by EBV specific CD⁺ T cell clones was analyzed by Ifn-γ ELISA. B cells were isolated using the B cell isolation Kit II (Miltenyi) from blood of donors with a matching HLA allele. They were infected with a MoI of 0.1 GRU/cell and assayed for recognition at the indicated day after infection. For recognition assays, triplicates of 10000 specific T cells and 20000 infected B cells were co-incubated for 18 hours on 96-well V-bottom plates in total volumes of 200µl. Ifn-γ levels were measured by ELISA (Mabtech) with 100µl of cell free supernatant from these co-cultures. Sample values were subtracted from putatively obtained basal Ifn-γ secretion of 10000 T cells without targets. In time course analyses, Ifn-γ values were normalized to the value of T cells that were coincubated with established LCLs of matching HLA (this value was set to 1). The normalization corrected for putative unequal performance of the T cells during the time course and inaccuracies of T cell counting.

2.4.4 Cytokine response of complete PBMCs to EBV infection

5×10^6 PBMCs of an EBV-positive donor were infected at a MoI of 0.1 GRU/B cell and incubated in 2ml, which of 500 μ l were sampled for analysis and replaced with fresh medium every three days. For analysis of Th1 and Th2 cytokines, the Th1/Th2 11plex FlowCytomix Kit (BenderMedSystems) was used according to the manufacturers instructions. Antibody coated beads of the kit were mixed and incubated with the sample. Soluble biotin-coupled antibodies against the analytes were added, followed by counterstaining with streptavidin-PE. Analyte prevalence was derived from PE signal intensity of the sample. Size and APC fluorescence of the beads defined the respective analyte. Data were acquired on a FACSCalibur (BD) and analyzed with FlowCytomixTM Pro 2.4 software

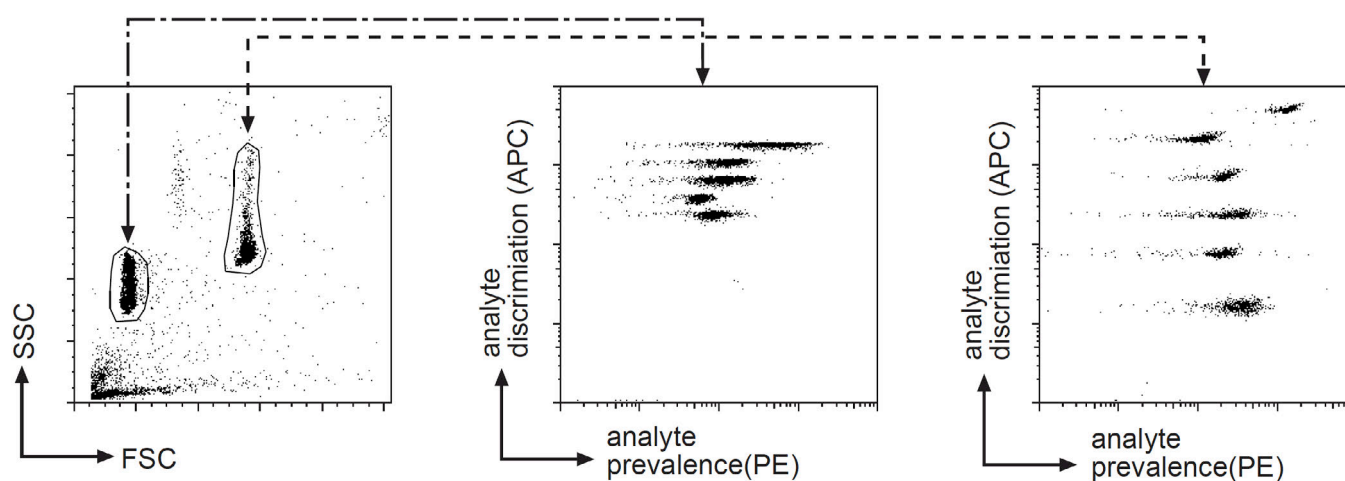


Figure 5.5: FACS based Multiplex ELISA. Different bead sizes resulted in two distinct populations in the FSC/SSC analysis (left panel). Both populations were gated and plotted for APC and PE values. The combination of bead size and defined APC values discriminated the eleven analytes, respective PE signal intensity indicated the prevalence of the analyte in the sample.

(BenderMedSystems).

2.4.5 Killing assays with NK cells

The cytotoxic activity of NK cells towards infected B cells was assessed by Calcein release from lysed cells as described in a previous report (Wiesner et al., 2008). B cells were isolated from PBMCs as described above, EBV infected and cultured for three days. On day 3 after infection, autologous CD56⁺ cells and CD4⁺ cells were isolated by positive MACS sort (Miltenyi). Infected B cells were labeled with calcein (Calcein-AM, Invitrogen) by incubation of 2×10^6 cells in 500 μ l medium containing 10 μ g/m Calcein-AM for 30min at 37°C. Subsequently, cells were washed three times in an excess of PBS and counted. Defined ratios of effector (NK) and target (B) cells were then incubated together in 96-well V-bottom plates, with 1 unit representing 1000 cells in a total volume of 200 μ l. After three hours, fluorescence

of the supernatant was measured in a Wallac Victor plate reader (Perkin-Elmer). Values were corrected for spontaneous release of calcein by subtraction of the value obtained with labeled cells without effectors (negative control). Maximum lysis of cells was induced by addition of detergent (TritonX, 0.5% final, positive control) and also corrected for spontaneous release. Specific lysis represents the ratio of corrected sample values to corrected maximum lysis values.

2.4.6 Limiting dilutions and regression assays

The transformation capacities of the recombinant viruses were assessed by limiting dilution of the virus as described (Wilson and May, 2001). In brief, serial dilutions of virus were added to 48 replicates of 1×10^5 B cells prepared from adenoids in 96-well flat bottom plates and incubated for 6 weeks with weekly supply of fresh medium. The presence of living cells was analyzed by MTT assay.

Regression assays assessed the successful establishment of virus infections in the presence of immune effectors. To this end, PBMCs were used in total or depleted of the CD56+ or CD4+ cells by magnetic cell sorting (Miltenyi) and infected overnight with a MoI of 0.1 GRU/B cell. After supplying fresh medium, cells were plated in 24 replicates on 96-well flat bottom plates in doubling dilutions, ranging from 100000 to 100 cells/well. After 6 weeks of culture with weekly supply of fresh medium, the number of wells with growing cells was assessed by MTT assay.

The principle of this assay has been described before (Rickinson et al., 1984) and in case of complete PBMCs leads to a characteristic distribution of wells with growing cells: i) at low cell numbers/well the present amount of B cells is insufficient to form a growing culture, ii) at intermediate cell numbers/well, infected B cells can form a LCL culture and insufficient amounts of effectors do not hamper B cell growth, iii) at high cell numbers/well, the amount of B cells would be sufficient for outgrowth, but effectors are present in sufficient amounts to eliminate infected cells. The sequence of (i) not growing / (ii) growing / (iii) not growing cells follows a logarithmic Gaussian distribution. The effects of virus mutants on successful outgrowth in presence of effector cells was determined by comparison of these distributions for similarity (see also figures 2.10 and 2.11).

ABBREVIATIONS

aa	Amino acid	maxiEBV	EBV-genome encoding BAC
ActD	Actinomycin D	MFI	Mean fluorescence intensity
AP	Alkaline phosphatase	MHC	Major histocompatibility complex
APC	Allophycocyanin	miR	MicroRNA
APS	Ammonium persulfate	MoI	Multiplicity of infection
ARE	AU rich element	mRNA	Messenger RNA
ARM	Arginine rich motif	MTT	3-(4,5-Dimethylthiazol-2-yl)-2,5-diphenyltetrazolium bromide
BAC	Bacterial artificial chromosome	n.d.	Not detected
BL	Burkitt lymphoma	NK	Natural killer cell
bp	Base pair	NKT	Natural killer T cells
CD	Cluster of differentiation	NPC	Naso-pharynx carcinoma
cDNA	Complementary DNA	nt	Nucleotide
CHX	Cycloheximide	o/n	Overnight
Cy5	Cyanine 5	OD	Optical density
dpi	Day(s) post infection	ORF	Open reading frame
E	Early	p-NPP	Phospho-nitrophenyl phosphate
EBV	Epstein-Barr virus	PAGE	Polyacrylamide gelelectrophoresis
ELISA	Enzyme linked immunosorbent assay	PAMP	Pathogen associated molecular pattern
ER	endoplasmatic reticulum	PBMC	Peripheral blood monocytic cells
FACS	Fluorescence-activated cell sorting	PBS	Phosphate buffered saline
FCS	Fetal calf serum	PE	Phycoerythrin
g	Relative centrifugal force	PEI	Polyethylenimine
GFP	Green fluorescent protein	PEL	Primary effusion lymphoma
gp	Glycoprotein	PerCP	Peridinin Chlorophyll protein complex
GRU	Green Raji unit	PRR	PAMP recognition receptor
Gy	Gray, absorbed dose of ionizing radiation	PTLD	Post transplant lymphoproliferative disease
hCMV	Human Cytomegalovirus	qPCR	Quantitative PCR
HHV	Human Herpes virus	R ²	Coefficient of determination
HLA	Human leukocyte antigen	rpm	Rounds per minute
hpi	Hour(s) post infection	RT	Room temperature
HSV I	Herpes simplex virus I	SDS	Sodium dodecylsulfate
IE	Immediate early	TAP	Transporter associated with antigen processing
Ifn	Interferon	TBS	Tris buffered saline
Ig	Immunoglobulin	TCR	T cell receptor
IL	Interleukin	Th	T helper cell
IM	Infectious mononucleosis	TNF	Tumor necrosis factor
IS	Immune system	TR	Terminal repeat
KSHV	Kaposi sarcoma Herpes virus	TTP	Tristetraprolin
KIR	Killing inhibitory receptor	XLD	X-linked lymphoproliferative disease
LCL	Lymphoblastoid cell line		

LITERATURE

- Akdis, C.A., and Blaser, K. (2001). Mechanisms of interleukin-10-mediated immune suppression. *Immunology* 103, 131-136.
- Al Tabaa, Y., Tuailon, E., Bollore, K., Foulongne, V., Petitjean, G., Seigneurin, J.M., Duperray, C., Desgranges, C., and Vendrell, J.P. (2009). Functional Epstein-Barr virus reservoir in plasma cells derived from infected peripheral blood memory B cells. *Blood* 113, 604-611.
- Altmann, M., and Hammerschmidt, W. (2005). Epstein-Barr virus provides a new paradigm: a requirement for the immediate inhibition of apoptosis. *PLoS Biol* 3, e404.
- Ambagala, A.P., Gopinath, R.S., and Srikumaran, S. (2003). Inhibition of TAP by pseudorabies virus is independent of its vhs activity. *Virus Res* 96, 37-48.
- Amon, W., Binne, U.K., Bryant, H., Jenkins, P.J., Karstegl, C.E., and Farrell, P.J. (2004). Lytic cycle gene regulation of Epstein-Barr virus. *J Virol* 78, 13460-13469.
- Baer, R., Bankier, A.T., Biggin, M.D., Deininger, P.L., Farrell, P.J., Gibson, T.J., Hatfull, G., Hudson, G.S., Satchwell, S.C., Seguin, C., and et al. (1984). DNA sequence and expression of the B95-8 Epstein-Barr virus genome. *Nature* 310, 207-211.
- Barth, S., Pfuhl, T., Mamiani, A., Ehses, C., Roemer, K., Kremmer, E., Jaker, C., Hock, J., Meister, G., and Grasser, F.A. (2008). Epstein-Barr virus-encoded microRNA miR-BART2 down-regulates the viral DNA polymerase BALF5. *Nucleic Acids Res* 36, 666-675.
- Batisse, J., Manet, E., Middeldorp, J., Sergeant, A., and Gruffat, H. (2005). Epstein-Barr virus mRNA export factor EB2 is essential for intranuclear capsid assembly and production of gp350. *J Virol* 79, 14102-14111.
- Bayliss, G.J., and Wolf, H. (1981). The regulated expression of Epstein-Barr virus. III. Proteins specified by EBV during the lytic cycle. *J Gen Virol* 56, 105-118.
- Bechtel, J., Grundhoff, A., and Ganem, D. (2005). RNAs in the virion of Kaposi's sarcoma-associated herpesvirus. *J Virol* 79, 10138-10146.
- Beck, S., and Barrell, B.G. (1988). Human cytomegalovirus encodes a glycoprotein homologous to MHC class-I antigens. *Nature* 331, 269-272.
- Bejarano, M.T., and Masucci, M.G. (1998). Interleukin-10 abrogates the inhibition of Epstein-Barr virus-induced B-cell transformation by memory T-cell responses. *Blood* 92, 4256-4262.
- Berg, D.J., Leach, M.W., Kuhn, R., Rajewsky, K., Muller, W., Davidson, N.J., and Rennick, D. (1995). Interleukin 10 but not interleukin 4 is a natural suppressant of cutaneous inflammatory responses. *The Journal of experimental medicine* 182, 99-108.
- Bergbauer, M., Kalla, M., Schmeinck, A., Gobel, C., Rothbauer, U., Eck, S., Benet-Pages, A., Strom, T.M., and Hammerschmidt, W. (2010). CpG-methylation regulates a class of Epstein-Barr virus promoters. *PLoS Pathog* 6.

- Biron, C.A. (1994). Cytokines in the generation of immune responses to, and resolution of, virus infection. *Curr Opin Immunol* 6, 530-538.
- Blackshear, P.J. (2002). Tristetraprolin and other CCCH tandem zinc-finger proteins in the regulation of mRNA turnover. *Biochemical Society transactions* 30, 945-952.
- Blazar, B., Patarroyo, M., Klein, E., and Klein, G. (1980). Increased sensitivity of human lymphoid lines to natural killer cells after induction of the Epstein-Barr viral cycle by superinfection or sodium butyrate. *J Exp Med* 151, 614-627.
- Bogedain, C., Wolf, H., Modrow, S., Stuber, G., and Jilg, W. (1995). Specific cytotoxic T lymphocytes recognize the immediate-early transactivator Zta of Epstein-Barr virus. *J Virol* 69, 4872-4879.
- Bollard, C.M., Cooper, L.J., and Heslop, H.E. (2008). Immunotherapy targeting EBV-expressing lymphoproliferative diseases. Best practice & research. *Clinical haematology* 21, 405-420.
- Boname, J.M., de Lima, B.D., Lehner, P.J., and Stevenson, P.G. (2004). Viral degradation of the MHC class I peptide loading complex. *Immunity* 20, 305-317.
- Bouaziz, J.D., Yanaba, K., and Tedder, T.F. (2008). Regulatory B cells as inhibitors of immune responses and inflammation. *Immunol Rev* 224, 201-214.
- Bouillie, S., Barel, M., Drane, P., Cassinat, B., Balbo, M., Holers, V.M., and Frade, R. (1995). Epstein-Barr virus/C3d receptor (CR2, CD21) activated by its extracellular ligands regulates pp105 phosphorylation through two distinct pathways. *Eur J Immunol* 25, 2661-2667.
- Bresnahan, W.A., and Shenk, T. (2000). A subset of viral transcripts packaged within human cytomegalovirus particles. *Science* 288, 2373-2376.
- Burrows, S.R., Gardner, J., Khanna, R., Steward, T., Moss, D.J., Rodda, S., and Suhrbier, A. (1994). Five new cytotoxic T cell epitopes identified within Epstein-Barr virus nuclear antigen 3. *J Gen Virol* 75 (Pt 9), 2489-2493.
- Busch, L.K., and Bishop, G.A. (1999). The EBV transforming protein, latent membrane protein 1, mimics and cooperates with CD40 signaling in B lymphocytes. *J Immunol* 162, 2555-2561.
- Callan, M.F., Steven, N., Krausa, P., Wilson, J.D., Moss, P.A., Gillespie, G.M., Bell, J.I., Rickinson, A.B., and McMichael, A.J. (1996). Large clonal expansions of CD8+ T cells in acute infectious mononucleosis. *Nature medicine* 2, 906-911.
- Carballo, E., Lai, W.S., and Blackshear, P.J. (1998). Feedback inhibition of macrophage tumor necrosis factor-alpha production by tristetraprolin. *Science* 281, 1001-1005.
- Chen, C., Ridzon, D.A., Broomer, A.J., Zhou, Z., Lee, D.H., Nguyen, J.T., Barbisin, M, Xu, N.L., Mahuvakar, V.R., Andersen, M.R., Lao, K.Q., Livak, K.J. and Guegler, K.J. (2005). Real-time quantification of microRNAs by stem-loop RT-PCR. *Nucleic Acid Res.* 33, e179.
- Cheung, R.K., Miyazaki, I., and Dosch, H.M. (1993). Unexpected patterns of Epstein-Barr virus gene expression during early stages of B cell transformation. *Int Immunol* 5, 707-716.

- Cohen, J.I. (1999). The biology of Epstein-Barr virus: lessons learned from the virus and the host. *Curr Opin Immunol* *11*, 365-370.
- Cooper, M.A., Fehniger, T.A., and Caligiuri, M.A. (2001). The biology of human natural killer-cell subsets. *Trends in immunology* *22*, 633-640.
- Countryman, J., Jenson, H., Seibl, R., Wolf, H., and Miller, G. (1987). Polymorphic proteins encoded within BZLF1 of defective and standard Epstein-Barr viruses disrupt latency. *J Virol* *61*, 3672-3679.
- Croft, N.P., Shannon-Lowe, C., Bell, A.I., Horst, D., Kremmer, E., Rensing, M.E., Wiertz, E.J., Middeldorp, J.M., Rowe, M., Rickinson, A.B., and Hislop, A.D. (2009). Stage-specific inhibition of MHC class I presentation by the Epstein-Barr virus BNLF2a protein during virus lytic cycle. *PLoS Pathog* *5*, e1000490.
- de Brouwer, A.P., van Bokhoven, H. and Kremer, H. (2006). Comparison of 12 reference genes for normalization of gene expression levels in Epstein-Barr virus-transformed lymphoblastoid cell lines and fibroblasts. *Mol Diagn Ther* *10*, 197-204
- de Waal Malefyt, R., Abrams, J., Bennett, B., Figdor, C.G., and de Vries, J.E. (1991a). Interleukin 10(IL-10) inhibits cytokine synthesis by human monocytes: an autoregulatory role of IL-10 produced by monocytes. *The Journal of experimental medicine* *174*, 1209-1220.
- de Waal Malefyt, R., Haanen, J., Spits, H., Roncarolo, M.G., te Velde, A., Figdor, C., Johnson, K., Kastelein, R., Yssel, H., and de Vries, J.E. (1991b). Interleukin 10 (IL-10) and viral IL-10 strongly reduce antigen-specific human T cell proliferation by diminishing the antigen-presenting capacity of monocytes via downregulation of class II major histocompatibility complex expression. *J Exp Med* *174*, 915-924.
- Delecluse, H.J., Feederle, R., Behrends, U., and Mautner, J. (2008). Contribution of viral recombinants to the study of the immune response against the Epstein-Barr virus. *Semin Cancer Biol* *18*, 409-415.
- Delecluse, H.J., Hilsendegen, T., Pich, D., Zeidler, R., and Hammerschmidt, W. (1998). Propagation and recovery of intact, infectious Epstein-Barr virus from prokaryotic to human cells. *Proc Natl Acad Sci U S A* *95*, 8245-8250.
- Delecluse, H.J., Pich, D., Hilsendegen, T., Baum, C., and Hammerschmidt, W. (1999). A first-generation packaging cell line for Epstein-Barr virus-derived vectors. *Proc Natl Acad Sci U S A* *96*, 5188-5193.
- Deutsch, M.J., Ott, E., Papior, P., and Schepers, A. (2010). The latent origin of replication of Epstein-Barr virus directs viral genomes to active regions of the nucleus. *Journal of virology* *84*, 2533-2546.
- Ding, Y., Qin, L., Kotenko, S.V., Pestka, S., and Bromberg, J.S. (2000). A single amino acid determines the immunostimulatory activity of interleukin 10. *J Exp Med* *191*, 213-224.
- Dolken, L., Malterer, G., Erhard, F., Kothe, S., Friedel, C.C., Suffert, G., Marcinowski, L., Motsch, N., Barth, S., Beitzinger, M., *et al.* (2010). Systematic analysis of viral and cellular microRNA targets in cells latently infected with human gamma-herpesviruses by RISC immunoprecipitation assay. *Cell Host Microbe* *7*, 324-334.

- Epstein, M.A., and Achong, B.G. (1979). *The Epstein-Barr virus* (Berlin ; New York: Springer-Verlag).
- Fiorentino, D.F., Bond, M.W., and Mosmann, T.R. (1989). Two types of mouse T helper cell. IV. Th2 clones secrete a factor that inhibits cytokine production by Th1 clones. *The Journal of experimental medicine* *170*, 2081-2095.
- Fiorentino, D.F., Zlotnik, A., Vieira, P., Mosmann, T.R., Howard, M., Moore, K.W., and O'Garra, A. (1991). IL-10 acts on the antigen-presenting cell to inhibit cytokine production by Th1 cells. *Journal of immunology* *146*, 3444-3451.
- Flamand, L., Stefanescu, I., Ablashi, D.V., and Menezes, J. (1993). Activation of the Epstein-Barr virus replicative cycle by human herpesvirus 6. *J Virol* *67*, 6768-6777.
- Fleming, S.B., McCaughan, C.A., Andrews, A.E., Nash, A.D., and Mercer, A.A. (1997). A homolog of interleukin-10 is encoded by the poxvirus orf virus. *J Virol* *71*, 4857-4861.
- Fowlkes, B.J., Kruisbeek, A.M., Ton-That, H., Weston, M.A., Coligan, J.E., Schwartz, R.H., and Pardoll, D.M. (1987). A novel population of T-cell receptor alpha beta-bearing thymocytes which predominantly expresses a single V beta gene family. *Nature* *329*, 251-254.
- Gazzinelli, R.T., Oswald, I.P., James, S.L., and Sher, A. (1992). IL-10 inhibits parasite killing and nitrogen oxide production by IFN-gamma-activated macrophages. *Journal of immunology* *148*, 1792-1796.
- Germain, R.N. (1994). MHC-dependent antigen processing and peptide presentation: providing ligands for T lymphocyte activation. *Cell* *76*, 287-299.
- Go, N.F., Castle, B.E., Barrett, R., Kastelein, R., Dang, W., Mosmann, T.R., Moore, K.W., and Howard, M. (1990). Interleukin 10, a novel B cell stimulatory factor: unresponsiveness of X chromosome-linked immunodeficiency B cells. *The Journal of experimental medicine* *172*, 1625-1631.
- Godfrey, D.I., MacDonald, H.R., Kronenberg, M., Smyth, M.J., and Van Kaer, L. (2004). NKT cells: what's in a name? *Nat Rev Immunol* *4*, 231-237.
- Gottschalk, S., Heslop, H.E., and Rooney, C.M. (2005a). Adoptive immunotherapy for EBV-associated malignancies. *Leukemia & lymphoma* *46*, 1-10.
- Gottschalk, S., Rooney, C.M., and Heslop, H.E. (2005b). Post-transplant lymphoproliferative disorders. *Annual review of medicine* *56*, 29-44.
- Graham, F.L., Smiley, J., Russell, W.C., and Nairn, R. (1977). Characteristics of a human cell line transformed by DNA from human adenovirus type 5. *J Gen Virol* *36*, 59-74.
- Gregorovic, G., Bosshard, R., Karstegl, C.E., White, R.E., Pattle, S., Chiang, A.K., Dittrich-Breiholz, O., Kracht, M., Russ, R., and Farrell, P.J. (2011). Cell gene expression correlating with EBER expression in Epstein-Barr virus infected lymphoblastoid cell lines. *J Virol*.
- Greijer, A.E., Dekkers, C.A., and Middeldorp, J.M. (2000). Human cytomegalovirus virions differentially incorporate viral and host cell RNA during the assembly process. *J Virol* *74*, 9078-9082.

- Griffin, B.D., Verweij, M.C., and Wiertz, E.J. (2010). Herpesviruses and immunity: the art of evasion. *Veterinary microbiology* 143, 89-100.
- Groux, H., O'Garra, A., Bigler, M., Rouleau, M., Antonenko, S., de Vries, J.E., and Roncarolo, M.G. (1997). A CD4+ T-cell subset inhibits antigen-specific T-cell responses and prevents colitis. *Nature* 389, 737-742.
- Gruffat, H., Batisse, J., Pich, D., Neuhierl, B., Manet, E., Hammerschmidt, W., and Sergeant, A. (2002). Epstein-Barr virus mRNA export factor EB2 is essential for production of infectious virus. *J Virol* 76, 9635-9644.
- Grundhoff, A., Sullivan, C.S., and Ganem, D. (2006). A combined computational and microarray-based approach identifies novel microRNAs encoded by human gamma-herpesviruses. *Rna* 12, 733-750.
- Guo, Q., Qian, L., Guo, L., Shi, M., Chen, C., Lv, X., Yu, M., Hu, M., Jiang, G., and Guo, N. (2010). Transactivators Zta and Rta of Epstein-Barr virus promote G0/G1 to S transition in Raji cells: a novel relationship between lytic virus and cell cycle. *Mol Immunol* 47, 1783-1792.
- Hammerschmidt, W., and Sugden, B. (1989). Genetic analysis of immortalizing functions of Epstein-Barr virus in human B lymphocytes. *Nature* 340, 393-397.
- Hansen, T.H., and Bouvier, M. (2009). MHC class I antigen presentation: learning from viral evasion strategies. *Nat Rev Immunol* 9, 503-513.
- Hardy, M.P., Owczarek, C.M., Jermin, L.S., Ejdeback, M., and Hertzog, P.J. (2004). Characterization of the type I interferon locus and identification of novel genes. *Genomics* 84, 331-345.
- He, L., and Hannon, G.J. (2004). MicroRNAs: small RNAs with a big role in gene regulation. *Nature reviews. Genetics* 5, 522-531.
- Hettich, E., Janz, A., Zeidler, R., Pich, D., Hellebrand, E., Weissflog, B., Moosmann, A., and Hammerschmidt, W. (2006). Genetic design of an optimized packaging cell line for gene vectors transducing human B cells. *Gene therapy* 13, 844-856.
- Hill, A., Jugovic, P., York, I., Russ, G., Bennink, J., Yewdell, J., Ploegh, H., and Johnson, D. (1995). Herpes simplex virus turns off the TAP to evade host immunity. *Nature* 375, 411-415.
- Hiriart, E., Bardouillet, L., Manet, E., Gruffat, H., Penin, F., Montserret, R., Farjot, G., and Sergeant, A. (2003a). A region of the Epstein-Barr virus (EBV) mRNA export factor EB2 containing an arginine-rich motif mediates direct binding to RNA. *J Biol Chem* 278, 37790-37798.
- Hiriart, E., Farjot, G., Gruffat, H., Nguyen, M.V., Sergeant, A., and Manet, E. (2003b). A novel nuclear export signal and a REF interaction domain both promote mRNA export by the Epstein-Barr virus EB2 protein. *J Biol Chem* 278, 335-342.
- Hislop, A.D., Palendira, U., Leese, A.M., Arkwright, P.D., Rohrlich, P.S., Tangye, S.G., Gaspar, H.B., Lankester, A.C., Moretta, A., and Rickinson, A.B. (2010). Impaired Epstein-

- Barr virus-specific CD8⁺ T-cell function in X-linked lymphoproliferative disease is restricted to SLAM family-positive B-cell targets. *Blood* *116*, 3249-3257.
- Hislop, A.D., Rensing, M.E., van Leeuwen, D., Pudney, V.A., Horst, D., Koppers-Lalic, D., Croft, N.P., Neefjes, J.J., Rickinson, A.B., and Wiertz, E.J. (2007). A CD8⁺ T cell immune evasion protein specific to Epstein-Barr virus and its close relatives in Old World primates. *J Exp Med* *204*, 1863-1873.
- Horst, D., van Leeuwen, D., Croft, N.P., Garstka, M.A., Hislop, A.D., Kremmer, E., Rickinson, A.B., Wiertz, E.J., and Rensing, M.E. (2009). Specific targeting of the EBV lytic phase protein BNLF2a to the transporter associated with antigen processing results in impairment of HLA class I-restricted antigen presentation. *J Immunol* *182*, 2313-2324.
- Hsu, D.H., de Waal Malefyt, R., Fiorentino, D.F., Dang, M.N., Vieira, P., de Vries, J., Spits, H., Mosmann, T.R., and Moore, K.W. (1990). Expression of interleukin-10 activity by Epstein-Barr virus protein BCRF1. *Science* *250*, 830-832.
- Iskra, S., Kalla, M., Delecluse, H.J., Hammerschmidt, W., and Moosmann, A. (2010). Toll-like receptor agonists synergistically increase proliferation and activation of B cells by Epstein-Barr virus. *J Virol* *84*, 3612-3623.
- Iwakiri, D., and Takada, K. (2010). Role of EBERs in the pathogenesis of EBV infection. *Advances in cancer research* *107*, 119-136.
- Iwakiri, D., Zhou, L., Samanta, M., Matsumoto, M., Ebihara, T., Seya, T., Imai, S., Fujieda, M., Kawa, K., and Takada, K. (2009). Epstein-Barr virus (EBV)-encoded small RNA is released from EBV-infected cells and activates signaling from Toll-like receptor 3. *J Exp Med* *206*, 2091-2099.
- Janeway, C. (2005). *Immunobiology : the immune system in health and disease*, 6th edn (New York: Garland Science).
- Janssen, E.M., Lemmens, E.E., Wolfe, T., Christen, U., von Herrath, M.G., and Schoenberger, S.P. (2003). CD4⁺ T cells are required for secondary expansion and memory in CD8⁺ T lymphocytes. *Nature* *421*, 852-856.
- Joseph, A.M., Babcock, G.J., and Thorley-Lawson, D.A. (2000). EBV persistence involves strict selection of latently infected B cells. *Journal of immunology* *165*, 2975-2981.
- Kalla, M., Schmeink, A., Bergbauer, M., Pich, D., and Hammerschmidt, W. (2010). AP-1 homolog BZLF1 of Epstein-Barr virus has two essential functions dependent on the epigenetic state of the viral genome. *Proc Natl Acad Sci U S A* *107*, 850-855.
- Kanai, K., Satoh, Y., Yamanaka, H., Kawaguchi, A., Horie, K., Sugata, K., Hoshikawa, Y., Sata, T., and Sairenji, T. (2007). The vIL-10 gene of the Epstein-Barr virus (EBV) is conserved in a stable manner except for a few point mutations in various EBV isolates. *Virus Genes* *35*, 563-569.
- Kanda, T., Otter, M., and Wahl, G.M. (2001). Coupling of mitotic chromosome tethering and replication competence in Epstein-Barr virus-based plasmids. *Mol Cell Biol* *21*, 3576-3588.
- Kawai, T., and Akira, S. (2008). Toll-like receptor and RIG-I-like receptor signaling. *Annals of the New York Academy of Sciences* *1143*, 1-20.

- Klein, E., Klein, G., Nadkarni, J.S., Nadkarni, J.J., Wigzell, H., and Clifford, P. (1968). Surface IgM-kappa specificity on a Burkitt lymphoma cell in vivo and in derived culture lines. *Cancer Res* 28, 1300-1310.
- Komano, J., Sugiura, M., and Takada, K. (1998). Epstein-Barr virus contributes to the malignant phenotype and to apoptosis resistance in Burkitt's lymphoma cell line Akata. *J Virol* 72, 9150-9156.
- Kotenko, S.V., Gallagher, G., Baurin, V.V., Lewis-Antes, A., Shen, M., Shah, N.K., Langer, J.A., Sheikh, F., Dickensheets, H., and Donnelly, R.P. (2003). IFN-lambdas mediate antiviral protection through a distinct class II cytokine receptor complex. *Nat Immunol* 4, 69-77.
- Kotenko, S.V., Sacconi, S., Izotova, L.S., Mirochnitchenko, O.V., and Pestka, S. (2000). Human cytomegalovirus harbors its own unique IL-10 homolog (cmvIL-10). *Proc Natl Acad Sci U S A* 97, 1695-1700.
- Krishnan, H.H., Naranatt, P.P., Smith, M.S., Zeng, L., Bloomer, C., and Chandran, B. (2004). Concurrent expression of latent and a limited number of lytic genes with immune modulation and antiapoptotic function by Kaposi's sarcoma-associated herpesvirus early during infection of primary endothelial and fibroblast cells and subsequent decline of lytic gene expression. *J Virol* 78, 3601-3620.
- Kuhn, R., Lohler, J., Rennick, D., Rajewsky, K., and Muller, W. (1993). Interleukin-10-deficient mice develop chronic enterocolitis. *Cell* 75, 263-274.
- Kuppers, R. (2003). B cells under influence: transformation of B cells by Epstein-Barr virus. *Nat Rev Immunol* 3, 801-812.
- Lautscham, G., Mayrhofer, S., Taylor, G., Haigh, T., Leese, A., Rickinson, A., and Blake, N. (2001). Processing of a multiple membrane spanning Epstein-Barr virus protein for CD8(+) T cell recognition reveals a proteasome-dependent, transporter associated with antigen processing-independent pathway. *J Exp Med* 194, 1053-1068.
- Lautscham, G., Rickinson, A., and Blake, N. (2003). TAP-independent antigen presentation on MHC class I molecules: lessons from Epstein-Barr virus. *Microbes Infect* 5, 291-299.
- Lauw, F.N., Pajkrt, D., Hack, C.E., Kurimoto, M., van Deventer, S.J., and van der Poll, T. (2000). Proinflammatory effects of IL-10 during human endotoxemia. *J Immunol* 165, 2783-2789.
- Lee, S.P., Thomas, W.A., Blake, N.W., and Rickinson, A.B. (1996). Transporter (TAP)-independent processing of a multiple membrane-spanning protein, the Epstein-Barr virus latent membrane protein 2. *Eur J Immunol* 26, 1875-1883.
- Lee, S.P., Thomas, W.A., Murray, R.J., Khanim, F., Kaur, S., Young, L.S., Rowe, M., Kurilla, M., and Rickinson, A.B. (1993). HLA A2.1-restricted cytotoxic T cells recognizing a range of Epstein-Barr virus isolates through a defined epitope in latent membrane protein LMP2. *J Virol* 67, 7428-7435.
- Lerner, M.R., Andrews, N.C., Miller, G., and Steitz, J.A. (1981). Two small RNAs encoded by Epstein-Barr virus and complexed with protein are precipitated by antibodies from patients with systemic lupus erythematosus. *Proc Natl Acad Sci U S A* 78, 805-809.

- Liu, Y., de Waal Malefyt, R., Briere, F., Parham, C., Bridon, J.M., Banchereau, J., Moore, K.W., and Xu, J. (1997). The EBV IL-10 homologue is a selective agonist with impaired binding to the IL-10 receptor. *J Immunol* *158*, 604-613.
- Lo, A.K., To, K.F., Lo, K.W., Lung, R.W., Hui, J.W., Liao, G., and Hayward, S.D. (2007). Modulation of LMP1 protein expression by EBV-encoded microRNAs. *Proc Natl Acad Sci U S A* *104*, 16164-16169.
- London, C.A., Lodge, M.P., and Abbas, A.K. (2000). Functional responses and costimulator dependence of memory CD4+ T cells. *Journal of immunology* *164*, 265-272.
- Long, E.O. (1999). Regulation of immune responses through inhibitory receptors. *Annu Rev Immunol* *17*, 875-904.
- Long, H.M., Taylor, G.S., and Rickinson, A.B. (2011). Immune defence against EBV and EBV-associated disease. *Curr Opin Immunol*.
- Luscher, B., and Eisenman, R.N. (1988). c-myc and c-myb protein degradation: effect of metabolic inhibitors and heat shock. *Mol Cell Biol* *8*, 2504-2512.
- MacNeil, I.A., Suda, T., Moore, K.W., Mosmann, T.R., and Zlotnik, A. (1990). IL-10, a novel growth cofactor for mature and immature T cells. *J Immunol* *145*, 4167-4173.
- Mahot, S., Sergeant, A., Drouet, E., and Gruffat, H. (2003). A novel function for the Epstein-Barr virus transcription factor EB1/Zta: induction of transcription of the hIL-10 gene. *J Gen Virol* *84*, 965-974.
- Maldonado, R.A., Irvine, D.J., Schreiber, R., and Glimcher, L.H. (2004). A role for the immunological synapse in lineage commitment of CD4 lymphocytes. *Nature* *431*, 527-532.
- Maldonado, R.A., Soriano, M.A., Perdomo, L.C., Sigrist, K., Irvine, D.J., Decker, T., and Glimcher, L.H. (2009). Control of T helper cell differentiation through cytokine receptor inclusion in the immunological synapse. *J Exp Med* *206*, 877-892.
- Mancao, C., Altmann, M., Jungnickel, B., and Hammerschmidt, W. (2005). Rescue of "crippled" germinal center B cells from apoptosis by Epstein-Barr virus. *Blood* *106*, 4339-4344.
- Marcu, K.B., Bossone, S.A., and Patel, A.J. (1992). myc function and regulation. *Annual review of biochemistry* *61*, 809-860.
- Martorelli, D., Muraro, E., Merlo, A., Turrini, R., Rosato, A., and Dolcetti, R. (2010). Role of CD4+ cytotoxic T lymphocytes in the control of viral diseases and cancer. *Int Rev Immunol* *29*, 371-402.
- McKenna, S.A., Lindhout, D.A., Shimoike, T., Aitken, C.E., and Puglisi, J.D. (2007). Viral dsRNA inhibitors prevent self-association and autophosphorylation of PKR. *J Mol Biol* *372*, 103-113.
- Meijer, E., and Cornelissen, J.J. (2008). Epstein-Barr virus-associated lymphoproliferative disease after allogeneic haematopoietic stem cell transplantation: molecular monitoring and early treatment of high-risk patients. *Current opinion in hematology* *15*, 576-585.

- Messeguer, X., Escudero, R., Farre, D., Nunez, O., Martinez, J., and Alba, M.M. (2002). PROMO: detection of known transcription regulatory elements using species-tailored searches. *Bioinformatics* 18, 333-334.
- Metzger, H. (1990). Fc receptors and the action of antibodies (Washington, D.C.: American Society for Microbiology).
- Meylan, E., and Tschopp, J. (2006). Toll-like receptors and RNA helicases: two parallel ways to trigger antiviral responses. *Mol Cell* 22, 561-569.
- Miller, G., El-Guindy, A., Countryman, J., Ye, J., and Gradoville, L. (2007). Lytic cycle switches of oncogenic human gammaherpesviruses. *Advances in cancer research* 97, 81-109.
- Miller, G., and Lipman, M. (1973). Release of infectious Epstein-Barr virus by transformed marmoset leukocytes. *Proc Natl Acad Sci U S A* 70, 190-194.
- Miller, G., Shope, T., Lisco, H., Stitt, D., and Lipman, M. (1972). Epstein-Barr virus: transformation, cytopathic changes, and viral antigens in squirrel monkey and marmoset leukocytes. *Proc Natl Acad Sci U S A* 69, 383-387.
- Miyazaki, I., Cheung, R.K., and Dosch, H.M. (1993). Viral interleukin 10 is critical for the induction of B cell growth transformation by Epstein-Barr virus. *J Exp Med* 178, 439-447.
- Mocellin, S., Marincola, F., Rossi, C.R., Nitti, D., and Lise, M. (2004). The multifaceted relationship between IL-10 and adaptive immunity: putting together the pieces of a puzzle. *Cytokine Growth Factor Rev* 15, 61-76.
- Modlin, R.L., and Nutman, T.B. (1993). Type 2 cytokines and negative immune regulation in human infections. *Curr Opin Immunol* 5, 511-517.
- Moore, K.W., de Waal Malefyt, R., Coffman, R.L., and O'Garra, A. (2001). Interleukin-10 and the interleukin-10 receptor. *Annu Rev Immunol* 19, 683-765.
- Moore, K.W., Vieira, P., Fiorentino, D.F., Trounstein, M.L., Khan, T.A., and Mosmann, T.R. (1990). Homology of cytokine synthesis inhibitory factor (IL-10) to the Epstein-Barr virus gene BCRF1. *Science* 248, 1230-1234.
- Moosmann, A., Bigalke, I., Tischer, J., Schirrmann, L., Kasten, J., Tippmer, S., Leeping, M., Prevalsek, D., Jaeger, G., Ledderose, G., *et al.* (2010). Effective and long-term control of EBV PTLD after transfer of peptide-selected T cells. *Blood* 115, 2960-2970.
- Mosmann, T. (1983). Rapid colorimetric assay for cellular growth and survival: application to proliferation and cytotoxicity assays. *J Immunol Methods* 65, 55-63.
- Mosser, D.M., and Zhang, X. (2008). Interleukin-10: new perspectives on an old cytokine. *Immunol Rev* 226, 205-218.
- Murphy, S. (1999). The HLA system : basic biology and clinical applications (Bethesda, Md.: American Association of Blood Banks).

- Nachmani, D., Stern-Ginossar, N., Sarid, R., and Mandelboim, O. (2009). Diverse herpesvirus microRNAs target the stress-induced immune ligand MICB to escape recognition by natural killer cells. *Cell Host Microbe* 5, 376-385.
- Nakayama, S., Murata, T., Murayama, K., Yasui, Y., Sato, Y., Kudoh, A., Iwahori, S., Isomura, H., Kanda, T., and Tsurumi, T. (2009). Epstein-Barr virus polymerase processivity factor enhances BALF2 promoter transcription as a coactivator for the BZLF1 immediate-early protein. *J Biol Chem* 284, 21557-21568.
- Nanbo, A., Inoue, K., Adachi-Takasawa, K., and Takada, K. (2002). Epstein-Barr virus RNA confers resistance to interferon-alpha-induced apoptosis in Burkitt's lymphoma. *EMBO J* 21, 954-965.
- Nemerow, G.R., Mold, C., Schwend, V.K., Tollefson, V., and Cooper, N.R. (1987). Identification of gp350 as the viral glycoprotein mediating attachment of Epstein-Barr virus (EBV) to the EBV/C3d receptor of B cells: sequence homology of gp350 and C3 complement fragment C3d. *Journal of virology* 61, 1416-1420.
- Neuhierl, B., and Delecluse, H.J. (2006). The Epstein-Barr virus BMRF1 gene is essential for lytic virus replication. *J Virol* 80, 5078-5081.
- Neuhierl, B., Feederle, R., Hammerschmidt, W., and Delecluse, H.J. (2002). Glycoprotein gp110 of Epstein-Barr virus determines viral tropism and efficiency of infection. *Proc Natl Acad Sci U S A* 99, 15036-15041.
- O'Garra, A., and Arai, N. (2000). The molecular basis of T helper 1 and T helper 2 cell differentiation. *Trends Cell Biol* 10, 542-550.
- Ojala, P.M., Sodeik, B., Ebersold, M.W., Kutay, U., and Helenius, A. (2000). Herpes simplex virus type 1 entry into host cells: reconstitution of capsid binding and uncoating at the nuclear pore complex in vitro. *Mol Cell Biol* 20, 4922-4931.
- Opal, S.M., Wherry, J.C., and Grint, P. (1998). Interleukin-10: potential benefits and possible risks in clinical infectious diseases. *Clin Infect Dis* 27, 1497-1507.
- Pan, S.H., Tai, C.C., Lin, C.S., Hsu, W.B., Chou, S.F., Lai, C.C., Chen, J.Y., Tien, H.F., Lee, F.Y., and Wang, W.B. (2009). Epstein-Barr virus nuclear antigen 2 disrupts mitotic checkpoint and causes chromosomal instability. *Carcinogenesis* 30, 366-375.
- Papadopoulos, E.B., Ladanyi, M., Emanuel, D., Mackinnon, S., Boulad, F., Carabasi, M.H., Castro-Malaspina, H., Childs, B.H., Gillio, A.P., Small, T.N., and et al. (1994). Infusions of donor leukocytes to treat Epstein-Barr virus-associated lymphoproliferative disorders after allogeneic bone marrow transplantation. *N Engl J Med* 330, 1185-1191.
- Pappworth, I.Y., Wang, E.C., and Rowe, M. (2007). The switch from latent to productive infection in Epstein-Barr virus-infected B cells is associated with sensitization to NK cell killing. *J Virol* 81, 474-482.
- Parato, K.G., Kumar, A., Badley, A.D., Sanchez-Dardon, J.L., Chambers, K.A., Young, C.D., Lim, W.T., Kravcik, S., Cameron, D.W., and Angel, J.B. (2002). Normalization of natural killer cell function and phenotype with effective anti-HIV therapy and the role of IL-10. *AIDS* 16, 1251-1256.

- Petersson, M., Charo, J., Salazar-Onfray, F., Noffz, G., Mohaupt, M., Qin, Z., Klein, G., Blankenstein, T., and Kiessling, R. (1998). Constitutive IL-10 production accounts for the high NK sensitivity, low MHC class I expression, and poor transporter associated with antigen processing (TAP)-1/2 function in the prototype NK target YAC-1. *J Immunol* *161*, 2099-2105.
- Pfeffer, S., Sewer, A., Lagos-Quintana, M., Sheridan, R., Sander, C., Grasser, F.A., van Dyk, L.F., Ho, C.K., Shuman, S., Chien, M., *et al.* (2005). Identification of microRNAs of the herpesvirus family. *Nature methods* *2*, 269-276.
- Pfeffer, S., Zavolan, M., Grasser, F.A., Chien, M., Russo, J.J., Ju, J., John, B., Enright, A.J., Marks, D., Sander, C., and Tuschl, T. (2004). Identification of virus-encoded microRNAs. *Science* *304*, 734-736.
- Pieters, J. (2000). MHC class II-restricted antigen processing and presentation. *Adv Immunol* *75*, 159-208.
- Pudney, V.A., Leese, A.M., Rickinson, A.B., and Hislop, A.D. (2005). CD8+ immunodominance among Epstein-Barr virus lytic cycle antigens directly reflects the efficiency of antigen presentation in lytically infected cells. *J Exp Med* *201*, 349-360.
- Pulvertaft, J.V. (1964). Cytology of Burkitt's Tumour (African Lymphoma). *Lancet* *1*, 238-240.
- Purcell, A.W., and Elliott, T. (2008). Molecular machinations of the MHC-I peptide loading complex. *Curr Opin Immunol* *20*, 75-81.
- Ragoczy, T., Heston, L., and Miller, G. (1998). The Epstein-Barr virus Rta protein activates lytic cycle genes and can disrupt latency in B lymphocytes. *J Virol* *72*, 7978-7984.
- Ralph, P., Nakoinz, I., Sampson-Johannes, A., Fong, S., Lowe, D., Min, H.Y., and Lin, L. (1992). IL-10, T lymphocyte inhibitor of human blood cell production of IL-1 and tumor necrosis factor. *Journal of immunology* *148*, 808-814.
- Ressing, M.E., Horst, D., Griffin, B.D., Tellam, J., Zuo, J., Khanna, R., Rowe, M., and Wiertz, E.J. (2008). Epstein-Barr virus evasion of CD8(+) and CD4(+) T cell immunity via concerted actions of multiple gene products. *Semin Cancer Biol* *18*, 397-408.
- Rickinson, A., and Kieff, E. (2007). Epstein Barr Virus. In *Fields virology*, B.N. Fields, D.M. Knipe, P.M. Howley, D.E. Griffin, M.A. Martin, and R.A. Lamb, eds. (Philadelphia: Wolters Kluwer Health/Lippincott Williams & Wilkins), pp. 2575-2672.
- Rickinson, A.B., and Moss, D.J. (1997). Human cytotoxic T lymphocyte responses to Epstein-Barr virus infection. *Annu Rev Immunol* *15*, 405-431.
- Rickinson, A.B., Rowe, M., Hart, I.J., Yao, Q.Y., Henderson, L.E., Rabin, H., and Epstein, M.A. (1984). T-cell-mediated regression of "spontaneous" and of Epstein-Barr virus-induced B-cell transformation in vitro: studies with cyclosporin A. *Cell Immunol* *87*, 646-658.
- Rock, K.L., and Shen, L. (2005). Cross-presentation: underlying mechanisms and role in immune surveillance. *Immunol Rev* *207*, 166-183.

- Rode, H.J., Janssen, W., Rosen-Wolff, A., Bugert, J.J., Thein, P., Becker, Y., and Darai, G. (1993). The genome of equine herpesvirus type 2 harbors an interleukin 10 (IL10)-like gene. *Virus Genes* 7, 111-116.
- Roizman, B. (2000). Redefining virology. *Science* 288, 2327-2328.
- Romagnani, S. (1999). Th1/Th2 cells. *Inflamm Bowel Dis* 5, 285-294.
- Rooney, C.M., Smith, C.A., Ng, C.Y., Loftin, S.K., Sixbey, J.W., Gan, Y., Srivastava, D.K., Bowman, L.C., Krance, R.A., Brenner, M.K., and Heslop, H.E. (1998). Infusion of cytotoxic T cells for the prevention and treatment of Epstein-Barr virus-induced lymphoma in allogeneic transplant recipients. *Blood* 92, 1549-1555.
- Rosa, M.D., Gottlieb, E., Lerner, M.R., and Steitz, J.A. (1981). Striking similarities are exhibited by two small Epstein-Barr virus-encoded ribonucleic acids and the adenovirus-associated ribonucleic acids VAI and VAII. *Mol Cell Biol* 1, 785-796.
- Rousset, F., Garcia, E., Defrance, T., Peronne, C., Vezzio, N., Hsu, D.H., Kastelein, R., Moore, K.W., and Banchereau, J. (1992a). Interleukin 10 is a potent growth and differentiation factor for activated human B lymphocytes. *Proceedings of the National Academy of Sciences of the United States of America* 89, 1890-1893.
- Rousset, F., Garcia, E., Defrance, T., Peronne, C., Vezzio, N., Hsu, D.H., Kastelein, R., Moore, K.W., and Banchereau, J. (1992b). Interleukin 10 is a potent growth and differentiation factor for activated human B lymphocytes. *Proc Natl Acad Sci U S A* 89, 1890-1893.
- Rowe, M., Glaunsinger, B., van Leeuwen, D., Zuo, J., Sweetman, D., Ganem, D., Middeldorp, J., Wiertz, E.J., and Rensing, M.E. (2007). Host shutoff during productive Epstein-Barr virus infection is mediated by BGLF5 and may contribute to immune evasion. *Proc Natl Acad Sci U S A* 104, 3366-3371.
- Ruf, I.K., Rhyne, P.W., Yang, H., Borza, C.M., Hutt-Fletcher, L.M., Cleveland, J.L., and Sample, J.T. (1999). Epstein-barr virus regulates c-MYC, apoptosis, and tumorigenicity in Burkitt lymphoma. *Mol Cell Biol* 19, 1651-1660.
- Ruiss, R., Jochum, S., Reisbach, G., Battke, C., Hammerschmidt, W., and Zeidler, R. (2011). A VLP-based Epstein Barr Virus vaccine. *Proc Natl Acad Sci U S A* *submitted*.
- Salek-Ardakani, S., Arrand, J.R., and Mackett, M. (2002). Epstein-Barr virus encoded interleukin-10 inhibits HLA-class I, ICAM-1, and B7 expression on human monocytes: implications for immune evasion by EBV. *Virology* 304, 342-351.
- Samanta, M., Iwakiri, D., Kanda, T., Imaizumi, T., and Takada, K. (2006). EB virus-encoded RNAs are recognized by RIG-I and activate signaling to induce type I IFN. *EMBO J* 25, 4207-4214.
- Samanta, M., and Takada, K. (2010). Modulation of innate immunity system by Epstein-Barr virus-encoded non-coding RNA and oncogenesis. *Cancer science* 101, 29-35.
- Sambrook, J., and Russell, D.W. (2001). *Molecular cloning : a laboratory manual*, 3rd edn (Cold Spring Harbor, N.Y.: Cold Spring Harbor Laboratory Press).

- Saulquin, X., Ibisch, C., Peyrat, M.A., Scotet, E., Hourmant, M., Vie, H., Bonneville, M., and Houssaint, E. (2000). A global appraisal of immunodominant CD8 T cell responses to Epstein-Barr virus and cytomegalovirus by bulk screening. *Eur J Immunol* 30, 2531-2539.
- Schoenborn, J.R., and Wilson, C.B. (2007). Regulation of interferon-gamma during innate and adaptive immune responses. *Adv Immunol* 96, 41-101.
- Schroder, K., Hertzog, P.J., Ravasi, T., and Hume, D.A. (2004). Interferon-gamma: an overview of signals, mechanisms and functions. *J Leukoc Biol* 75, 163-189.
- Sciortino, M.T., Suzuki, M., Taddeo, B., and Roizman, B. (2001). RNAs extracted from herpes simplex virus 1 virions: apparent selectivity of viral but not cellular RNAs packaged in virions. *J Virol* 75, 8105-8116.
- Sciortino, M.T., Taddeo, B., Poon, A.P., Mastino, A., and Roizman, B. (2002). Of the three tegument proteins that package mRNA in herpes simplex virions, one (VP22) transports the mRNA to uninfected cells for expression prior to viral infection. *Proc Natl Acad Sci U S A* 99, 8318-8323.
- Seto, E., Moosmann, A., Gromminger, S., Walz, N., Grundhoff, A., and Hammerschmidt, W. (2010). Micro RNAs of Epstein-Barr virus promote cell cycle progression and prevent apoptosis of primary human B cells. *PLoS Pathog* 6.
- Shannon-Lowe, C., Adland, E., Bell, A.I., Delecluse, H.J., Rickinson, A.B., and Rowe, M. (2009). Features distinguishing Epstein-Barr virus infections of epithelial cells and B cells: viral genome expression, genome maintenance, and genome amplification. *J Virol* 83, 7749-7760.
- Sharma, A., Kumar, M., Aich, J., Hariharan, M., Brahmachari, S.K., Agrawal, A., and Ghosh, B. (2009). Posttranscriptional regulation of interleukin-10 expression by hsa-miR-106a. *Proc Natl Acad Sci U S A* 106, 5761-5766.
- Shedlock, D.J., and Shen, H. (2003). Requirement for CD4 T cell help in generating functional CD8 T cell memory. *Science* 300, 337-339.
- Sheppard, P., Kindsvogel, W., Xu, W., Henderson, K., Schlutsmeyer, S., Whitmore, T.E., Kuestner, R., Garrigues, U., Birks, C., Roraback, J., *et al.* (2003). IL-28, IL-29 and their class II cytokine receptor IL-28R. *Nat Immunol* 4, 63-68.
- Siegel, M.R., and Sisler, H.D. (1963). Inhibition of Protein Synthesis in Vitro by Cycloheximide. *Nature* 200, 675-676.
- Sitkovsky, M.V. (1988). Mechanistic, functional and immunopharmacological implications of biochemical studies of antigen receptor-triggered cytolytic T-lymphocyte activation. *Immunological reviews* 103, 127-160.
- Snow, A.L., and Martinez, O.M. (2007). Epstein-Barr virus: evasive maneuvers in the development of PTLD. *American journal of transplantation : official journal of the American Society of Transplantation and the American Society of Transplant Surgeons* 7, 271-277.
- Sobell, H.M. (1985). Actinomycin and DNA transcription. *Proc Natl Acad Sci U S A* 82, 5328-5331.

- Sodeik, B., Ebersold, M.W., and Helenius, A. (1997). Microtubule-mediated transport of incoming herpes simplex virus 1 capsids to the nucleus. *The Journal of cell biology* *136*, 1007-1021.
- Spellberg, B., and Edwards, J.E., Jr. (2001). Type 1/Type 2 immunity in infectious diseases. *Clin Infect Dis* *32*, 76-102.
- Steinbrink, K., Wolf, M., Jonuleit, H., Knop, J., and Enk, A.H. (1997). Induction of tolerance by IL-10-treated dendritic cells. *J Immunol* *159*, 4772-4780.
- Steven, N.M., Leese, A.M., Annels, N.E., Lee, S.P., and Rickinson, A.B. (1996). Epitope focusing in the primary cytotoxic T cell response to Epstein-Barr virus and its relationship to T cell memory. *J Exp Med* *184*, 1801-1813.
- Stoecklin, G., Tenenbaum, S.A., Mayo, T., Chittur, S.V., George, A.D., Baroni, T.E., Blackshear, P.J., and Anderson, P. (2008). Genome-wide analysis identifies interleukin-10 mRNA as target of tristetraprolin. *J Biol Chem* *283*, 11689-11699.
- Strowig, T., Brilot, F., Arrey, F., Bougras, G., Thomas, D., Muller, W.A., and Munz, C. (2008). Tonsillar NK cells restrict B cell transformation by the Epstein-Barr virus via IFN-gamma. *PLoS Pathog* *4*, e27.
- Suzuki, T., Tahara, H., Narula, S., Moore, K.W., Robbins, P.D., and Lotze, M.T. (1995). Viral interleukin 10 (IL-10), the human herpes virus 4 cellular IL-10 homologue, induces local anergy to allogeneic and syngeneic tumors. *J Exp Med* *182*, 477-486.
- Swaminathan, S. (2008). Noncoding RNAs produced by oncogenic human herpesviruses. *Journal of cellular physiology* *216*, 321-326.
- Swaminathan, S., Tomkinson, B., and Kieff, E. (1991). Recombinant Epstein-Barr virus with small RNA (EBER) genes deleted transforms lymphocytes and replicates in vitro. *Proc Natl Acad Sci U S A* *88*, 1546-1550.
- Terhune, S.S., Schroer, J., and Shenk, T. (2004). RNAs are packaged into human cytomegalovirus virions in proportion to their intracellular concentration. *J Virol* *78*, 10390-10398.
- Theofilopoulos, A.N., Baccala, R., Beutler, B., and Kono, D.H. (2005). Type I interferons (alpha/beta) in immunity and autoimmunity. *Annual review of immunology* *23*, 307-336.
- Thomson, A.W., and Lotze, M.T. (2003). *The cytokine handbook*, 4th edn (Amsterdam ; Boston: Academic Press).
- Vieira, P., de Waal-Malefyt, R., Dang, M.N., Johnson, K.E., Kastelein, R., Fiorentino, D.F., deVries, J.E., Roncarolo, M.G., Mosmann, T.R., and Moore, K.W. (1991). Isolation and expression of human cytokine synthesis inhibitory factor cDNA clones: homology to Epstein-Barr virus open reading frame BCRF1. *Proc Natl Acad Sci U S A* *88*, 1172-1176.
- Vivier, E., Raulet, D.H., Moretta, A., Caligiuri, M.A., Zitvogel, L., Lanier, L.L., Yokoyama, W.M., and Ugolini, S. (2011). Innate or adaptive immunity? The example of natural killer cells. *Science* *331*, 44-49.

- Vivier, E., and Ugolini, S. (2009). Regulatory natural killer cells: new players in the IL-10 anti-inflammatory response. *Cell Host Microbe* 6, 493-495.
- Wagner, C.S., Ljunggren, H.G., and Achour, A. (2008). Immune modulation by the human cytomegalovirus-encoded molecule UL18, a mystery yet to be solved. *J Immunol* 180, 19-24.
- Wang, X., and Hutt-Fletcher, L.M. (1998). Epstein-Barr virus lacking glycoprotein gp42 can bind to B cells but is not able to infect. *Journal of virology* 72, 158-163.
- Wang, X., Kenyon, W.J., Li, Q., Mullberg, J., and Hutt-Fletcher, L.M. (1998). Epstein-Barr virus uses different complexes of glycoproteins gH and gL to infect B lymphocytes and epithelial cells. *Journal of virology* 72, 5552-5558.
- Warming, S., Costantino, N., Court, D.L., Jenkins, N.A., and Copeland, N.G. (2005). Simple and highly efficient BAC recombineering using galK selection. *Nucleic Acids Res* 33, e36.
- Wiesner, M., Zentz, C., Mayr, C., Wimmer, R., Hammerschmidt, W., Zeidler, R., and Moosmann, A. (2008). Conditional immortalization of human B cells by CD40 ligation. *PLoS One* 3, e1464.
- Wills, M.R., Ashiru, O., Reeves, M.B., Okecha, G., Trowsdale, J., Tomasec, P., Wilkinson, G.W., Sinclair, J., and Sissons, J.G. (2005). Human cytomegalovirus encodes an MHC class I-like molecule (UL142) that functions to inhibit NK cell lysis. *J Immunol* 175, 7457-7465.
- Wilson, A.D., and Morgan, A.J. (2002). Primary immune responses by cord blood CD4(+) T cells and NK cells inhibit Epstein-Barr virus B-cell transformation in vitro. *J Virol* 76, 5071-5081.
- Wilson, J.B., and May, G.H.W. (2001). *Epstein-Barr virus protocols* (Totowa, N.J.: Humana Press).
- Xia, T., O'Hara, A., Araujo, I., Barreto, J., Carvalho, E., Sapucaia, J.B., Ramos, J.C., Luz, E., Pedroso, C., Manrique, M., *et al.* (2008). EBV microRNAs in primary lymphomas and targeting of CXCL-11 by ebv-mir-BHRF1-3. *Cancer Res* 68, 1436-1442.
- Yoon, S.I., Jones, B.C., Logsdon, N.J., and Walter, M.R. (2005). Same structure, different function crystal structure of the Epstein-Barr virus IL-10 bound to the soluble IL-10R1 chain. *Structure* 13, 551-564.
- Young, L.S., and Rickinson, A.B. (2004). Epstein-Barr virus: 40 years on. *Nature reviews. Cancer* 4, 757-768.
- Yuan, J., Cahir-McFarland, E., Zhao, B., and Kieff, E. (2006). Virus and cell RNAs expressed during Epstein-Barr virus replication. *J Virol* 80, 2548-2565.
- Zeidler, R., Eissner, G., Meissner, P., Uebel, S., Tampe, R., Lazis, S., and Hammerschmidt, W. (1997). Downregulation of TAP1 in B lymphocytes by cellular and Epstein-Barr virus-encoded interleukin-10. *Blood* 90, 2390-2397.

DANKSAGUNG

Ich möchte mich ganz besonders bedanken bei

- **Prof. Dr. Reinhard Zeidler** für die Projekte und die freie Hand, die er mir ließ, um diese umzusetzen, sowie die vielen fruchtbaren Diskussionen, in denen nicht selten Pläne für neue Projekte entstanden,
- **Prof. Dr. Wolfgang Hammerschmidt** für die Diskussionen im Laborseminar oder auch zwischen Tür und Angel, für sehr hilfreiche, konstruktive Kritik und Überlegungen sowie für das Einarbeiten in die Technik der maxi-EBV Klonierung,
- **Prof. Dr. Horst Domdey** für die Übernahme der universitären Schirmherrschaft über meine Arbeit und die Fachvertretung an der Fakultät,
- **Prof. Dr. Wagner, Prof. Dr Förstemann, Prof. Dr. Martin und Prof. Dr. Hopfner** dafür, dass sie sich ebenfalls Zeit genommen haben, meine Arbeit zu begutachten,
- **Dr. Andreas Moosmann** für die T Zell Klone und weitere Schätze aus seinem Cryo-Stock- und Antikörper-Fundus, für tiefeschürfende Diskussionen und sein beeindruckendes Detailwissen bezüglich immunologischer Zusammenhänge, Kristallisationsvorgängen und anderer philosophischer Fragestellungen,
- **Dagmar Pich**, die mir viele technischen Tipps und Tricks vermittelte, welche entscheidend zum Erfolg der Arbeit beitrugen,
- **Prof. Dr. Dirk Eick** für sein Interesse an meiner Arbeit und seiner Arbeitsgruppe für das Aushelfen mit Antikörpern und verschiedenen Inhibitoren.

Außerdem gilt mein Dank

Andrea Schub für die hilfreichen Diskussionen diverser Projekte und dessen, was sich davon eventuell realisieren lässt, die unumstößliche gute Laune, die wiederholten Hinweise, das Kaffeepausen zwar nicht die Datenlage, aber auf jeden Fall die Stimmung verbessern, den Olympic-Games-News-Ticker und die Übernahme der Stammtisch-Organisation;

Antje Arnold, die das BNL2a-Paper im Journal Club vorgestellt hat und zumindest für einige Zeit die Fraktion der Labor-Zug'roastn verdoppelte;

Sebastian Grömminger für die EBV-microRNA Primer und die Einarbeitung in die Geheimnisse der qPCR;

Larissa Martin, für das stets bereitwillige Zur-Verfügung-Stellen ihrer persönlichen Flow, das Wechseln von Medium, wenn ich gerade verhindert war, der Gewährung labortechnischen Asyls beim Pipettieren des ein oder anderen PCRchens, sowie der Aktualisierung meines Kenntnisstandes bezüglich des tagesaktuellen Geschehens frei nach Radio Gong;

Marc Borath für meist gute Musik, für die Fachsimpeleien über egal was, als drittem „Big Player“ in der Kaffeepause, als Mückenwiesen-Flügelflitzer und „Core Processor“ des Stammtischs;

Markus Kalla für die hilfsbereite Unterstützung, das klaglose Ertragen wiederholten Schnorrens, das gemeinsame Klonieren induzierbarer Vektoren, die uns fast zum Durchbruch verholfen hätten, weitsichtiger Rad-Touren-Pläne, die bald schon in Erfüllung gehen könnten, und dafür, dass ich immer zuerst durch die Tür gehen musste;

der gesamten AG Moosmann dafür, dass sie mich in ihrem Labor wie einen der Ihren gewähren ließen – trotz meines Status als „externem Mitarbeiter“;

... und nicht zu vergessen:

Manuel Deutsch dafür, dass wir richtige Mikroskop-Freunde wurden und ich von jetzt an einen echten Scotch-Single-Malt höchstens alternierend mit einem Schluck seines Quellwassers genieße; Andi Thomae für die Erkenntnis, dass jedes Protein individuell ist; Stoffl Meyer für das mitunter unvermittelte Vermitteln vieler Fakten und noch mehr Wissen über Österreich und seine schlafwandlerische Kenntnis der Chemikalienvorräte; Christoph Hinzen für nerdige Mittagspausen, feinsten italienischen Caffé und weltbeste Sprüche in der Disziplin „locker bis lässig“; Kai, Stoffl und Sebastian (aka „Die drei von der Halle“) für meine Aufnahme in die Top-four der Badminton-Asse trotz nicht ganz hinreichender Fähigkeiten meinerseits; Christine, weil sie immer dafür sorgt, dass der Käse gegessen ist; Ugur für das Kicken auf der Mückenwiese (präsentiert mit freundlicher Unterstützung von der Abteilung Kommunikation, Schirmherr: Prof. Dr. Wess); der AG Imhof für die Socca5 Beteiligung; der Wanderschuh-Lobby; allen Labor-Kollegen für die klaglose Einsicht, dass sich fünf Minuten bei mir gelegentlich höchst relativ verhalten

...und natürlich allen anderen Kollegen der AGV, die immer für ein nettes, lustiges – aber natürlich nicht zu kuscheliges! ;-) – Arbeitsklima sorgten.

Ganz besonders bedanke ich mich bei meinen Eltern und meiner Schwester, die sich immer tapfer nach dem Stand der Dinge erkundigten und meiner Motivation immer mal wieder neue Energie geben konnten,

und vor allem bei meiner Freundin Anne Julie für ihr geduldiges Verständnis, dass ich so viele Stunden im Labor verbracht habe, ihr Interesse an meiner Arbeit und ihre Freude, wenn sie wusste, um was es in den Versuchen ging. Ihre Unterstützung hat ganz entscheidend dazu beigetragen, dass ich in allen Phasen der Arbeit am Ball blieb und es tatsächlich geschafft habe, auf dieser Seite anzukommen.

CURRICULUM VITAE

Name	Simon Jochum
Date of birth	5. April 1980
Place of birth	Koblenz, Germany
Nationality	German
1986-1992	Primary school, Waldesch, Germany
1992-1999	Secondary School, „Gymnasium auf der Karthause“, Koblenz, Germany
1999-2000	Civilian Service as a Paramedic, Deutsches Rotes Kreuz, Koblenz, Germany
2000-2006	Studies of Biology, Albert-Ludwigs-Universität, Freiburg, Germany Graduation in Immunobiology, Cellular Biology, Developmental Biology, Virology and Business Administration
2006-2007	Diploma Thesis: „Analysis of CDK Inhibitors in B-Cells during proliferation and development“ AG Prof. Dr. Hassan Jumaa, Department Prof. Dr. Michael Reth Max-Planck-Institute for Immunobiology, Freiburg, Germany
2007-2011	Doctoral Thesis: „RNA transfer by Epstein-Barr virus triggers early events that regulate cell fate and promote immune evasion“ AG Prof. Dr. Reinhard Zeidler, Department Prof. Dr. Wolfgang Hammerschmidt Helmholtz Zentrum München and Ludwig-Maximilians University, München, Germany

PUBLICATIONS AND PRESENTATIONS

- **Jochum S.**, Ruiss R., Moosmann A., Hammerschmidt W. and Zeidler R. (2012)
RNAs in Epstein-Barr virions control early steps of infection.
Proceedings of the National Academy of Sciences 109: E1396-E1404.
- **Jochum S.**, Moosmann A., Lang S., Hammerschmidt W. and Zeidler R. (2012)
The EBV immune evasion proteins vIL-10 and BNLF2a protect newly infected B cells from immune recognition and elimination.
PLoS Pathogens 8: e1002704.
- Ruiss R., **Jochum S.**, Wanner G., Reisbach G., Hammerschmidt W. and Zeidler R. (2011)
A virus-like particle-based Epstein-Barr virus vaccine. *J Virol* 85, 13105-13.
- Ruiss R., **Jochum S.**, Mocikat R., Hammerschmidt W., Zeidler R. (2011)
EBV-gp350 confers B-cell tropism to tailored exosomes and is a neo-antigen in normal and malignant B cells – a new option for the treatment of B-CLL. *PLoS One* 6, e25294
- Battke C., Ruiss R., Welsch U., Wimberger P., Lang S., **Jochum S.**, Zeidler R. (2011)
Tumour exosomes inhibit binding of tumour-reactive antibodies to tumour cells and reduce ADCC. *Cancer Immunol. Immunother.* 60, 639-48
- Talk at the 14th International Congress of Immunology, 22.-27.8.2010 in Kobe, Japan, workshop “Immunity to Virus Infections, title “The Impact of BCRF1 (viral IL-10) and BNLF2a on the Immune Evasion of Epstein-Barr Virus”
(supported by a travel grant of the Glaxo-Smith-Kline Foundation)
- Talk at the 3rd European EBV Meeting, 16. - 17.6.2011 in Lyon, France, with the title “EBV Particles Contain Functional RNAs that Trigger Early Events in Infection”